R. & M. No. 3801

R. & M. No. 3801

PROCUREMENT EXECUTIVE MINISTRY OF DEFENCE

AERONAUTICAL RESEARCH COUNCIL

REPORTS AND MEMORANDA

Low-Speed Wind-Tunnel Tests of the Longitudinal Stability Characteristics of some Swept-Wing Quiet Airbus Configurations

By D. A. KIRBY AND A. G. HEPWORTH

Aerodynamics Department, R.A.E., Farnborough, Hants.

LONDON: HER MAJESTY'S STATIONERY OFFICE

1977

£7 net

Low-Speed Wind-Tunnel Tests of the Longitudinal Stability Characteristics of some Swept-Wing Quiet Airbus Configurations

By D. A. KIRBY AND A. G. HEPWORTH
Aerodynamics Department, R.A.E., Farnborough, Hants.

Reports and Memoranda No. 3801*
March, 1976

Summary

Measurements of lift, drag and pitching moment have been made on model configurations representing rear-engined layouts, with large nacelles so positioned that both wing and tailplane will make a contribution to noise shielding. Only round nacelles were used with a high-wing model but both round and flat types of nacelle were tested on a low-wing model.

The investigation concentrated on the effects of the large lifting surfaces of the nacelles on the longitudinal stability and performance under the high-lift conditions appropriate to take-off and landing; the nacelles were not powered so the influence of the jet efflux was excluded. The results show that the influence of the nacelles on the downwash at the tailplane is such as to offset the lift losses and longitudinal stability changes incurred by adding the nacelles to models without tailplane; so that for the complete models the stability changes were small, and the effects on performance only became appreciable when the flat nacelles were tilted several degrees nose down with a landing-flap setting.

Included in the test programme were measurements of the distribution of total head at a hypothetical engine face inside the round nacelles for a number of model configurations and conditions.

* Replaces R.A.E. Technical Report 76029, A.R.C. 36 825

LIST OF CONTENTS

1. Introduction

2. Details of Models

3. Details of Tests

4. Calculation and Presentation of Results

5. Comparison of Results on High- and Low-Wing Models without Nacelles and Tailplane

6. Nacelle Internal Flow Characteristics
   6.1. Round Nacelles
   6.2. Flat Nacelles

7. Effect of Round Nacelles on the Longitudinal Stability Characteristics

8. Effect of Flat Nacelles on the Longitudinal Stability Characteristics
   8.1. Plain Nacelles
   8.2. Nacelles with Auxiliary Noise-Shielding Surfaces
   8.3. Blocked Nacelles
   8.4. Surface Flow Observations

9. Effect of Nacelles on the Mean Downwash at the Tailplane

10. Some Aspects of the Effects of the Nacelles on Performance

11. Concluding Remarks

List of Symbols

References

Tables—1 to 10

Illustrations—Figs. 1 to 57

Detachable Abstract Cards

1. Introduction

The increased emphasis on the need for reducing the levels of aircraft noise experienced on the ground gives rise to further factors which must be taken into account at an early stage in the design of a new aircraft. For several years, noise has been a serious consideration in the design of many of the components of the jet engine and with the imposition of stricter noise standards the external shape of the nacelle is being influenced more and more; in particular the lengths of intake and exhaust ducts have been increased to accommodate silencing material. It has also become clear that further noise reductions can be obtained by exploiting the potential of parts of the aircraft other than the nacelles to provide noise shielding and refraction; and this could result in the future in rear-engined aircraft having lifting surfaces of different proportions, for example—lower aspect ratio wings, larger tailplanes and shorter tailplane arms, than those in current use. In the longer term more novel layouts—twin fins, twin fuselages etc. for which design criteria are even less readily available may need to be investigated.

It is almost inevitable that the necessary resiting and resizing of aircraft parts for noise reduction will introduce new or magnify known interference effects, and may thus adversely effect the aircraft performance. The purpose of the work presented in this Report was to provide data which could be used to assess the low-speed longitudinal stability and performance of those twin-engined layouts where, by making the nacelles large enough to span the gap between wing and tailplane, several features favourable to noise shielding are achieved. For simplicity free-flow nacelles were used in the test programme, so that although distortions in the flow at the tailplane caused by the 'lifting' qualities of the nacelles were represented, the further changes in the velocity and downwash at the tailplane which would be caused by a jet efflux were not. These effects at low speed, and the forward effect of the nacelles on the wing characteristics at high speed, form important associated fields of research which are the basis of other parts of the overall wind-tunnel programme.

Two types of nacelle were used with model components including a wing typical of a modern transport aircraft, two fuselages so that either a high- or a low-wing position could be represented, and a low tailplane which was larger than necessary from longitudinal stability considerations but which would enhance the noise-shielding properties of the layouts investigated. The model details are described more fully in Section 2 of the Report.

The first pair of nacelles were round and the first series of tests were made with the nacelles mounted above the fuselage of a high-wing configuration—it being assumed that the maximum benefits in noise shielding could thus be obtained. However, since there are considered to be distinct advantages in structural efficiency in using a low-wing position, the next set of tests was made with the nacelles mounted above the fuselage of a low-wing model using the same wing and tailplane and the same relative fore and aft positions of the nacelles, wing and tailplane. For both the high- and low-wing configurations, measurements of the total-head distribution in the nacelles at a typical engine-face position were made to allow some evaluation of the effects of the close proximity of the nacelles to the wing on the engine performance.

From ground clearance considerations, particularly during rotation at take-off, some degree of upsweep is necessary on the fuselage rear end and for a low-wing configuration it is not possible to position the tailplane in line with the wing. This means that unless the nacelles are inclined downwards some of the noise-shielding potential of the wing is lost. Flattening of the nacelle intake and exit could also be beneficial since the noise sources should then be somewhat closer to the noise-shielding surfaces. Such a flattened shape is more likely than the round nacelle to shed vortices of sufficient strength to have a major effect on the flow field at the tailplane. Therefore in order to find if any adverse effects on performance and stability result from such developments, tests have been made on the low-wing model with flattened nacelles fixed on the side of the body at three alternative inclinations. Following a suggestion by Hawker Siddeley Aviation for increasing the noise-shielding qualities, these flat nacelles were extended over the tailplane for some of the configurations. The details of these 'auxiliary noise-shielding surfaces' and the nacelles in general are given in Section 2 and in the figures and tables at the end of the Report.

In Section 3 the range of the tests for each configuration is described, and the method of calculation and presentation of the results is covered by Section 4.

A short discussion comparing the lift, drag and pitching moment of the basic high- and low-wing models, including some comment on the efficacy of fitting a fillet in the wing-body junction of the high wing model, is made in Section 5.

The main discussion is concerned with the results with the nacelles in position and this is undertaken in Sections 6 to 10. Of these Sections, 6 is devoted to the internal flow characteristics of the nacelles and 7 and 8 are concerned with the effects of the various types of nacelle on the longitudinal stability characteristics. The reasons for the changes in stability and trim when the nacelles are added become more apparent when the changes in downwash at the tailplane are calculated—Section 9. Finally some assessment of the various layouts

from a performance viewpoint is made in Section 10 using trimmed lift and drag coefficients calculated at model Reynolds number.

2. Details of Models

The general arrangement of the high- and low-wing models is shown in Figs. 1 and 2 respectively. The wing used for both models was the wing of Ref. 1 in the configuration representative of a rear-engined transport aircraft with a low-wing position*. This wing is of aspect ratio 7·53 and has a high-lift system consisting of a full-span leading-edge slat and a tabbed Fowler flap which can be deployed full or part span. Full details of this system are given in the tables and figures of Ref. 1 and only the main dimensions are reproduced in Table 1 of this Report. The combinations of the high-lift components used in the present investigation were the clean wing, that is flaps and slats undeflected, or slats 25 degrees and flaps 10, 25 or 40 degrees. The flap span used was 80 per cent of the overall wing span and the tab at the rear of the flap was never deflected.

Both the fuselages were of the wide-bodied type, the body of Ref. 1 being used for the low-wing model. The centre and rear sections of another existing body were rebuilt to provide the high-wing model. Although of the same diameter and nose shape as the body of the low-wing model the converted body was longer and the rear fuselage was more upswept in keeping with the higher wing and tailplane positions. Details of the bodies, wing heights and of the wing-body angles, which were slightly different for the two models, are given in Table 1. For all the tests with the high-lift system deflected, the inboard ends of the slats and flaps were in the vertical plane of the maximum fuselage width so that, except for the high-wing tests with a fillet in the wing-body junction described in Section 5, there were gaps between the bodies and the high-lift devices.

Because of the emphasis on noise-shielding, the tailplane made specially for the tests was larger in area relative to the wing compared with the tailplanes used on the various wide-bodied transport aircraft currently flying. The tailplane arm was the same for both models and the tailplane pivoted at two thirds of the centre-line chord about shafts passing through the bodies and the metal tongues securing the fins to their respective bodies. For convenience in speed of model manufacture existing fins were used; although these are of rather different style the differences were not considered to be important in relation to the work described in this Report. The sides of both the bodies were flattened in the region of the tailplane so that the tailplane angle could be varied without introducing spanwise gaps.

The round nacelles were axisymmetric with a cowl shape derived by stretching cowl 2 of Ref. 2 but blunting the nose to delay any propensity to flow separation. Also the trailing edge was distorted in order to increase the exit area and ensure that the velocity through the nacelles was raised (as far as is possible with free-flow nacelles) towards the high values of entry velocity ratio appropriate to the take-off and climb phases of flight. The maximum diameter of these nacelles was 0·625 times that of the bodies and they were aligned parallel to the body centre-lines. For all the force tests they were mounted just in contact with the body surface and the gap between the nacelles was 0·125 of a body diameter. This gap was doubled for some of the tests in which the measuring rake fitted inside the port nacelle was used to investigate the flow characteristics at a hypothetical engine face. Details of the nacelles and the disposition of the pitot and static tubes and holes are shown in Fig. 3. For both the positions used the nacelles were each held in place by two bolts fitted with spacers, no attempt being made to fill in with a realistic pylon the gap between nacelle and body.

The flat nacelles were more complex in shape and were designed in consultation with Hawker Siddeley Aviation Limited (Hatfield) to have suitable external lines and entry and exit areas in relation to the rest of the model components.† For ease of manufacture the internal cross-sectional shapes were made near-rectangular merging smoothly with the near-elliptic entry section and allowing easy fitting of the half-open ducts which were added behind the nacelle in some of the tests to provide an auxiliary noise-shielding surface, filling the gap between the nacelles proper and the tailplane. Because the nacelle internal shape was unrealistic, there was no point in investigating the distribution of total head etc. at a likely engine position but a pitot-static rake fitted 0·0343 m ahead of the port nacelle exit was used to determine the entry velocity ratio.

---

* It was appreciated that the kinked planform was not very appropriate for high-wing aircraft, since for such layouts it is more sensible to retract the landing-gear into the fuselage or special blisters on the fuselage side—thus removing one of the constraints on the wing design. However, using the kinked wing gave the larger wing chords in the root region required for noise shielding and permitted a more direct appreciation of the effect of wing height.

† At this stage of the research programme it was realised that, in the enthusiasm for finding the effects of adding some really large nacelles, the round nacelles were made rather oversize in relation to the fuselage etc.

These flat nacelles were attached to the body of the low-wing model by bolts which could be fitted in different positions so that the nacelles could be tested in three alternative settings. One of these was parallel to the fuselage centre-line and the entry face was then in the fore and aft position used for the round nacelles. For the two nose-down settings, approximately 4 and 8 degrees, the nacelles rotated about the centre of the exit plane. The nacelles just touched the body for all the settings; so, since they were always parallel to the plane of symmetry of the model they moved slightly further outboard as the angle of tilt increased. As for the round nacelles only the holding bolts and the spacers around them linked the nacelles and the body. Full details of the nacelle locations are given in Table 1 and the relative positions of the nacelles, wing with flaps deflected and tailplane are shown in Fig. 4. Since the auxiliary noise-shielding surfaces were attached to the nacelles, they moved away from the tailplane when the nacelles were tilted.

Photographs showing the round nacelles fitted to the high-wing model and to the low-wing model are reproduced in Figs. 5a and 5b respectively. Two views of the low-wing model fitted with the flat nacelles and their auxiliary noise-shielding extensions are reproduced in Fig. 6.

3. Details of Tests

The low-wing model was originally tested in the No. 2 $11\frac{1}{2}$ ft $\times 8\frac{1}{2}$ ft wind tunnel at speeds up to 76 m/s with the high-lift devices deflected but without nacelles[1]. Because the working section of that tunnel and its equipment were undergoing an extensive modernisation in the latter half of 1972 and first half of 1973 all the work described in this Report was done in the No. 1 $11\frac{1}{2}$ ft $\times 8\frac{1}{2}$ ft wind tunnel where the strut rig is a comparatively light structure, Fig. 5a, and the tunnel speed had to be restricted. A speed of 37·1 m/s was used for most of the tests. The Reynolds number of the tests was therefore only $0{\cdot}72 \times 10^6$, based on the standard mean chord, and compared with the previous work done mainly at $1{\cdot}48 \times 10^6$ in the No. 2 $11\frac{1}{2}$ ft $\times 8\frac{1}{2}$ ft wind tunnel the stall naturally occurred at a lower angle of incidence and the maximum obtainable values of lift coefficient were less. Thus, the maximum lift coefficient for the low-wing model with slats 25 degrees and flaps 40 degrees was reduced from 2·6 to 2·3 with proportionate reductions at the other flap settings. However, the lift curve slopes were very similar at the two values of Reynolds number and in the working range of lift coefficient appropriate to low speed flight the flow was still unseparated; thus valid comparisons can be made of the effects on the stability and performance of adding the nacelles. The stall like that at the higher Reynolds number began on the outer wing and was therefore not representative of what would be required on a transport aircraft where the aim is to make the inner wing stall first so that safe stalling characteristics satisfying the airworthiness requirements can be achieved.

Beyond the stall, when the flow over the wing is completely separated, scale effect is small and the further reduction in tunnel speed to 24·6 m/s made from safety considerations should not affect the conclusions regarding the superstall characteristics made in Section 7. For these superstall tests the range of angle of incidence was extended to just beyond 40 degrees. Normally the range was from about −3 to 24 degrees in steps of 1·5 degrees for the main tests with more limited ranges as applicable for the tailsettings other than zero or −5 degrees. Transition was fixed on the fuselages by a wire round the nose for the pre-stall work but for the tests beyond the stall, an additional wire was fixed along the body length, following the method found suitable for superstall investigations in Ref. 3. The usual practice of leaving transition free on the main lifting surfaces for general work was followed.

A summary of the configurations on which force tests were made is given in the table overleaf. For every configuration a test without tailplane was made but the tailsettings used varied and were those required to provide data for the analysis of the mean downwash angle at the tailplane position and of the trimmed lift and drag. In most cases $\eta_B = -5$ and 0 degrees were tested and the full range can be found in Tables 3 to 10 at the end of this Report where the results are listed. Except for the two configurations where the flat nacelles were completely blocked, all the tests were made with free flow through the nacelles.

The wing alone was also tested but only with the slats and flaps undeflected. The results are given in Table 2.

Measurements of the total head and static pressure distribution inside the port round nacelle were made for the high-wing, high-wing with fillets and low-wing models at flap deflections of 10 and 40 degrees with zero angle of sideslip. The nacelle spacing was 0·125 of the body diameter, D, but for the high-wing layout the measurements were repeated with the increased spacing of 0·25 of the body diameter. The range of incidence covered was up to $\alpha = 21$ degrees at 37·1 m/s with extensions to $\alpha = 41$ degrees at 24·6 m/s for some cases. For two configurations—the high-wing with fillets and the low-wing, both with slats 25 degrees, flaps 40 degrees—measurements were also made at $\alpha = 8$ and 14·5 degrees over a range of sideslip angle from −15 to +15 degrees.

Slats (degrees)	Flaps (degrees)	Nacelles							
				Flat			Flat with auxiliary noise-shielding surfaces		
		None	Round	Parallel	4 degrees nose down	8 degrees nose down	Parallel	4 degrees nose down	8 degrees nose down
High wing									
0	0	√	√						
25	10	√	√						
25	25	√							
25	40	√	√						
High wing with fillet									
0	0	√							
25	10	√							
25	25	√							
25	40	√							
Low wing									
0	0	√	√	√	√	√	√		√
25	10	√	√	√	√	√	√		√
25	25								
25	40	√	√	√ also blocked	√	√	√ also blocked		√

With the flat nacelles similar measurements were made only at zero sideslip, the angle of incidence ranging from about $-1{\cdot}5$ to 21 degrees at a tunnel speed of $37{\cdot}1$ m/s.

The test programme was concluded with some observations at $37{\cdot}1$ m/s of the surface flow over the flat nacelles and rear body using a suspension of Dayglo powder in paraffin.

4. Calculation and Presentation of Results

Following removal of the rig contributions the values of lift, drag and pitching moment were non-dimensionalised relative to the dynamic head, gross wing area and standard mean chord of the gross wing. The coefficients were then corrected for tunnel constraint, including wake blockage, by the methods given in Ref. 4. For both models the pitching moment coefficients were converted to a moment centre on the centre-line chord at $0{\cdot}25\,\bar{c}$ before tabulation and plotting at the end of the Report. The angle of incidence used throughout is that of the wing datum but as the various tailsettings had during manufacture been set as exact numbers relative to the body datum lines these settings, η_B, are retained for ease of reference.

In the figures showing the effects of the various nacelle arrangements on the forces and pitching moment a consistent set of symbols has been used according to the following table.

Configuration	Symbol
High-wing model without nacelles	×
Low-wing model without nacelles	+
Models with round nacelles	⊙
Flat nacelles at	
0 degrees	⊡
−4 degrees	◇
−8 degrees	▽

5. Comparison of Results on High- and Low-Wing Models without Nacelles and Tailplane

The lift, drag and pitching moment coefficients measured on the high- and low-wing models without the nacelles and tailplane are compared in Figs. 7–9. The wing with slats and flaps retracted was also tested without either body; Fig. 7 shows that although adding the body to form the low-wing model caused negligible change in lift coefficient there was a reduction of about 0·05 throughout the incidence range for the high-wing model compared with the low-wing model. Some of the detailed difference in loading may be associated with the different body shapes but the overall loss in lift coefficient must arise mainly from the change in wing position. The so-called low-wing position of a modern wide-bodied transport is so close to a mid-wing position that the usual results of little loss in lift coefficient at low incidence for a mid-wing position at low wing-body angles and a large loss with a large offset position, such as for the high-wing model, were found in the present tests.

It is noticeable in Fig. 7 that when the circulation round the wing was increased by deflecting the flaps to 10 degrees the difference in lift coefficient between the high- and low-wing models increased to 0·1, but that for the still higher circulation with flaps at 40 degrees the difference was down again, to about 0·03. This latter behaviour probably occurs because the spanwise gap between the flaps and the body is reducing as flap deflection increases for the high-wing but is increasing for the low-wing model. When this gap was still further reduced on the high-wing model by fitting a fillet to tidy up the flow in the wing-body junction the lift curves for the low- and high-wing models with 40 degrees of flap deflection were virtually identical. At this deflection a modification to the lower region of the fuselage of the low-wing model to close the gaps should be beneficial, but at 10 degrees of deflection these gaps evidently matter less and despite the introduction of the junction fillet for the high-wing model less lift is still measured for the high- compared with the low-wing position (Fig. 7).

The fillets in the high-wing-body junction were developed with the flaps at 25 degrees rather than 40 degrees because there was evidence of some trailing-edge separation on the flap at the higher deflection[1]. Basically, each fillet consisted of a vertical surface slightly inboard of the maximum body diameter, faired smoothly fore and aft into the body. Filling the slight spanwise gaps remaining between the flaps and the fillets and the slats and the fillets with plasticine made very little difference to lift coefficient, so the more practical arrangement of leaving small gaps was used in the force and moment tests which gave the coefficients plotted in Figs. 7–9; this also applied to the investigation of internal flow characteristics of the nacelles, discussed in Section 6.

The fitting of the fillets also reduced the drag, Fig. 8, and for the configurations with slats and flaps deflected the drag of the high-wing model was thereby reduced below that of the low-wing model; however under these conditions improvements would be expected if the lower region of the fuselage of the low-wing model was in turn modified to reduce the spanwise gaps.

The improved lifting characteristics of the flaps when the fillets were added, naturally increased the nose-down pitching moment coefficient, *see* Fig. 9. This figure also shows the larger destabilising effect resulting from the longer forebody of the high- compared with the low-wing model. Estimates of $\partial \Delta C_{m_{body}}/\partial \alpha$ using slender body theory for the forebody lift are related to the overall effect of adding the bodies to the clean wing in the following table:

Destablising effect of bodies, $\partial \Delta C_{m_{body}}/\partial \alpha$ *(per degree) with slats and flaps at* 0 *degrees*

	High wing	Low wing
Estimated	0·0166	0·0131
Measured	0·0144	0·0095

This comparison confirms past experience[5] that most of the destablising effect is associated with the forebody and it is inferred that the load carried on the rear body must be small; particularly in the case of the high-wing model since the rear body is then immersed more in the stronger part of the downwash field of the wing.

The foregoing remarks are concerned with changes in the slope $\partial C_m/\partial \alpha$ and hence in the slope $\partial C_m/\partial C_L$. The precise effect on pitching moment coefficient at a fixed angle of incidence of adding a body depends on various factors including the wing-body angle, wing-body junction shape, wing height, rear body upsweep, the presence of flow separations etc. and is not readily calculable especially when the slats and flaps are deflected. Nevertheless the importance of the forebody lift in determining the longitudinal static stability margin is

illustrated by the similarity of the difference in $\partial C_m/\partial C_L$ between the high- and low-wing models with various flap settings viz. 0·07 for slats and flaps 0 degrees, 0·07 for slats 25 degrees, flaps 10 degrees and 0·08 for slats 25 degrees, flaps 40 degrees in the attached flow region. These values can be compared with the slender body theory estimate of 0·05.

6. Nacelle Internal Flow Characteristics

6.1. Round Nacelles

The measurements of total head and static pressure made at an assumed engine face for the round nacelles have been analysed to find the mean total heads, distortion parameters* and flow ratios; and the results with the larger flap deflection are presented in Figs. 10–12. Calculations of the mean entry velocity through the highlight area gave values of $\bar{V}_i/V_0$ very close to unity at low angles of incidence for all the combinations tested (see Fig. 12). Thus the internal expansion at the rear of the nacelles was sufficient to ensure conditions where the possibility of external separations from the lips of the nacelles would be minimised. At high angles of incidence the flow rates reflect the extent to which the boundary layers of the body and wing and any flow separations in the wing-body junction pass into the nacelle but even in the worst case encountered in the pre-superstall tests, $\bar{V}_i/V_0$ only dropped to about 0·85. The few tests made under superstall conditions showed that $\bar{V}_i/V_0$ had fallen to 0·5 at $\alpha = 30$ degrees and at about this incidence there were indications that regions of reversed flow were occurring inside the nacelle.

The effect of aircraft layout on the total head distribution and consequently on the extent of the design problem for the internal shaping of the nacelle and for the engine is illustrated by Figs. 10 and 11. For the low-wing position only the boundary layer on the body is likely to affect the flow through the nacelles and the results show that even with the nacelles touching the body (nacelles 0·125 D apart) the entry is sufficiently distant from the body surface to provide an adequate boundary layer bypass, so that the measured mean total head is close to unity with only small losses mainly attributable to the nacelle internal boundary layer.

However when the wing is raised parts of the wing wake and of the complex flows round the wing-body junctions and inboard ends of the flaps would naturally be expected to pass into the nacelles and reductions in $\bar{P}/q_0$ and increases in $\Delta P/q_0$ do occur and are particularly severe at high angles of incidence. Improving the flow in the junctions by providing a fillet is beneficial and at low angles of incidence there is considerable advantage in moving the nacelles horizontally outboard from a 0·125 D to a 0·25 D spacing, again showing the significance of the junction. The reasons for the differences in $\bar{P}/q_0$ and in $\Delta P/q_0$ between the various configurations can be more easily understood by reference to Fig. 13 where the total head contours (neglecting the internal boundary layers) are plotted for three angles of incidence. In addition to showing the improvements for the high-wing model mentioned above it is interesting to see the slight improvement in total head distribution for the low-wing model between $\alpha = 11.5$ and 20.5 degrees. This could be due to the action of vortices shed from the forebody thinning the boundary layer on the body at angles of incidence above about 10 degrees and would account for the shape of the curve of distortion parameter against incidence in Fig. 11, i.e. some of the small loss in mean total head at the 'engine face' noted for the low-wing model could result from ingestion of part of a body boundary layer. Since no measurements of flow direction were made this hypothesis cannot be verified at the present time. All the configurations should of course benefit by the increase in Reynolds number between model and full scale.

With the nacelle spacing of 0·125 D the angle of sideslip was varied at two angles of incidence for the low wing and the high wing with fillets. Measurements were only made for the port nacelle and naturally the quality of the flow inside the nacelle deteriorated considerably at positive angles of sideslip since the starboard nacelle, body and wing (for the high-wing model) were then all creating boundary layers and flow disturbances ahead of the port nacelle, Figs. 14 and 15. Again the effects can be seen most clearly by looking at the total head contours, Fig. 16. In the worst cases where $\bar{P}/q_0$ fell to 0·8 $\Delta P/q_0$ was over 0·2 (a peak value of 0·27 was found on the low-wing model at $\alpha = 14{\cdot}5$ degress, $\beta = 15$ degrees).

Measurements in more detail of swirl angle as well as of total head and velocity would be required before any realistic assessment of the effect of the various parameters on engine design could be formulated but the results presented in this Report give an indication of the broad effects of some configuration changes.

---

* These tests were only intended to give an indication of the problems which would occur for various conditions and the number of pitots was not sufficient to allow use of one of the more fashionable parameters, such as DC_{60}, so the root mean square of the differences between the local total head and the mean total head has been used throughout this Report and the calculations have been made over the whole internal diameter, i.e. there is no allowance for hubs etc.

6.2. Flat Nacelles

As stated in Section 2 the internal geometry of the flat nacelles was unrepresentative, and the measurements of total head and static pressure made using a rake at the rear of the port nacelle were aimed solely at providing sufficient data to calculate the entry velocity ratio, Fig. 17. The combination of the closeness to the wing of the entry when the nacelles were tilted 8 degrees nose down and the supervelocity with the flaps at 40 degrees increased $\bar{V}_i/V_0$ to 0·9 compared with a general level of 0·85 for flaps 0 degrees. A disadvantage of moving the entry close to the wing to improve the noise shielding is the loss in engine performance when the wing stalls. That this is likely to occur is demonstrated in Fig. 17 by the large loss of flow rate through the nose-down nacelles at high incidence with the slats and flaps at 0 degrees.

7. Effect of Round Nacelles on the Longitudinal Stability Characteristics

The effects on the lift, drag and pitching moment coefficients of adding the round nacelles with 0·125 D spacing are shown in Figs. 18–22 for the high-wing model and in Figs. 23–27 for the low-wing model. The nacelles are lifting bodies but the extent of their contribution to the overall lift is dependent on their angle of incidence relative to the local flow and indeed on their effect on the local flow. The lift coefficients plotted in Figs. 18 and 23 for the models without tailplane indicate that the mean downward component of the flow past the nacelles is increased, as would be expected, by the increased circulation round the wing when the flaps are deflected; but there is also a loss in lift coefficient caused by adding the nacelles when the basic models are at zero lift. This is partly due to the wing camber and wing-body angle ensuring that the nacelles mounted parallel to the body are nose down relative to the local stream, but interference between the nacelle and wing and/or rear body may contribute. An understanding of the complexities of adding nacelles to the fuselage in close proximity to the clean wing at low angles of incidence will be essential before an optimum design for cruise can be determined and a series of experiments up to high subsonic Mach number on a smaller model of the same wing and body proportions as the low-wing model discussed in this Report is being made in the R.A.E. 8 ft × 6 ft transonic wind tunnel.

For all the configurations, the addition of nacelles causes an increase in lift curve slope, pre-stall, since the downwash angle at the nacelle positions increases less rapidly than the geometrical incidence.

Figs. 19 and 24 show that at constant lift coefficient the nacelles increase the drag coefficient by roughly 0·01 for all configurations and all lift coefficients. However, examination of the coefficients listed in Table 6 shows that, for the high-wing model with slats 25 degrees and flaps 40 degrees, the increase in drag coefficient caused by the addition of the nacelles at constant incidence falls from 0·010 at $\alpha = -1$ degree to −0·005 just pre-stall at $\alpha = 16$ degrees; this compares with a variation from 0·011 to 0·008 over the same incidence range for the low-wing model, Table 10. The value of 0·01 results mainly from the increased wetted surface area with the nacelles present but the nacelles are sited in a strong downwash field for the high wing configuration and therefore, at high wing incidences, generate sufficient negative lift normal to the local stream to offset the increase in profile drag, and thus cause an overall decrement in drag. A similar behaviour was observed for the flat nacelles fitted to the low-wing model when the flaps were deflected and the relevance of the local stream direction is discussed further in Section 8 where the greater quantity of data available for the flat nacelles is used to make a detailed analysis.

A full assessment of the effect on the performance of adding the nacelles needs to take account of the trimming aspect so the main discussion on the implications of the changes in lift and drag is deferred to Section 10.

Pitching moment coefficients for the three flap settings are plotted in Figs. 20–22 for the high-wing model and in Figs. 25–27 for the low-wing model. All these figures show that at low angles of incidence, the addition of nacelles to a model *without tailplane* causes a nose-up pitching moment; this is consistent with a download on or near the nacelles as discussed at the beginning of this section. Analysis of the data shows that the effective point of action of this lift decrement is ahead of the nacelle entry at low values of incidence and wing lift, and moves further forward with increase of incidence. This confirms that the changes caused by adding the nacelles are of a complex nature, arising from changes in pressure distribution on the wing and body as well as on the nacelles. It is not therefore surprising that although there is the stabilising effect appropriate to a lifting body introduced aft of the moment centre, the crossover point between the pitching moment curves with and without nacelles varies with the wing position and flap setting; *see* also Section 8.1.

This stabilising effect is not obtained when the tailplane is present, neither the longitudinal stability nor the stalling behaviour being affected to any extent by the addition of the nacelles. This implies that the downwash field at the tailplane position is changed by the different distribution of bound and trailing vorticity of the models when the round nacelles are added in such a manner as to counteract their stabilising effect on the

pitching moment without tailplane. Considering the complexities of the flow, the similarity in shape of the curves with and without nacelles shown in Figs. 20–22 and 25–27 for the models with tailplane is quite remarkable; the only change being the change of trim corresponding to about one degree of tailplane angle. This simplicity may of course be particular to the nacelle and tailplane arrangement tested and the changes in downwash are analysed and discussed further in Section 9.

A few configurations were tested over a wider range of incidence to find if the addition of large rear-engined nacelles introduced a deterioration in longitudinal stability beyond the stall which could lead to a superstall problem. The results for lift and pitching moment are presented in Figs. 28–31. The detailed behaviour at the stall is naturally dependent on the Reynolds number but above about 30 degress of incidence, when the wing will be completely stalled even at full scale conditions, the wind tunnel results are valid. The figures show the conventional behaviour at high angles of incidence for a low tailplane position[3] and the nacelles have little effect.

8. Effect of Flat Nacelles on the Longitudinal Stability Characteristics

8.1. Plain Nacelles

As explained in the introduction to this Report the flat nacelles were derived from considerations of how to maximise the noise shielding potential of low-wing layouts. The loss of lift coefficient and the increase of lift curve slope when nacelles are attached parallel to the fuselage behind the wing were again observed and the magnitude of the negative lift coefficient which can be generated by the flat nacelles is illustrated by the curves for the model without tailplane, slats and flaps undeflected, plotted in Fig. 32. The addition of nacelles, tilted 8 degrees nose down, gave a loss in lift coefficient of 0·2 at an incidence (−1 degree) where the lift of the datum model, and hence the downwash behind the wing, were small. The increased downwash when the flaps were deflected 40 degrees increased this decrement in lift coefficient at low angles of incidence to 0·3, *see* Fig. 33. As with the round nacelles increasing wing incidence reduced the size of the lift losses so the effect of the nacelles on the maximum lift coefficient was less than the effect at low incidence; but, the changes in lift coefficient due to tilt at constant wing incidence, i.e. rotating the nacelles but keeping them substantially in a fixed downwash field, naturally remained constant over the whole range of incidence up to the stall.

The drag coefficients for the model without tailplane are plotted in Fig. 34, and Figs. 35 and 36 show the incremental changes in both lift and drag coefficient caused by the flat nacelles. With the nacelles parallel to the body the increases in drag coefficient when the nacelles were added were similar to those measured for the round nacelles but when the nacelles were tilted downwards a higher drag was obtained at low angles of incidence, as shown in Fig. 35. However at higher angles of incidence, where there is a large downwash angle of the flow field behind the wing, the resultant force on the nacelles actually acts in a forward direction so that the drag at constant incidence is reduced by the addition of nacelles which generate large negative lifts. Because of this large lift loss the behaviour at constant lift coefficient is more straightforward, i.e. the nacelles always cause an increase in the drag—Fig. 34.

A better understanding of the contribution of the flat nacelles to the overall lift and drag of the model without tailplane and of the different behaviour exhibited in Fig. 34 for the various flap configurations is obtained if the changes in lift and drag coefficient ΔC_{L_N} and ΔC_{D_N} are expressed relative to the local stream direction at the nacelle position. No measurements of the local downwash angle were made during the tests; but consideration of the results of Ref. 6, of a mean downwash indicated by the tilted nacelles acting as lifting surface and of the relative position of nacelles and tailplane led to the assumption that the mean downwash at the nacelle position would be similar to that calculated at the tailplane position from the pitching moment coefficients without nacelles present—*see* Section 9. As the analysis proceeded, this assumption was refined slightly and the local nacelle incidences α_N used in plotting Fig. 36 were calculated taking the ratio of the mean downwash angle at the nacelle location to the mean downwash angle at the tailplane as 0·8 for flaps 0 degrees, 1·0 for flaps 10 degrees and 0·9 for flaps 40 degrees. These values allow roughly for the different positions of the wing trailing-edge relative to the nacelles.

Fig. 36 shows that, when referred to local stream axes, the changes in lift and drag caused by adding the flat nacelles at different tilt angles can be correlated quite closely and proves that the negative drag increments noted previously were associated with the use of free stream rather than local stream axes in calculating the changes caused by the nacelles.

The existence of two separate curves for the lift changes shown in Fig. 36a is consistent with the increased interference of the nacelles with the wing flow when the lifting surface of the wing is extended rearwards by deploying the flaps. This dependence on flap condition is less marked for the changes in drag coefficient and it is questionable that a distinction exists amongst the scatter of the points plotted in Fig. 36b. The better collapse

of the lift data compared with the drag data in Fig. 36 is attributed to the presumption that although the changes in lift caused by adding a nacelle will be made up of several factors (including the lift on the nacelle itself, carry-over lift on the body and interference with the wing) these are all likely to be directly dependent on the lift on the nacelles themselves, whereas the drag results from the complex balance of pressures and suctions acting on forward- and aft-facing surfaces of the various components of the model and may thus be more dependent on the precise configuration.

The extent to which the lift changes are not purely those occurring on the nacelles themselves can be gauged from the fact that in a special test at a tunnel speed of 37·1 m/s with an isolated flat nacelle and then with two nacelles in side by side contact, lift curve slopes of 0·0019 and 0·0065 per degree are measured compared with the minimum slope $\partial\Delta C_{L_N}/\partial\alpha$ of 0·011 shown by Fig. 36a. The drag coefficient at zero lift for the two nacelles touching, which is a similar situation to the nacelles touching the body, was 0·009; compare the value of $\Delta C_{D_N} = 0{\cdot}008$ found for the low values of α_N in Fig. 36b.

The effects on pitching moment of adding the flat nacelles are shown in Figs. 37–39. They were similar in kind to those observed for the round nacelles; the stabilising contributions of the nacelles, tailplane off, were again offset by the changes in the downwash field at the tailplane so that for the complete model the longitudinal static stability margin was virtually unchanged by the addition of the nacelles. The changes in trim, however, were more pronounced, and the importance of the change in downwash angle at the tailplane (discussed further in Section 9) is indicated by the pitching moment changes caused by tilting the nacelles being of opposite sign when the tailplane is present compared with those for the model without tailplane.

As in the case of the round nacelles the effective point of action of the overall change in lift caused by the addition of nacelles, derived from the pitching moments measured without tailplane, is ahead of the nacelle entry plane. The following table gives values of Δx_N, the distance of the point of action of the lift change behind the model moment centre, calculated directly from Tables 8 to 10 for the angles of incidence closest to zero.

Δx_N as a fraction of the mean chord, $\bar{c}$

Nacelle tilt (degrees)	Flap deflection (degrees)		
	0	10	40
0	0·22	0·41	0·67
−4	0·67	0·63	0·72
−8	0·77	0·70	0·72

The effect of changes in drag are omitted in this simple calculation but the values of $\Delta x_N/\bar{c}$ are of sufficient accuracy to establish that the lift change is effectively acting ahead of the nacelle entry plane, which is located $0{\cdot}90\bar{c}$ aft of the moment centre.

In the tests on the nacelles alone the test with two nacelles touching showed that the nacelle lift acted just ahead of the entry plane (about $0{\cdot}02\bar{c}$). As far as the nacelle loads are concerned, this configuration is similar to that of the nacelle alongside a body but the less forward lift position compared with those shown in the table and the smaller lift slope noted previously establish that an additional negative lift is induced on the wing and body. Detailed pressure plotting of the model would be necessary before a complete analysis of the force and moment changes caused by the addition of the nacelles could be attempted.

8.2. Nacelles with Auxiliary Noise-Shielding Surfaces

The effect of fitting auxiliary noise-shielding surfaces to the rear of the nacelles was fairly straightforward in that the additional lifting surface so far behind the model moment centre further increased the longitudinal stability margin without the tailplane; and much of the gain in stability was retained when the tailplane was added, presumably because the additional shielding surface was near to and partially above the tailplane and therefore scarcely affected the mean downwash at the tailplane position. Figs. 40–42 contrast the pitching moment coefficients with and without the auxiliary noise-shielding surfaces.

The overall changes in lift, drag and pitching moment arising from the addition of these noise-shielding surfaces was not large, but because the extended nacelles overlapped both wing and tailplane they (rather than the less extreme plain nacelles) have been taken as the flat nacelle configuration which is analysed in detail in the later sections dealing with downwash angle and performance.

8.3. Blocked Nacelles

Rather larger changes in all three components were obtained in tests made to investigate the effect of blocking the nacelles, *see* Table 10. Both nacelles were completely blocked in order to highlight some of the changes which would occur in the event of an engine failure. In practice, even with an engine reduced to windmilling, there would be some flow through the nacelle and it is estimated that rather less than half the changes caused by completely blocking both nacelles (Figs. 43 and 44) need be recognised. This means that with the exit close to the tailplane, as for the auxiliary noise-shielding configuration, about half of a degree change in tailplane angle to trim could result from the large reduction in flow through the nacelle. This may be a small term compared with the changes in trim caused by the removal of the effect of the jet efflux close to the tailplane.

8.4. Surface Flow Observations

Some tests were made with the flat nacelles in which the surface flow over the nacelles and rear fuselage was observed using a suspension of Dayglo powder in paraffin. A few photographs were taken and those for the slats 25 degrees, flaps 40 degrees configuration at $\alpha = 10$ degrees are reproduced in Fig. 45. They illustrate the complexities of the flow in the vicinity of the nacelles and show that when the nacelles are tilted down 8 degrees the crossflow can be sufficient to cause a separation along the whole length of the nacelles which rolls up to form strong tip vortices from the effective nacelle lifting area, viz. the nacelles and adjacent body. Vorticity appropriate to the nacelle lift will of course be shed for all nacelle configurations but it is presumably the separation from the whole edge region for the larger lift changes which gives the non-linearity in the curves of Fig. 36a. The photographs also show that 'bubble type' separations with reattachment are present near the entry lips and that areas of separated flow can occur on the rear body ahead of the tailplane.

9. Effect of Nacelles on the Mean Downwash at the Tailplane

The mean downwash angle, $\bar{\varepsilon}_T$, at the tailplane position has been calculated for several configurations by using the pitching moment coefficients measured for different tailplane settings to deduce the tailplane setting for which zero change in pitching moment coefficient would occur when the tailplane was added; that is when the effective angle of the tailplane to the local stream $\bar{\alpha}_T$ $(=\alpha_B + \eta_B - \bar{\varepsilon}_T)$ equalled zero. Inherent in this method is the assumption that the drag of the tailplane at zero mean lift is so small and acts at such a small moment arm that its contribution to pitching moment is negligible. For the present analysis the maximum error involved is less than 1/50th of a degree.

The results for the basic models (Figs. 46 and 47) show, as is usual, an increase in mean downwash angle at a tailplane position when the circulation round the wing is caused by an increase in the angle of incidence and/or the deflection of the flaps. The detailed shape of the curves with increasing incidence is controlled by the position of the tailplane relative to the wing wake. For example, because the tailplane is lower relative to the high wing than to the low wing, it has moved further from the wing wake at high angles of incidence for the high- than for the low-wing model and $\partial\bar{\varepsilon}_T/\partial\alpha$ is smaller for the flap deflections of 0 and 10 degrees. Presumably this does not happen with the flaps at 40 degrees because the region of high downwash angle behind the wing is then more extensive and is lowered by the increased flap deflection to affect the two tailplane positions more equally. A further complication shown by the results is that for the low-wing model the tailplane is evidently still sufficiently high at the higher angles of incidence to be subjected to the increased rise in downwash angle which occurs when the outer wing stalls and the trailing vorticity is concentrated more inboard.

Figs. 18, 23, 32 and 33 show that adding the nacelles caused losses in lift coefficient at low angles of incidence but increases in the lift curve slope, because the lifting force on the nacelles increased positively with incidence. This means that initially the changes in the mean downwash angle at the tailplane when the nacelles are added will be negative, because of the direction of rotation of the shed vorticity associated with the negative lift of the nacelles, but that $\partial\bar{\varepsilon}_T/\partial\alpha$ should be higher with the nacelles on, see Figs. 48–51. Whether or not the mean downwash angle at a fixed incidence is higher or lower than without the nacelles is dependent on the extent of the download on the nacelles at low angles of incidence. For example, Fig. 51 shows the results of the downwash analysis for several nacelle configurations, and with the flat nacelles tilted 8 degrees nose down in the strong cross-flow generated with the flaps at 40 degrees the shed vorticity is sufficient to reduce the mean downwash angle at the tailplane by 6 degrees at $\alpha = 0$ degrees.

It is because of the increase in $\partial\bar{\varepsilon}/\partial\alpha$, i.e. the reduction in $(1 - \partial\bar{\varepsilon}/\partial\alpha)$ and hence in tailplane effectiveness when the nacelles are added, that the stabilising tendency of the nacelles observed without the tailplane fitted is eliminated and the main effect of adding the nacelles for all the complete aircraft configurations is an

unfavourable change in trim resulting from the reduction in $\bar{\varepsilon}_T$, Figs. 20–22, 25–27, 37–39 and 40–42. The implications of this change on performance are discussed further in the next Section but it is pertinent to emphasise that the effects of jet efflux were not present in this investigation.

10. Some Aspects of the Effects of the Nacelles on Performance

A full appreciation of the effect on aircraft aerodynamic performance of large nacelles of the types which have been tested is obviously beyond the scope of this Report, since no attempt was made to represent the engine flow correctly and the tests were made at a low Reynolds number and Mach number. Even so some measure of the major effects under high-lift conditions can be obtained from examination of the trimmed lift and drag coefficients. These have been calculated for the round nacelles and the flat nacelles with auxiliary noise-shielding surfaces, and the results are presented for the model moment centre at $0{\cdot}25\ \bar{c}$ in Figs. 52–57.

For all configurations addition of the nacelles without a tailplane present caused a nose-up increment in pitching moment at low angles of incidence and for most of the flap settings and nacelle tilts this effect persisted to higher incidences. Consequently smaller elevator or tailplane angles would be required to trim with the nacelles added and the losses in trimmed lift coefficient at a fixed angle of incidence caused by the nacelles are less than the corresponding losses without the tailplane, for example compare the values plotted in Fig. 55 with those given in Tables 9 and 10. Moreover the increased lift curve slope with nacelles present ensures that the losses in the maximum $C_{L_{\text{trimmed}}}$ are smaller than the losses in $C_{L_{\text{trimmed}}}$ noted at lower wing incidences. Therefore unless the nacelles cause a radical change in the stalling behaviour of an aircraft, the maximum usable lift coefficient could, as for the model, be only slightly degraded by the presence of the large nacelles. There would probably need to be some redesign of the undercarriage and/or rear fuselage shape to permit the use of slightly higher angles of incidence, but this is an aspect which cannot be examined fully without a knowledge of the engine thrust effects including the interference of the jet efflux on the tailplane. However, such thrust effects should be small on the approach with the engines at low power, so the model results with the flaps deflected to 40 degrees have been used to take the analysis a little further in the following paragraphs.

Under approach and landing conditions, with flaps 40 degrees, the low-wing layout should develop, at full scale Reynolds number, a maximum lift coefficient $C_{L_{\max}}$ of approximately 2·7 with the correct stall pattern. The airworthiness regulations allow usable lift coefficients of up to about two-thirds $C_{L_{\max}}$, so this yields an approach C_L of 1·8. Fig. 55 implies that adding the round or flat nacelles parallel to the body will scarcely affect $C_{L_{\max}}$ and shows that at $C_L = 1{\cdot}8$ only a half a degree of incidence separates the no-nacelle and with-nacelle curves. If flat nacelles at a tilt angle of 8 degrees nose-down were to be used Fig. 55 implies some loss in $C_{L_{\max}}$, and therefore some slight loss in usable C_L, together with a need to increase the approach angle of incidence by about one and a half degrees (compared with the no-nacelle datum) in order to realise the new usable C_L. This increase might not be possible because of limitations imposed by the design of the undercarriage and the rear fuselage shape.

The effects on the trimmed drag coefficient, *see* Figs. 56 and 57, differ considerably for the take-off and landing configurations. With flaps deflected 10 degrees the lift-drag polar is very similar for all the nacelle configurations tested on the low-wing model and the increase in trimmed drag coefficient at constant trimmed lift coefficient caused by the flat and round nacelles are about the same, $\Delta C_D \simeq 0{\cdot}01$, as the basic drag coefficient of the round nacelles observed from the tests with the high-lift system undeflected, Fig. 24. The smaller effects for the high-wing model compared with the low-wing model noted previously in Section 7 were still present.

For the landing flap deflection of 40 degrees, the large increases in drag caused by the flat nacelles on the model without tailplane, Fig. 34, were also obtained for the trimmed state and although the curves with and without nacelles are approaching each other at the assumed usable lift coefficient of about 1·8, the penalty in drag for using nacelles tilted 8 degrees nose-down would be high, Fig. 57. The noise benefits of such a layout would therefore be reduced since more engine thrust would be needed.

In comparing the drag curves for flaps 10 and 40 degrees, the differences in the effect of the nacelles are very striking, but the analysis made in Section 8 shows that these differences are explicable when account is taken of the local flow directions.

11. Concluding Remarks

Measurements of lift, drag and pitching moment have been made on model configurations representing rear-engined layouts with large nacelles positioned so that both wing and tailplane would be noise-shielding surfaces. The results with flap arrangements appropriate to take-off and landing have been analysed in detail to provide information on the effects of such nacelles on the longitudinal stability and performance of high-

and low-wing transport aircraft of the airbus type; that is with a large capacity fuselage of considerably greater width relative to the wing span and chords than the first generation of jet transports.

The model nacelles were made to represent nacelles larger than those in current use in order to allow for the developments in engine silencing, such as more acoustic lining and coaxial exit nozzles, now envisaged for the future. Despite this increase in size, the overall effects of the nacelles on the longitudinal stability, judged on the contributions of the nacelles as lifting bodies, were reassuringly small, since the changes in the aerodynamic characteristics caused by the nacelles when fitted to the models without tailplane were largely offset by the effects of the nacelles on the tailplane. The reason for this is shown by an analysis of the mean downwash at the tailplane.

Some performance aspects also look encouraging. At a take-off flap setting of 10 degrees, flat nacelles fitted with auxiliary noise shielding surfaces and tilted down 8 degrees relative to the fuselage, in order to maximise the noise-shielding potential, showed no higher trimmed drag than much simpler round nacelles mounted parallel to the fuselage. However, with this nacelle tilt there were adverse effects on the trimmed drag at a 40 degree flap setting, and on the trimmed lift for both take-off and landing settings; but the results indicate that more moderate tilt angles could be employed with small performance penalties very similar to those obtained with nacelles of flat or round type at zero tilt. An analysis of the contributions of the flat nacelles to lift and drag showed how the effects for different nacelle tilts and flap settings can be correlated and this provides a means for estimating the contributions for other nacelle and flap settings.

Although the results of these tests are promising in giving confidence that large nacelles can be fitted close to the wing and tailplane without causing major losses in longitudinal stability and performance, it must be emphasised that only free-flow nacelles were used in this preliminary work and that many other aerodynamic aspects must be considered before the noise-shielding possibilities of the rear-engine layout can be properly assessed.

LIST OF SYMBOLS

A	Aspect ratio
b	Overall span
C_D	Drag coefficient
C_L	Lift coefficient
C_m	Pitching moment coefficient
$\bar{c}$	Standard mean chord
D	Body diameter
$\bar{P}$	Mean total head at engine face
ΔP	Difference between local total head and mean total head at engine face
q_0	Free stream dynamic pressure
V_i	Mean velocity at nacelle entry
V_0	Free stream velocity
Δx_N	Distance of point of action of a lift change behind the moment centre
α	Angle of incidence of wing
α_B	Angle of incidence of body
α_N	Incidence of nacelle to local flow
β	Angle of sideslip
$\bar{\varepsilon}_T$	Mean downwash angle at tailplane
η_B	Tailplane angle relative to body datum

Subscripts

B	Body
N	Nacelle
T	Tailplane

REFERENCES

No.	*Author(s)*	*Title, etc.*
1	D. A. Lovell	A wind-tunnel investigation of the effects of flap span and deflection angle, wing planform and a body on the high-lift performance of a 28 degree swept wing. A.R.C. C.P. No. 1372 (1977)
2	C. Young	An investigation of annular aerofoils for turbofan engine cowls. A.R.C. R. & M. No. 3688 (1972)
3	D. J. Kettle and D. A. Kirby	Low-speed wind-tunnel tests on the effects of tailplane and nacelle position on the superstall characteristics of transport aircraft. A.R.C. R. & M. No. 3571 (1969)
4	H. C. Garner, E. W. E. Rogers, W. E. A. Acum and E. C. Maskell ...	Subsonic wind-tunnel wall corrections. AGARDograph 109 (1966)
5	J. Weber, D. A. Kirby and D. J. Kettle	An extension of Multhopp's method of calculating the spanwise loading of wing-fuselage combinations. A.R.C. R. & M. No. 2872 (1956)
6	A. G. Hepworth and D. A. Kirby	An investigation of the downwash distribution under high-lift conditions at possible engine intake positions close behind the wing of an airbus model. Unpublished MOD(PE) paper.

TABLE 1

Geometric Details of Models

Wing		
Gross area, S	$0{\cdot}6126\ m^2$	
Gross span, b	2·1476 m	
Aspect ratio, A	7·529	
Standard mean chord, $\bar{c}$	0·2853 m	
Centre-line chord	0·5393 m	
Kink chord	0·2931 m	
Tip chord	0·1334 m	
Spanwise position of kink	0·3809 m	
Thickness/chord ratio	10·7 per cent	
Section	*see Ref* 1	
Leading-edge sweepback	30·51 degrees	
Quarter-chord sweepback (outer wing)	28 degrees	
Trailing-edge sweepback		
(inner wing)	−3.24 degrees	
(outer wing)	19·73 degrees	
Distance of the mean quarter-chord point aft of the wing apex	0·3292 m	
Dihedral	0	
Slat chord	16 per cent of local wing chord	
Flap chord		
(outer wing)	34 per cent of local wing chord	
(inner wing)	0·0967 m	
	High-wing model	Low-wing model
Distance of wing apex aft of body nose	0·9528 m	0·7161 m
Height of wing apex above body datum	0·1255 m	−0·0368 m
Wing-body angle	1·27 degrees	1·10 degrees
Tailplane		
Gross area, S_T	$0{\cdot}2090\ m^2$	
Gross span, b_T	0·9144 m	
Aspect ratio, A_T	4	
Standard mean chord, $\bar{c}_T$	0.2286 m	
Centre-line chord	0·3658 m	
Tip chord	0·0914 m	
Thickness/chord ratio	10 per cent	
Section	NACA 0010	
Quarter-chord sweepback	35 degrees	
Distance of the mean quarter-chord point aft of the tailplane apex	0·2195 m	
Dihedral	0	
Tailplane arm (mean quarter-chord point of wing to mean quarter-chord point of tailplane) measured along body datum	0·9538 m	
	High-wing model	Low-wing model
Tailplane height above body datum (for zero tailsetting)	0·0889 m	0·0392 m
Distance of tailplane pivot point aft of apex	0·2438 m	
Tailplane volume coefficient	1·1406	

TABLE 1 (continued)

	High-wing model	Low-wing model
Fins		
Gross area (projected to body datum)	0·1786 m^2	0·1531 m^2
Height above body datum	0·4860 m	0·5137 m
Chord at body datum	0·4541 m	0·4449 m
Tip chord	0·2808 m	0·1512 m
Thickness/chord ratio	10 per cent	10 per cent
Section	NACA 0010	NACA 0010
Quarter-chord sweepback	43·25 degrees	40 degrees
Distance of the mean quarter-chord point aft of the fin leading-edge at the body datum	0·3241 m	0·2913 m
Fin arm	0·9224 m	0·9510 m
Fin volume coefficient	0·1252	0·1107
Bodies		
Diameter	0·3048 m	0·3048 m
Overall length	2·4607 m	2·2385 m
Length of nose	0·4333 m	0·4333 m
Length of parallel portion	0·8844 m	1·0432 m
Length of rear-fuselage	1·1430 m	0·7620 m
Round nacelles		
Overall length	0·5687 m	
Maximum diameter	0·1905 m at 38 per cent of length	
Thickness/chord ratio of section	4·5 per cent	
Section	*see* Section 2 of Report	
Entry cross-sectional area (highlight)	0·1998 m^2	
Exit cross-sectional area	0·2154 m^2	
Cross-sectional area at rake position	0·1526 m^2	
Distance of entry aft of wing apex	0·5849 m	
Nacelle-body angle	0	
Height above body datum	0·2167 m	
Spanwise positions of nacelle centre-line	0·1143 and 0·1334 m	
Flat nacelles		
Overall length (without auxiliary surfaces)	0·5334 m	
Maximum width	0·1727 m	
Maximum depth	0·1502 m	
Section	*see* Section 2 of Report	
Entry cross-sectional area (highlight)	0·1183 m^2	
Exit cross-sectional area	0·1065 m^2	
Cross-sectional area at rake position	0·1040 m^2	
Distance of entry aft of wing apex at zero nacelle-body angle	0·5849 m	
Height of nacelle above body datum at zero wing nacelle-body angle	0·1097 m	
Spanwise position of nacelle centre-line at zero nacelle-body angle	0·2133 m	
Nacelle-body angles relative to body centre-line	0, −4·2 and −8·1 degrees	
Auxiliary noise-shielding surfaces extended nacelle length by	0·0762 m inboard 0·2222 m outboard	

TABLE 2

Wing Alone with Slats and Flaps 0 Degrees

α_{deg}	C_L	C_D	C_m
−4·31	−0·234	0·0168	−0·0255
−2·76	−0·124	0·0132	−0·0370
−1·20	0	0·0101	−0·0487
+0·36	0·121	0·0101	−0·0540
1·90	0·224	0·0110	−0·0553
3·45	0·330	0·0157	−0·0590
5·00	0·439	0·0172	−0·0616
6·55	0·545	0·0225	−0·0642
8·10	0·650	0·0325	−0·0644
9·64	0·742	0·0617	−0·0627
11·16	0·787	0·0926	−0·0415
12·67	0·814	0·1150	−0·0230
14·19	0·829	0·1532	−0·0035
15·69	0·842	0·1875	+0·0012
17·20	0·857	0·2203	0·0002

TABLE 3

High Wing with Slats and Flaps 0 Degrees

	No tailplane			$\eta_B = -5$ degrees			$\eta_B = 0$ degrees		
α_{deg}	C_L	C_D	C_m	C_L	C_D	C_m	C_L	C_D	C_m
				No nacelles					
−3·02				−0·361	0·0412	0·3689	−0·260	0·0330	+0·0734
−1·47	−0·071	0·0244	−0·1098	−0·210	0·0325	0·3149	−0·110	0·0266	+0·0105
+0·09	+0·048	0·0223	−0·0949	−0·073	0·0281	0·2721	+0·033	0·0241	−0·0370
1·64	0·161	0·0224	−0·0743	+0·060	0·0262	0·2221	0·159	0·0242	−0·0618
3·19	0·271	0·0254	−0·0551	0·182	0·0268	0·2002	0·278	0·0274	−0·0873
4·74	0·375	0·0289	−0·0384	0·305	0·0295	0·1822	0·404	0·0313	−0·1130
6·29	0·487	0·0340	−0·0183	0·433	0·0337	0·1454	0·535	0·0376	−0·1583
7·84	0·594	0·0412	+0·0010	0·562	0·0405	0·0971	0·662	0·0470	−0·2055
9·38	0·694	0·0599	0·0281	0·684	0·0595	0·0530	0·782	0·0677	−0·2516
10·91	0·754	0·0931	0·0674	0·764	0·0952	0·0316	0·869	0·1083	−0·2814
12·43	0·795	0·1229	0·0944	0·813	0·1279	0·0207	0·916	0·1426	−0·2890
13·93	0·791	0·1650	0·1356	0·827	0·1701	+0·0010	0·932	0·1864	−0·3080
15·44	0·804	0·2005	0·1604	0·864	0·2092	−0·0488	0·965	0·2294	−0·3469
16·95	0·821	0·2351	0·1742	0·899	0·2462	−0·1040	0·993	0·2711	−0·3941
				Round nacelles parallel to body					
−3·06	−0·279	0·0419	−0·0584	−0·409	0·0528	0·3418	−0·312	0·0446	+0·0532
−1·49	−0·133	0·0351	−0·0639	−0·247	0·0432	0·2828	−0·157	0·0368	−0·0091
+0·06	−0·008	0·0315	−0·0641	−0·107	0·0377	0·2424	−0·006	0·0335	−0·0599
1·62	+0·116	0·0307	−0·0565	+0·030	0·0314	0·1944	+0·131	0·0320	−0·0925
3·17	0·232	0·0322	−0·0465	0·158	0·0350	0·1676	0·256	0·0346	−0·1179
4·72	0·346	0·0356	−0·0375	0·288	0·0372	0·1411	0·385	0·0389	−0·1532
6·28	0·469	0·0407	−0·0291	0·428	0·0415	0·0947	0·522	0·0454	−0·1991
7·83	0·580	0·0478	−0·0139	0·559	0·0484	0·0566	0·654	0·0550	−0·2406
9·38	0·684	0·0644	−0·0045	0·680	0·0653	+0·0230	0·780	0·0758	−0·2867
10·91	0·751	0·0995	+0·0286	0·767	0·1028	−0·0038	0·857	0·1138	−0·3072
12·44	0·800	0·1292	0·0627	0·833	0·1351	−0·0231	0·924	0·1503	−0·3220
13·95	0·821	0·1717	0·0975	0·847	0·1798	−0·0350	0·931	0·1963	−0·3294
15·45	0·810	0·2053	0·1332	0·876	0·2159	−0·0731	0·959	0·2362	−0·3682
16·95	0·820	0·2380	0·1524	0·912	0·2535	−0·1217	0·997	0·2768	−0·4117

TABLE 4

High Wing with Slats 25 Degrees and Flaps 10 Degrees

	No tailplane			$\eta_B = -5$ degrees			$\eta_B = 0$ degrees		
α_{deg}	C_L	C_D	C_m	C_L	C_D	C_m	C_L	C_D	C_m
				No nacelles					
−2·99	−0·114	0·0951	−0·1933	−0·255	0·1080	0·2435	−0·172	0·0994	−0·0291
−1·45	−0·041	0·0818	−0·1698	−0·176	0·0905	0·2473	−0·083	0·0833	−0·0309
+0·11	+0·096	0·0677	−0·1708	−0·036	0·0750	0·2150	+0·063	0·0696	−0·0692
1·70	0·296	0·0579	−0·1901	+0·173	0·0615	0·1619	0·277	0·0591	−0·1283
3·28	0·467	0·0574	−0·1904	0·364	0·0588	0·1180	0·461	0·0589	−0·1665
4·85	0·615	0·0612	−0·1795	0·526	0·0611	0·0794	0·621	0·0631	−0·1962
6·41	0·753	0·0679	−0·1694	0·690	0·0675	0·0449	0·778	0·0712	−0·2291
7·98	0·897	0·0766	−0·1570	0·849	0·0761	+0·0102	0·942	0·0818	−0·2706
9·54	1·042	0·0870	−0·1456	1·001	0·0869	−0·0215	1·103	0·0941	−0·3089
11·11	1·182	0·0992	−0·1303	1·164	0·1005	−0·0553	1·260	0·1102	−0·3518
12·67	1·321	0·1157	−0·1080	1·317	0·1172	−0·0894	1·418	0·1296	−0·3939
14·23	1·449	0·1339	−0·0862	1·475	0·1382	−0·1343	1·571	0·1528	−0·4419
15·78	1·572	0·1546	−0·0651	1·617	0·1629	−0·1855	1·720	0·1783	−0·4920
17·34	1·686	0·1768	−0·0390	1·753	0·1888	−0·2359	1·848	0·2064	−0·5269
18·88	1·780	0·2010	−0·0097	1·871	0·2172	−0·2693	1·964	0·2383	−0·5553
20·41	1·833	0·2291	+0·0449	1·934	0·2486	−0·2709	2·025	0·2732	−0·5546
21·91	1·816	0·2583	0·1065	1·937	0·2848	−0·2708	2·029	0·3141	−0·5523
23·41	1·808	0·2923	0·1518	1·953	0·3256	−0·2990	2·031	0·3597	−0·5630
				Round nacelles parallel to body					
−3·01	−0·177	0·1120	−0·1678	−0·300	0·1226	0·2199	−0·208	0·1130	−0·0635
−1·48	−0·100	0·0950	−0·1450	−0·221	0·1020	0·2202	−0·124	0·0954	−0·0631
+0·08	+0·029	0·0810	−0·1451	−0·089	0·0858	0·1898	+0·015	0·0806	−0·1066
1·67	0·226	0·0685	−0·1694	+0·120	0·0711	0·1213	0·224	0·0683	−0·1658
3·25	0·401	0·0661	−0·1792	0·328	0·0663	0·0680	0·424	0·0665	−0·2162
4·82	0·560	0·0683	−0·1802	0·497	0·0678	+0·0283	0·591	0·0704	−0·2449
6·39	0·709	0·0748	−0·1826	0·659	0·0737	−0·0080	0·754	0·0785	−0·2784
7·96	0·863	0·0833	−0·1704	0·823	0·0825	−0·0430	0·921	0·0891	−0·3172
9·53	1·010	0·0932	−0·1642	0·985	0·0929	−0·0755	1·086	0·1012	−0·3590
11·10	1·162	0·1066	−0·1550	1·150	0·1066	−0·1090	1·252	0·1182	−0·4006
12·66	1·304	0·1226	−0·1451	1·316	0·1250	−0·1471	1·418	0·1385	−0·4521
14·22	1·437	0·1421	−0·1311	1·469	0·1464	−0·1934	1·574	0·1624	−0·4953
15·78	1·565	0·1626	−0·1164	1·623	0·1711	−0·2439	1·717	0·1884	−0·5369
17·34	1·685	0·1866	−0·1015	1·756	0·1974	−0·2950	1·853	0·2166	−0·5752
18·88	1·778	0·2116	−0·0736	1·877	0·2273	−0·3238	1·975	0·2508	−0·6110
20·42	1·845	0·2404	−0·0291	1·938	0·2619	−0·3209	2·024	0·2873	−0·5985
21·41	1·833	0·2690	+0·0269	1·951	0·2966	−0·3171	2·048	0·3293	−0·5965
23·42	1·828	0·3036	0·0787	1·964	0·3365	−0·3288	2·047	0·3754	−0·5972

TABLE 4 (continued)

	No tailplane			$\eta_B = -10$ degrees		
	C_L	C_D	C_m	C_L	C_D	C_m
			No nacelles			
11·11	1·182	0·0992	−0·1303	1·071	0·0955	0·2343
12·67	1·321	0·1157	−0·1080	1·218	0·1107	0·2131
14·23	1·449	0·1339	−0·0862	1·370	0·1291	0·1746
15·78	1·572	0·1546	−0·0651	1·512	0·1505	0·1317
17·34	1·686	0·1768	−0·0390	1·655	0·1756	0·0772
18·88	1·780	0·2010	−0·0097	1·769	0·2016	0·0449
20·41	1·833	0·2291	+0·0449	1·842	0·2318	0·0306
21·91	1·816	0·2583	0·1065	1·846	0·2642	+0·0275
23·41	1·808	0·2923	0·1518	1·866	0·3029	−0·0087
			Round nacelles parallel to body			
11·10	1·162	0·1066	−0·1550	1·056	0·1020	0·1727
12·66	1·304	0·1226	−0·1451	1·207	0·1166	0·1447
14·22	1·437	0·1421	−0·1311	1·364	0·1362	0·1056
15·78	1·565	0·1626	−0·1164	1·513	0·1586	0·0628
17·34	1·685	0·1866	−0·1015	1·658	0·1844	+0·0070
18·88	1·778	0·2116	−0·0736	1·773	0·2116	−0·0276
20·42	1·845	0·2404	−0·0291	1·846	0·2424	−0·0309
21·41	1·833	0·2690	−0·0269	1·861	0·2760	−0·0363
23·42	1·828	0·3036	−0·0787	1·876	0·3135	−0·0518

TABLE 5

High Wing with Slats and Flaps 25 Degrees

	No tailplane			$\eta_B = -5$ degrees			$\eta_B = 0$ degrees		
α_{deg}	C_L	C_D	C_m	C_L	C_D	C_m	C_L	C_D	C_m
				No nacelles					
−2·92	0·031	0·1010	−0·2451				−0·070	0·1039	+0·0764
−1·32	0·239	0·0859	−0·2854	0·040	0·0943	0·2723	+0·145	0·0868	−0·0076
+0·32	0·564	0·0778	−0·3658	0·395	0·0808	0·1359	0·502	0·0774	−0·1451
1·93	0·788	0·0848	−0·3873	0·631	0·0842	0·0797	0·729	0·0831	−0·1966
3·51	0·961	0·0954	−0·3862	0·819	0·0922	0·0485	0·914	0·0928	−0·2328
5·07	1·110	0·1071	−0·3808	0·983	0·1018	+0·0174	1·078	0·1043	−0·2693
6·64	1·253	0·1190	−0·3722	1·146	0·1126	−0·0082	1·239	0·1165	−0·3002
8·21	1·403	0·1346	−0·3590	1·300	0·1271	−0·0282	1·396	0·1345	−0·3298
9·77	1·538	0·1521	−0·3396	1·452	0·1448	−0·0600	1·555	0·1541	−0·3682
11·33	1·671	0·1713	−0·3151	1·607	0·1660	−0·1013	1·698	0·1763	−0·4006
12·89	1·793	0·1928	−0·2884	1·748	0·1887	−0·1380	1·842	0·2015	−0·4257
14·44	1·911	0·2171	−0·2610	1·881	0·2132	−0·1664	0·980	0·2292	−0·4474
15·99	2·017	0·2420	−0·2399	2·018	0·2417	−0·1960	2·106	0·2586	−0·4752
17·53	2·102	0·2667	−0·1941	2·118	0·2727	−0·2075	2·207	0·2888	−0·4918
19·03	2·102	0·2932	−0·0996	2·146	0·3016	−0·1737	2·215	0·3193	−0·4558
20·53	2·072	0·3269	−0·0365	2·110	0·3355	−0·1530	2·198	0·3592	−0·4492
22·02	2·034	0·3577	−0·0316	2·107	0·3769	−0·1796	2·194	0·4012	−0·4755

TABLE 6

High Wing with Slats 25 Degrees and Flaps 40 Degrees

	No tailplane			$\eta_B = -5$ degrees			$\eta_B = 0$ degrees		
α_{deg}	C_L	C_D	C_m	C_L	C_D	C_m	C_L	C_D	C_m
				No nacelles					
−2·79	0·305	0·1166	−0·3485	0·044	0·1392	0·3600	0·143	0·1178	+0·0747
−1·10	0·721	0·1152	−0·4873	0·464	0·1247	0·1738	0·579	0·1137	−0·1222
+0·51	0·972	0·1252	−0·5289	0·772	0·1292	0·0682	0·872	0·1224	−0·2171
2·09	1·149	0·1392	−0·5289	0·974	0·1376	+0·0111	1·063	0·1350	−0·2605
3·66	1·298	0·1532	−0·5251	1·141	0·1481	−0·0323	1·235	0·1495	−0·2957
5·22	1·430	0·1664	−0·5078	1·290	0·1597	−0·0606	1·382	0·1622	−0·3224
6·78	1·562	0·1829	−0·4951	1·433	0·1739	−0·0864	1·524	0·1795	−0·3507
8·34	1·683	0·2011	−0·4722	1·568	0·1896	−0·1120	1·666	0·1979	−0·3778
9·89	1·805	0·2242	−0·4487	1·714	0·2126	−0·1364	1·798	0·2199	−0·3943
11·45	1·920	0·2465	−0·4179	1·850	0·2345	−0·1536	1·937	0·2450	−0·4102
13·00	2·045	0·2684	−0·3920	1·982	0·2568	−0·1739	2·070	0·2716	−0·4259
14·56	2·159	0·2972	−0·3608	2·109	0·2864	−0·1905	2·200	0·3008	−0·4451
16·10	2·255	0·3248	−0·3342	2·219	0·3158	−0·1995	2·303	0·3322	−0·4533
17·60	2·249	0·3493	−0·2467	2·228	0·3410	−0·1478	2·306	0·3606	−0·3997
19·08	2·193	0·3791	−0·1496	2·175	0·3748	−0·0775	2·268	0·3964	−0·3447
20·58	2·174	0·4113	−0·0800	2·163	0·4096	−0·0542	2·263	0·4352	−0·3328
				Round nacelles parallel to body					
−2·86	0·153	0·1341	−0·2746	−0·026	0·1435	0·2849	0·053	0·1340	+0·0304
−1·20	0·517	0·1250	−0·3957	+0·324	0·1295	0·1371	0·428	0·1234	−0·1266
+0·45	0·841	0·1342	−0·4858	0·685	0·1347	+0·0139	0·781	0·1317	−0·2517
2·04	1·038	0·1459	−0·5003	0·901	0·1439	−0·0377	0·998	0·1430	−0·2981
3·62	1·207	0·1597	−0·5025	1·081	0·1545	−0·0761	1·160	0·1550	−0·3312
5·18	1·348	0·1722	−0·4970	1·238	0·1646	−0·0989	1·323	0·1678	−0·3588
6·74	1·481	0·1872	−0·4831	1·389	0·1782	−0·1326	1·471	0·1841	−0·3934
8·30	1·606	0·2022	−0·4676	1·531	0·1929	−0·1573	1·614	0·2026	−0·4166
9·86	1·735	0·2227	−0·4424	1·669	0·2138	−0·1807	1·757	0·2234	−0·4397
11·42	1·869	0·2459	−0·4259	1·815	0·2377	−0·2033	1·888	0·2497	−0·4559
12·98	1·992	0·2689	−0·4019	1·951	0·2617	−0·2231	2·030	0·2773	−0·4752
14·53	2·100	0·2932	−0·3771	2·079	0·2886	−0·2439	2·161	0·3092	−0·4945
16·07	2·200	0·3202	−0·3450	2·200	0·3199	−0·2576	2·274	0·3358	−0·5095
17·58	2·199	0·3442	−0·2625	2·221	0·3454	−0·2181	2·289	0·3659	−0·4605
19·07	2·154	0·3733	−0·1722	2·165	0·3772	−0·1482	2·250	0·3973	−0·4037
20·56	2·134	0·4070	−0·1120	2·165	0·4125	−0·1322	2·251	0·4414	−0·4020

	No tailplane			$\eta_B = -10$ degrees			$\eta_B = +5$ degrees		
α_{deg}	C_L	C_D	C_m	C_L	C_D	C_m	C_L	C_D	C_m
				No nacelles					
−2·79	0·305	0·1166	−0·3485				0·226	0·1157	−0·1968
−1·10	0·721	0·1152	−0·4873				0·672	0·1127	−0·4146
+0·51	0·972	0·1252	−0·5289				0·952	0·1235	−0·5036
2·09	1·149	0·1392	−0·5289				1·149	0·1382	−0·5478
3·66	1·298	0·1532	−0·5251				1·310	0·1532	−0·5724
5·22	1·430	0·1664	−0·5078				1·459	0·1688	−0·5959
6·78	1·562	0·1829	−0·4951				1·599	0·1869	−0·6215
8·34	1·683	0·2011	−0·4722				1·742	0·2067	−0·6427
9·89	1·805	0·2242	−0·4487						
11·45	1·920	0·2465	−0·4179	1·767	0·2288	0·1151			
13·00	2·045	0·2684	−0·3920	1·897	0·2514	0·0779			
14·56	2·159	0·2972	−0·3608	2·017	0·2753	0·0628			
16·10	2·255	0·3248	−0·3342	2·128	0·3029	0·0549			
17·60	2·249	0·3493	−0·2467	2·155	0·3262	0·1012			
19·08	2·193	0·3791	−0·1496	2·084	0·3527	0·1749			
20·58	2·174	0·4113	−0·0800	2·067	0·3846	0·2065			
				Round nacelles parallel to body					
11·42	1·869	0·2459	−0·4259	1·727	0·2316	0·0547			
12·98	1·992	0·2689	−0·4019	1·863	0·2540	0·0307			
14·53	2·100	0·2932	−0·3771	1·993	0·2794	+0·0015			
16·07	2·200	0·3202	−0·3450	2·102	0·3051	−0·0116			
17·58	2·199	0·3442	−0·2625	2·137	0·3289	+0·0230			
19·07	2·154	0·3733	−0·1722	2·091	0·3593	0·1001			
20·56	2·134	0·4070	−0·1120	2·090	0·3954	0·1224			

TABLE 7

High Wing, No Tailplane and Nacelles with Fillet in Wing Body Junction

	Slats 0 degrees Flaps 0 degrees		
α_{deg}	C_L	C_D	C_m
−1·43	(−0·060)	0·0239	−0·1040
+0·08	+0·038	0·0223	−0·0908
1·64	0·155	0·0225	−0·0756
3·19	0·267	0·0249	−0·0562
4·74	0·374	0·0288	−0·0360
6·29	0·489	0·0338	−0·0184
7·84	0·593	0·0404	+0·0026
9·38	0·691	0·0600	0·0266
10·91	0·752	0·0959	0·0660
12·43	0·788	0·1262	0·1037
13·94	0·795	0·1665	0·1377
15·45	0·811	0·2028	0·1570
16·96	0·834	0·2366	0·1726

	Slats 25 degrees Flaps 25 degrees		
α_{deg}	C_L	C_D	C_m
−2·92	0·024	0·0989	−0·2490
−1·30	0·288	0·0825	−0·3158
+0·35	0·623	0·0768	−0·3943
1·95	0·832	0·0844	−0·4111
3·53	1·010	0·0959	−0·4094
5·10	1·169	0·1082	−0·4035
6·66	1·304	0·1211	−0·3890
8·23	1·454	0·1379	−0·3684
9·78	1·562	0·1516	−0·3448
11·35	1·710	0·1742	−0·3186
12·91	1·843	0·1977	−0·2955
14·46	1·966	0·2220	−0·2697
16·01	2·063	0·2463	−0·2431
17·55	2·139	0·2729	−0·1938
19·04	2·113	0·2994	−0·1091
20·54	2·107	0·3391	−0·0349
22·04	2·076	0·3697	+0·0218

	Slats 25 degrees Flaps 10 degrees		
α_{deg}	C_L	C_D	C_m
−2·96	(−0·112)	0·0949	−0·2012
−1·45	−0·047	0·0797	−0·1775
+0·12	+0·109	0·0652	−0·1866
1·71	0·311	0·0564	−0·2038
3·29	0·488	0·0553	−0·2036
4·86	0·635	0·0597	−0·1918
6·42	0·781	0·0675	−0·1807
7·99	0·932	0·0768	−0·1686
9·55	1·067	0·0873	−0·1543
11·12	1·214	0·1008	−0·1369
12·68	1·353	0·1173	−0·1167
14·24	1·485	0·1370	−0·0944
15·80	1·615	0·1582	−0·0741
17·36	1·731	0·1818	−0·0503
18·90	1·828	0·2077	−0·0200
20·43	1·874	0·2392	+0·0366
21·93	1·868	0·2705	0·0925
23·43	1·859	0·3052	0·1353

	Slats 25 degrees Flaps 40 degrees		
α_{deg}	C_L	C_D	C_m
−2·82	0·252	0·1132	−0·3341
−1·09	0·761	0·1115	−0·5076
+0·52	0·999	0·1232	−0·5424
2·10	1·173	0·1370	−0·5450
3·68	1·335	0·1529	−0·5314
5·24	1·462	0·1668	−0·5120
6·79	1·590	0·1831	−0·4887
8·35	1·704	0·2004	−0·4595
9·91	1·837	0·2216	−0·4304
11·46	1·949	0·2431	−0·4071
13·02	2·083	0·2694	−0·3827
14·57	2·196	0·2955	−0·3544
16·11	2·286	0·3209	−0·3107
17·61	2·273	0·3483	−0·2184
19·10	2·227	0·3789	−0·1324
20·59	2·197	0·4164	−0·0645

Note: Values in brackets deduced

TABLE 8

Low Wing with Slats and Flaps 0 Degrees

	No tailplane			$\eta_B = -5$ degrees			$\eta_B = 0$ degrees		
α_{deg}	C_L	C_D	C_m	C_L	C_D	C_m	C_L	C_D	C_m
				No nacelles					
−3·18	−0·166	0·0257	−0·0874	−0·341	0·0377	0·4297	−0·203	0·0528	0·1144
−1·62	−0·037	0·0217	−0·0858	−0·187	0·0305	0·3671	−0·072	0·0431	0·0529
−0·06	+0·081	0·0208	−0·0768	−0·042	0·0264	0·3176	+0·063	0·0375	+0·0026
+1·49	0·193	0·0218	−0·0634	+0·076	0·0257	0·2804	0·229	0·0371	−0·0480
3·04	0·301	0·0248	−0·0492	0·201	0·0270	0·2363	0·341	0·0384	−0·0820
4·59	0·413	0·0288	−0·0392	0·328	0·0297	0·1925	0·435	0·0424	−0·1124
6·14	0·525	0·0344	−0·0285	0·468	0·0348	0·1447	0·585	0·0485	−0·1523
7·69	0·629	0·0423	−0·0151	0·588	0·0414	0·1120	0·680	0·0554	−0·1746
9·23	0·726	0·0676	+0·0004	0·701	0·0672	0·0808	0·792	0·0842	−0·2039
10·76	0·781	0·1009	0·0300	0·762	0·1001	0·0751	0·888	0·1194	−0·2190
12·27	0·813	0·1356	0·0652	0·800	0·1373	0·0858	0·905	0·1569	−0·1948
13·78	0·819	0·1754	0·0858	0·807	0·1761	0·1017	0·906	0·1967	−0·1855
15·29	0·829	0·2086	0·1002	0·837	0·2095	+0·0609	0·941	0·2347	−0·2316
16·79	0·839	0·2411	0·1110	0·868	0·2477	−0·0112	0·969	0·2711	−0·2965
18·29	0·822	0·2690	0·1077	0·886	0·2694	−0·0672			
19·78	0·808	0·2991	0·0971						
				Round nacelles parallel to body					
−3·21	−0·237	0·0396	−0·0244	(−0·265)	0·0563	0·3993	−0·285	0·0428	0·1143
−1·65	−0·106	0·0343	−0·0314	−0·233	0·0477	0·3596	−0·127	0·0359	+0·0461
−0·09	+0·021	0·0315	−0·0309	−0·094	0·0424	0·3069	+0·012	0·0327	−0·0065
+1·46	0·142	0·0320	−0·0277	+0·045	0·0404	0·2568	0·149	0·0330	−0·0518
3·02	0·258	0·0337	−0·0263	0·174	0·0415	0·2086	0·281	0·0357	−0·0920
4·57	0·372	0·0376	−0·0240	0·306	0·0462	0·1597	0·417	0·0405	−0·1340
6·12	0·492	0·0426	−0·0231	0·436	0·0480	0·1164	0·546	0·0476	−0·1730
7·68	0·604	0·0503	−0·0171	0·571	0·0562	0·0749	0·672	0·0566	−0·2060
9·22	0·709	0·0744	−0·0123	0·693	0·0839	0·0392	0·792	0·0845	−0·2369
10·75	0·768	0·1076	+0·0149	0·761	0·1182	0·0334	0·853	0·1271	−0·2501
12·27	0·808	0·1407	0·0452	0·794	0·1506	0·0529	0·898	0·1609	−0·2333
13·78	0·813	0·1800	0·0710	0·808	0·1887	0·0706	0·900	0·2076	−0·2185
15·29	0·829	0·2134	0·0862	0·840	0·2240	+0·0321	0·935	0·2421	−0·2572
16·80	0·840	0·2468	0·0964	0·881	0·2618	−0·0349	0·960	0·2797	−0·3193
18·30	0·838	0·2762	0·0990	0·899	0·2823	−0·0848	0·984	0·3195	−0·4062
19·79				0·893	0·2935	−0·1230			
				Flat nacelles parallel to body					
−3·22	−0·256	0·0421	−0·0352	−0·390	0·0531	0·3666	−0·284	0·0437	+0·0719
−1·65	−0·108	0·0358	−0·0523	−0·234	0·0439	0·3163	−0·125	0·0369	+0·0142
−0·09	+0·024	0·0325	−0·0643	−0·084	0·0385	0·2693	+0·004	0·0342	−0·0244
+1·47	0·152	0·0326	−0·0662	+0·057	0·0358	0·2223	0·155	0·0338	−0·0692
3·02	0·270	0·0349	−0·0614	0·185	0·0366	0·2038	0·283	0·0363	−0·1010
4·58	0·390	0·0375	−0·0565	0·321	0·0386	0·1572	0·418	0·0408	−0·1395
6·13	0·515	0·0431	−0·0559	0·461	0·0429	0·1221	0·547	0·0470	−0·1726
7·69	0·627	0·0509	−0·0475	0·597	0·0507	0·0787	0·682	0·0575	−0·2143
9·24	0·735	0·0740	−0·0418	0·709	0·0731	0·0498	0·796	0·0812	−0·2421

TABLE 8 (continued)

	No tailplane			$\eta_B = -5$ degrees			$\eta_B = 0$ degrees		
α_{deg}	C_L	C_D	C_m	C_L	C_D	C_m	C_L	C_D	C_m
				Flat nacelles parallel to body (concluded)					
10·77	0·797	0·1092	−0·0148	0·787	0·1093	0·0365	0·875	0·1212	−0·2538
12·29	0·838	0·1431	0·0172	0·831	0·1421	0·0435	0·919	0·1541	−0·2499
13·79	0·834	0·1826	0·0476	0·835	0·1843	0·0674	0·925	0·1991	−0·2297
15·30	0·852	0·2178	0·0651	0·865	0·2197	+0·0356	0·954	0·2395	−0·2706
16·81	0·866	0·2490	0·0737	0·896	0·2554	−0·0151	0·988	0·2784	−0·3243
18·31	0·861	0·2788	0·0742	0·917	0·2867	−0·1255	1·010	0·3154	−0·4252
19·80	0·830	0·2970	0·0705	0·934	0·3135	−0·2700	1·014	0·3455	−0·5651
				Flat nacelles 4·2 degrees nose down relative to body					
−3·25	−0·326	0·0478	0·0342	−0·435	0·0574	0·3634	−0·340	0·0488	+0·0754
−1·68	−0·173	0·0404	0·0125	−0·273	0·0472	0·3065	−0·179	0·0405	+0·0180
−0·12	−0·036	0·0360	+0·0020	−0·127	0·0412	0·2601	−0·026	0·0360	−0·0354
+1·44	+0·093	0·0345	−0·0055	+0·021	0·0379	0·2174	+0·117	0·0341	−0·0782
3·00	0·216	0·0360	−0·0029	0·148	0·0379	0·1853	0·251	0·0368	−0·1118
4·55	0·340	0·0392	−0·0070	0·292	0·0395	0·1525	0·386	0·0404	−0·1444
6·11	0·468	0·0431	−0·0119	0·432	0·0436	0·1122	0·520	0·0462	−0·1828
7·67	0·589	0·0501	−0·0091	0·567	0·0497	0·0752	0·658	0·0545	−0·2157
9·22	0·698	0·0714	−0·0028	0·683	0·0706	0·0437	0·771	0·0785	−0·2401
10·75	0·763	0·1058	+0·0212	0·760	0·1065	0·0352	0·846	0·1154	−0·2472
12·27	0·804	0·1379	0·0521	0·811	0·1392	0·0418	0·895	0·1515	−0·2384
13·77	0·805	0·1772	0·0870	0·814	0·1798	0·0701	0·899	0·1918	−0·2147
15·28	0·816	0·2092	0·1095	0·841	0·2140	+0·0403	0·923	0·2285	−0·2481
16·79	0·828	0·2407	0·1203	0·879	0·2486	−0·0251	0·955	0·2652	−0·3176
18·29	0·821	0·2664	0·1209	0·899	0·2802	−0·1371	0·968	0·2963	−0·4252
19·77	0·784	0·2809	0·1103	0·912	0·3068	−0·2876	0·994	0·3340	−0·5521
				Flat nacelles 8·1 degrees nose down relative to body					
−3·28	−0·397	0·0555	0·0988	−0·489	0·0636	0·3669	−0·381	0·0531	+0·0633
−1·71	−0·246	0·0470	0·0802	−0·320	0·0515	0·3041	−0·222	0·0441	+0·0117
−0·15	−0·106	0·0411	0·0669	−0·173	0·0440	0·2580	−0·064	0·0388	−0·0415
+1·41	+0·028	0·0384	0·0649	−0·024	0·0397	0·2204	+0·081	0·0359	−0·0863
2·97	0·149	0·0381	0·0620	+0·105	0·0388	0·1882	0·216	0·0372	−0·1210
4·52	0·274	0·0395	0·0561	0·251	0·0398	0·1443	0·351	0·0406	−0·1594
6·09	0·407	0·0430	0·0509	0·386	0·0428	0·1075	0·493	0·0464	−0·1976
7·64	0·528	0·0486	0·0489	0·528	0·0486	0·0667	0·624	0·0541	−0·2288
9·19	0·644	0·0667	0·0495	0·649	0·0676	0·0325	0·744	0·0763	−0·2526
10·73	0·715	0·1006	0·0682	0·731	0·1027	0·0275	0·821	0·1118	−0·2554
12·25	0·761	0·1306	0·0946	0·781	0·1311	0·0343	0·872	0·1453	−0·2485
13·76	0·767	0·1698	0·1279	0·795	0·1728	0·0681	0·878	0·1873	−0·2222
15·26	0·776	0·2011	0·1489	0·821	0·2080	+0·0348	0·905	0·2246	−0·2598
16·77	0·793	0·2314	0·1615	0·861	0·2420	−0·0306	0·942	0·2607	−0·3231
18·28	0·792	0·2578	0·1620	0·880	0·2730	−0·1336	0·964	0·2981	−0·4267
19·76	0·764	0·2827	0·1180	0·895	0·3051	−0·2653	0·971	0·3365	−0·5390

TABLE 8 (concluded)

α_{deg}	No tailplane			$\eta_B = -5$ degrees			$\eta_B = 0$ degrees		
	C_L	C_D	C_m	C_L	C_D	C_m	C_L	C_D	C_m
	Flat nacelles with auxiliary surfaces parallel to body								
−3·23	−0·286	0·0437	−0·0059	−0·402	0·0556	0·3696	−0·298	0·0453	+0·0721
−1·65	−0·118	0·0367	−0·0458	−0·243	0·0463	0·3229	−0·136	0·0388	+0·0177
−0·09	+0·031	0·0332	−0·0650	−0·082	0·0398	0·2665	+0·027	0·0351	−0·0364
+1·47	0·155	0·0331	−0·0697	+0·039	0·0381	0·2374	0·165	0·0353	−0·0796
3·03	0·278	0·0354	−0·0746	0·186	0·0383	0·1939	0·288	0·0379	−0·1080
4·58	0·401	0·0394	−0·0743	0·318	0·0410	0·1594	0·434	0·0434	−0·1531
6·13	0·513	0·0446	−0·0706	0·464	0·0457	0·1123	0·552	0·0499	−0·1852
7·69	0·644	0·0534	−0·0715	0·598	0·0526	0·0702	0·684	0·0596	−0·2237
9·24	0·750	0·0775	−0·0680	0·714	0·0769	0·0430	0·812	0·0886	−0·2630
10·77	0·812	0·1127	−0·0415	0·793	0·1135	0·0253	0·887	0·1263	−0·2745
12·29	0·852	0·1482	−0·0102	0·837	0·1460	0·0335	0·930	0·1638	−0·2702
13·80	0·853	0·1898	+0·0221	0·842	0·1861	0·0518	0·935	0·2040	−0·2509
15·30	0·860	0·2199	0·0427	0·868	0·1848	+0·0301	0·963	0·2462	−0·2883
16·81	0·875	0·2549	0·0493	0·901	0·1930	−0·0276	0·991	0·2842	−0·3462
18·31	0·871	0·2825	0·0544	0·924	0·2079	−0·1174	0·997	0·3167	−0·4208
19·80	0·850	0·2950	0·0582	0·932	0·2242	−0·2552	1·018	0·3516	−0·5774
	Flat nacelles with auxiliary surfaces 8·1 degrees nose down relative to body								
−3·29	−0·420	0·0601	0·1454	−0·492	0·0661	0·3852	−0·377	0·0539	+0·0674
−1·71	−0·251	0·0487	0·1017	−0·326	0·0537	0·3265	−0·216	0·0447	+0·0144
−0·15	−0·106	0·0421	0·0842	−0·166	0·0457	0·2697	−0·062	0·0391	−0·0394
+1·41	+0·023	0·0391	0·0760	−0·024	0·0413	0·2256	+0·088	0·0369	−0·0867
2·97	0·150	0·0386	0·0675	+0·111	0·0401	0·1868	0·229	0·0385	−0·1283
4·53	0·287	0·0399	0·0568	0·253	0·0409	0·1446	0·362	0·0417	−0·1652
6·09	0·413	0·0429	0·0484	0·402	0·0444	0·0986	0·497	0·0472	
7·64	0·537	0·0486	0·0410	0·532	0·0501	0·0607	0·637	0·0555	−0·2416
9·20	0·647	0·0656	0·0417	0·659	0·0696	0·0262	0·761	0·0789	−0·2680
10·73	0·725	0·1024	0·0606	0·737	0·1048	0·0176	0·836	0·1154	−0·2751
12·26	0·771	0·1321	0·0832	0·789	0·1353	0·0269	0·888	0·1519	−0·2637
13·76	0·784	0·1718	0·1153	0·796	0·1777	0·0587	0·891	0·1922	−0·2427
15·27	0·783	0·2048	0·1453	0·821	0·2102	+0·0270	0·917	0·2280	−0·2735
16·78	0·804	0·2350	0·1563	0·863	0·2440	−0·0381	0·955	0·2649	−0·3380
18·28	0·800	0·2602	0·1508	0·887	0·2763	−0·1405	0·985	0·3034	−0·4443
19·78	0·797	0·2889	0·0528	0·918	0·3115	−0·2896	1·012	0·3459	−0·5831

TABLE 9

Low Wing with Slats 25 Degrees and Flaps 10 Degrees

	No tailplane			$\eta_B = -5$ degrees			$\eta_B = 0$ degrees		
α_{deg}	C_L	C_D	C_m	C_L	C_D	C_m	C_L	C_D	C_m
				No nacelles					
−3·14	−0·079	0·0893	−0·1878	−0·243	0·1014	0·3398	−0·162	0·0931	+0·0507
−1·59	+0·011	0·0781	−0·1711	−0·152	0·0858	0·3377	−0·061	0·0796	+0·0219
−0·02	0·173	0·0650	−0·1836	+0·022	0·0746	0·2840	+0·113	0·0649	−0·0418
+1·56	0·855	0·0569	−0·1975	0·229	0·0595	0·2118	0·326	0·0562	−0·1136
3·14	0·527	0·0576	−0·2013	0·412	0·0576	0·1594	0·507	0·0571	−0·1612
4·71	0·674	0·0627	−0·1972	0·579	0·0617	0·1128	0·666	0·0632	−0·2007
6·27	0·819	0·0710	−0·1957	0·741	0·0696	0·0634	0·830	0·0730	−0·2422
7·84	0·968	0·0799	−0·1908	0·911	0·0779	+0·0102	0·990	0·0828	−0·2832
9·41	1·115	0·0910	−0·1872	1·075	0·0896	−0·0371	1·158	0·0961	−0·3212
10·97	1·254	0·1054	−0·1795	1·227	0·1044	−0·0719	1·320	0·1141	−0·3561
12·53	1·389	0·1224	−0·1692	1·381	0·1224	−0·1097	1·473	0·1347	−0·3900
14·09	1·520	0·1420	−0·1566	1·521	0·1433	−0·1411	1·619	0·1587	−0·4214
15·65	1·637	0·1630	−0·1499	1·651	0·1660	−0·1674	1·755	0·1843	−0·4522
17·20	1·750	0·1856	−0·1260	1·789	0·1932	−0·1971	1·882	0·2126	−0·4740
18·74	1·833	0·2119	−0·0948	1·880	0·2234	−0·2019	1·968	0·2431	−0·4796
20·26	1·861	0·2400	−0·0415	1·925	0·2559	−0·1880	2·020	0·2784	−0·4688
21·76	1·852	0·2700	+0·0035	1·920	0·2943	−0·1899	2·012	0·3168	−0·4741
23·26	1·839	0·3044	+0·0377	1·932	0·3352	−0·2233	2·030	0·3650	−0·5290
				Round nacelles parallel to body					
−3·17	−0·148	0·1059	−0·1250	−0·295	0·1176	0·3244	−0·200	0·1098	+0·0274
−1·63	−0·063	0·0929	−0·1103	−0·203	0·1005	0·3146	−0·102	0·0963	+0·0059
−0·06	+0·094	0·0783	−0·1287	−0·032	0·0834	0·2558	+0·079	0·0792	−0·0626
+1·54	0·297	0·0678	−0·1565	−0·182	0·0706	0·1834	0·287	0·0690	−0·1337
3·11	0·469	0·0658	−0·1680	+0·370	0·0674	0·1254	0·471	0·0679	−0·1849
4·68	0·621	0·0701	−0·1736	0·542	0·0706	0·0774	0·649	0·0735	−0·2290
6·25	0·776	0·0772	−0·1785	0·707	0·0766	+0·0257	0·802	0·0816	−0·2691
7·83	0·933	0·0871	−0·1828	0·882	0·0863	−0·0285	0·976	0·0933	−0·3174
9·40	1·090	0·0989	−0·1869	1·043	0·0970	−0·0711	1·139	0·1067	−0·3575
10·96	1·226	0·1126	−0·1859	1·212	0·1123	−0·1126	1·310	0·1238	−0·3995
12·53	1·377	0·1310	−0·1875	1·364	0·1304	−0·1500	1·465	0·1447	−0·4376
14·09	1·512	0·1519	−0·1842	1·519	0·1531	−0·1875	1·607	0·1683	−0·4615
15·65	1·644	0·1733	−0·1787	1·668	0·1785	−0·2114	1·750	0·1946	−0·4860
17·20	1·760	0·1970	−0·1693	1·794	0·2057	−0·2356	1·875	0·2223	−0·5040
18·74	1·843	0·2237	−0·1411	1·892	0·2325	−0·2476	1·973	0·2523	−0·5181
20·27	1·895	0·2552	−0·1029	1·941	0·2683	−0·2700	2·001	0·2869	−0·4876
21·76	1·870	0·2850	−0·0543	1·946	0·3041	−0·2263			
23·27	1·879	0·3235	−0·0150	1·941	0·3465	−0·2484			

TABLE 9 (continued)

	No tailplane			$\eta_B = -5$ degrees			$\eta_B = 0$ degrees		
α_{deg}	C_L	C_D	C_m	C_L	C_D	C_m	C_L	C_D	C_m
				Flat nacelles parallel to body					
−3·18	−0·174	0·1080	−0·1300	−0·289	0·1189	0·2535	−0·214	0·1112	−0·0166
−1·64	−0·083	0·0928	−0·1200	−0·204	0·1013	0·2486	−0·119	0·0947	−0·0275
−0·07	+0·067	0·0783	−0·1405	−0·036	0·0837	0·1955	+0·056	0·0794	−0·0877
+1·52	0·264	0·0670	−0·1682	+0·178	0·0702	0·1314	0·266	0·0678	−0·1528
3·11	0·456	0·0645	−0·1893	0·355	0·0662	0·0898	0·453	0·0653	−0·1967
4·68	0·608	0·0683	−0·1955	0·526	0·0679	0·0530	0·618	0·0705	−0·2303
6·25	0·761	0·0758	−0·1969	0·694	0·0745	+0·0113	0·788	0·0785	−0·2710
7·82	0·915	0·0848	−0·2031	0·858	0·0831	−0·0328	0·966	0·0893	−0·3202
9·39	1·065	0·0954	−0·2062	1·032	0·0942	−0·0833	1·141	0·1036	−0·3737
10·96	1·220	0·1101	−0·2103	1·191	0·1086	−0·1228	1·294	0·1195	−0·4086
12·52	1·365	0·1269	−0·2088	1·357	0·1285	−0·1592	1·456	0·1406	−0·4457
14·08	1·500	0·1477	−0·2059	1·502	0·1490	−0·1876	1·599	0·1633	−0·4713
15·64	1·626	0·1683	−0·2065	1·648	0·1733	−0·2183	1·742	0·1891	−0·4969
17·20	1·747			1·775	0·1998	−0·2440	1·871	0·2179	−0·5227
18·74	1·834	0·2214	−0·1823	1·883	0·2307	−0·2524	1·971	0·2503	−0·5310
20·27	1·884	0·2548	−0·1402	1·925	0·2631	−0·2421	2·018	0·2857	−0·5176
21·77	1·885	0·2858	−0·1007	1·937	0·3020	−0·2381	2·029	0·3256	−0·5218
23·28	1·881	0·3242	−0·0683	1·955	0·3427	−0·2650	2·047	0·3703	−0·5606
				Flat nacelles 4·2 degrees nose down relative to body					
−3·20	−0·218	0·1229	−0·0794	−0·334	0·1247	0·2472	−0·249	0·1154	−0·0341
−1·66	−0·139	0·1033	−0·0627	−0·249	0·1052	0·2452	−0·159	0·0980	−0·0367
−0·10	+0·003	0·0874	−0·0765	−0·098	0·0877	0·2044	+0·011	0·0813	−0·0904
+1·49	0·200	0·0739	−0·1088	+0·111	0·0734	0·1405	0·213	0·0686	−0·1520
3·08	0·386	0·0650	−0·1302	0·313	0·0666	0·0893	0·407	0·0659	−0·1999
4·65	0·539	0·0671	−0·1374	0·482	0·0677	0·0515	0·585	0·0691	−0·2409
6·22	0·703	0·0728	−0·1476	0·647	0·0728	+0·0096	0·746	0·0761	−0·2794
7·79	0·866	0·0813	−0·1596	0·834	0·0812	−0·0438	0·921	0·0866	−0·3243
9·36	1·017	0·0918	−0·1694	1·008	0·0916	−0·0908	1·091	0·0993	−0·3690
10·94	1·179	0·1057	−0·1753	1·167	0·1055	−0·1358	1·257	0·1152	−0·4116
12·50	1·320	0·1228	−0·1703	1·323	0·1226	−0·1623	1·419	0·1349	−0·4441
14·06	1·452	0·1408	−0·1664	1·467	0·1443	−0·1923	1·569	0·1584	−0·4719
15·63	1·591	0·1630	−0·1636	1·616	0·1679	−0·2219	1·707	0·1835	−0·4933
17·18	1·713	0·1869	−0·1603	1·749	0·1930	−0·2440	1·839	0·2118	−0·5174
18·73	1·805	0·2148	−0·1421	1·857	0·2253	−0·2552	1·934	0·2429	−0·5229
20·25	1·857	0·2458	−0·1092	1·912	0·2574	−0·2477	1·996	0·2798	−0·5210
21·76	1·853	0·2762	−0·0682	1·923	0·2939	−0·2423	2·004	0·3193	−0·5328
23·26	1·853	0·3131	−0·0311	1·938	0·3338	−0·2651	2·034	0·3692	−0·5830
				Flat nacelles 8·1 degrees nose down relative to body					
−3·24	−0·296	0·1240	−0·0088	−0·383	0·1355	0·2407	−0·278	0·1189	−0·0605
−1·70	−0·227	0·1066	+0·0164	−0·288	0·1113	0·2334	−0·203	0·1029	−0·0566
−0·14	−0·093	0·0901	+0·0013	−0·152	0·0933	0·1985	−0·054	0·0866	−0·0915
+1·45	+0·107	0·0742	−0·0334	+0·055	0·0759	0·1364	+0·159	0·0718	−0·1600
3·03	0·295	0·0682	−0·0578	0·257	0·0685	0·0869	0·354	0·0664	−0·2122
4·61	0·459	0·0678	−0·0658	0·437	0·0688	+0·0379	0·531	0·0691	−0·2599
6·18	0·617	0·0727	−0·0746	0·603	0·0726	−0·0046	0·705	0·0755	−0·3036
7·76	0·784	0·0796	−0·0894	0·777	0·0799	−0·0542	0·880	0·0851	−0·3499
9·33	0·948	0·0889	−0·1102	0·951	0·0895	−0·0985	1·052	0·0970	−0·3911

TABLE 9 (continued)

	No tailplane			$\eta_B = -5$ degrees			$\eta_B = 0$ degrees		
α_{deg}	C_L	C_D	C_m	C_L	C_D	C_m	C_L	C_D	C_m
			Flat nacelles 8·1 degrees nose down relative to body (concluded)						
10·91	1·109	0·1015	−0·1178	1·134	0·1036	−0·1464	1·215	0·1119	−0·4243
12·47	1·248	0·1156	−0·1244	1·287	0·1195	−0·1773	1·378	0·1308	−0·4539
14·04	1·395	0·1346	−0·1207	1·438	0·1402	−0·2038	1·526	0·1529	−0·4827
15·60	1·528	0·1554	−0·1188	1·586	0·1635	−0·2325	1·671	0·1775	−0·5008
17·15	1·652	0·1770	−0·1236	1·695	0·1841	−0·2457	1·804	0·2046	−0·5235
18·70	1·748	0·2031	−0·1036	1·806	0·2144	−0·2582	1·911	0·2365	−0·5344
20·23	1·811	0·2353	−0·0722	1·871	0·2487	−0·2499	1·968	0·2711	−0·5340
21·74	1·820	0·2678	−0·0272	1·878	0·2825	−0·2432	1·981	0·3104	−0·5399
23·25	1·820	0·3013	+0·0059	1·906	0·3254	−0·2710	2·018	0·3571	−0·5828
			Flat nacelles with auxiliary surfaces parallel to body						
−3·18	−0·171	0·1093	−0·1395	−0·291	0·1195	0·2532	−0·204	0·1120	−0·0229
−1·64	−0·084	0·0939	−0·1227	−0·203	0·1031	0·2498	−0·108	0·0962	−0·0369
−0·07	+0·074	0·0787	−0·1467	−0·034	0·0845	0·1938	+0·065	0·0803	−0·0966
+1·53	0·275	0·0682	−0·1808	+0·169	0·0720	0·1359	0·264	0·0698	−0·1588
3·11	0·459	0·0659	−0·1993	0·367	0·0680	0·0838	0·459	0·0675	−0·2095
4·68	0·607	0·0695	−0·2060	0·543	0·0709	0·0445	0·626	0·0723	−0·2446
6·25	0·758	0·0768	−0·2102	0·704	0·0779	+0·0060	0·804	0·0813	−0·2995
7·82	0·918	0·0869	−0·2168	0·872	0·0860	−0·0428	0·961	0·0919	−0·3351
9·39	1·072	0·0983	−0·2237	1·035	0·0972	−0·0915	1·129	0·1057	−0·3877
10·96	1·224	0·1135	−0·2281	1·206	0·1128	−0·1363	1·303	0·1241	−0·4338
12·52	1·363	0·1299	−0·2314	1·368	0·1324	−0·1732	1·467	0·1457	−0·4671
14·09	1·517	0·1519	−0·2370	1·516	0·1552	−0·2084	1·617	0·1708	−0·5014
15·65	1·638	0·1737	−0·2450	1·659	0·1798	−0·2393	1·758	0·1984	−0·5255
17·21	1·766	0·1998	−0·2321	1·793	0·2078	−0·2632	1·887	0·2262	−0·5439
18·75	1·855	0·2288	−0·2180	1·890	0·2396	−0·2707	1·982	0·2594	−0·5568
20·27	1·901	0·2611	−0·1779	1·940	0·2734	−0·2599	2·035	0·2982	−0·5486
21·78	1·899	0·2940	−0·1337	1·943	0·3112	−0·2537	2·038	0·3347	−0·5458
23·28	1·897	0·3321	−0·0942	1·966	0·3537	−0·2764	2·059	0·3856	−0·5894
			Flat nacelles with auxiliary surfaces 8·1 degrees nose down relative to body						
−3·24	−0·312	0·1279	0·0126	−0·385	0·1343	0·2515	−0·291	0·1233	−0·0409
−1·71	−0·238	0·1091	0·0294	−0·304	0·1149	0·2557	−0·207	0·1044	−0·0470
−0·14	−0·089	0·0899	+0·0110	−0·159	0·0950	0·2150	−0·064	0·0883	−0·0875
+1·45	+0·109	0·0748	−0·0232	+0·068	0·0763	0·1427	+0·154	0·0724	−0·1588
3·03	0·288	0·0687	−0·0500	0·239	0·0699	0·0942	0·353	0·0669	−0·2154
4·61	0·459	0·0694	−0·0610	0·429	0·0708	+0·0438	0·531	0·0694	−0·2624
6·18	0·614	0·0731	−0·0704	0·599	0·0735	−0·0061	0·702	0·0764	−0·3126
7·76	0·780	0·0804	−0·0886	0·776	0·0805	−0·0604	0·880	0·0859	−0·3627
9·33	0·947	0·0901	−0·1068	0·946	0·0902	−0·1111	1·056	0·0981	−0·4099
10·90	1·100	0·1021	−0·1174	1·122	0·1036	−0·1474	1·227	0·1135	−0·4512
12·47	1·257	0·1183	−0·1262	1·279	0·1208	−0·1860	1·392	0·1336	−0·4836
14·04	1·398	0·1368	−0·1288	1·431	0·1410	−0·2157	1·542	0·1561	−0·5052
15·60	1·540	0·1592	−0·1289	1·585	0·1663	−0·2490	1·681	0·1808	−0·5321
17·16	1·669	0·1816	−0·1321	1·719	0·1903	−0·2738	1·824	0·2093	−0·5567
18·71	1·762	0·2078	−0·1174	1·814	0·2157	−0·2783	1·929	0·2427	−0·5713
20·23	1·811	0·2375	−0·0840	1·886	0·2548	−0·2762	1·991	0·2783	−0·5725
21·74	1·818	0·2709	−0·0445	1·890	0·2871	−0·2664	2·005	0·3194	−0·5780
23·25	1·823	0·3070	−0·0126	1·918	0·3299	−0·2905	2·010	0·3632	−0·6150

TABLE 9 (continued)

	No tailplane			$\eta_B = -10$ degrees			$\eta_B = -7{\cdot}5$ degrees		
α_{deg}	C_L	C_D	C_m	C_L	C_D	C_m	C_L	C_D	C_m
				No nacelles					
6·27	0·819	0·0710	−0·1957	0·648	0·0684	0·3541	0·690	0·0681	0·2222
7·84	0·968	0·0799	−0·1908	0·808	0·0761	0·3158	0·854	0·0766	0·1726
9·41	1·115	0·0910	−0·1872	0·970	0·0857	0·2704	1·028	0·0877	0·1236
10·97	1·254	0·1054	−0·1795	1·113	0·0991	0·2350	1·172	0·1008	0·0813
12·53	1·389	0·1224	−0·1692	1·295	0·1162	0·1892	1·332	0·1185	0·0422
14·09	1·520	0·1420	−0·1566	1·433	0·1350	0·1541	1·474	0·1391	+0·0017
15·65	1·637	0·1630	−0·1499	1·567	0·1557	0·1181	1·615	0·1612	−0·0329
17·20	1·750	0·1856	−0·1260	1·696	0·1798	0·0813	1·742	0·1859	−0·0587
18·74	1·833	0·2119	−0·0948	1·801	0·2088	0·0648	1·836	0·2139	−0·0702
20·26	1·861	0·2400	−0·0415	1·837	0·2387	0·0819	1·892	0·2456	−0·0577
21·76	1·852	0·2700	+0·0035	1·842	0·2735	0·0842	1·895	0·2807	−0·0478
23·26	1·839	0·3044	+0·0377	1·844	0·3144	0·0510	1·901	0·3199	−0·0761
				Round nacelles parallel to body					
6·25	0·776	0·0772	−0·1785	0·626	0·0768	0·3169	0·676	0·0766	0·1719
7·83	0·933	0·0871	−0·1828	0·791	0·0841	0·2699	0·844	0·0850	0·1217
9·40	1·090	0·0989	−0·1869	0·962	0·0942	0·2180	1·014	0·0961	0·0696
10·96	1·226	0·1126	−0·1859	1·121	0·1067	0·1833	1·165	0·1087	+0·0348
12·53	1·377	0·1310	−0·1875	1·282	0·1240	0·1384	1·327	0·1273	−0·0129
14·09	1·512	0·1519	−0·1842	1·426	0·1436	0·1051	1·471	0·1483	−0·0445
15·65	1·644	0·1733	−0·1787	1·579	0·1668	0·0562	1·619	0·1715	−0·0798
17·20	1·760	0·1970	−0·1693	1·697	0·1917	0·0375	1·742	0·1981	−0·1025
18·74	1·843	0·2237	−0·1411	1·806	0·2185	0·0221	1·843	0·2245	−0·1160
20·26	1·895	0·2552	−0·1029	1·861	0·2534	0·0224	1·893	0·2599	−0·1020
21·76	1·870	0·2850	−0·0543	1·866	0·2886	0·0363	1·905	0·2948	−0·0944
23·27	1·879	0·3235	−0·0150	1·880	0·3269	0·0076	1·911	0·3352	−0·1180
				Flat nacelles parallel to body					
15·64	1·626	0·1683	−0·2065	1·550	0·1614	0·0555			
17·20	1·747			1·685	0·1863	0·0222			
18·74	1·834	0·2214	−0·1823	1·793	0·2156	0·0073			
20·27	1·884	0·2548	−0·1402	1·848	0·2474	0·0157			
21·77	1·885	0·2858	−0·1007	1·857	0·2819	0·0274			
23·27	1·881	0·3242	−0·0683	1·871	0·3227	0·0083			
				Flat nacelles 4·2 degrees nose down relative to body					
15·63	1·591	0·1630	−0·1636	1·518	0·1567	0·0456			
17·18	1·713	0·1869	−0·1603	1·657	0·1812	0·0219			
18·73	1·805	0·2148	−0·1421	1·764	0·2090	0·0066			
20·25	1·857	0·2458	−0·1092	1·828	0·2410	0·0145			
21·75	1·853	0·2762	−0·0682	1·839	0·2761	0·0263			
23·26	1·853	0·3131	−0·0311	1·854	0·3140	0·0164			

TABLE 9 (concluded)

	No tailplane			$\eta_B = -10$ degrees			$\eta_B = -7{\cdot}5$ degrees		
α_{deg}	C_L	C_D	C_m	C_L	C_D	C_m	C_L	C_D	C_m
			Flat nacelles 8·1 degrees nose down relative to body						
12·47	1·248	0·1156	−0·1244	1·184	0·1138	0·1119			
14·04	1·395	0·1346	−0·1207	1·341	0·1321	0·0824			
15·60	1·528	0·1554	−0·1188	1·490	0·1526	0·0461			
17·15	1·652	0·1770	−0·1236	1·623	0·1764	+0·0137			
18·70	1·748	0·2031	−0·1036	1·732	0·2027	−0·0035			
20·23	1·811	0·2353	−0·0722	1·797	0·2346	+0·0130			
21·74	1·820	0·2678	−0·0272	1·814	0·2688	0·0246			
23·25	1·820	0·3013	+0·0059	1·828	0·3071	0·0089			
			Flat nacelles with auxiliary surfaces parallel to body						
6·25	0·758	0·0768	−0·2102	0·616	0·0777	0·2805			
7·82	0·918	0·0869	−0·2168	0·786	0·0851	0·2404			
9·39	1·072	0·0983	−0·2237	0·951	0·0947	0·2032			
10·96	1·224	0·1135	−0·2281	1·109	0·1074	0·1643			
12·52	1·363	0·1299	−0·2314	1·278	0·1248	0·1273			
14·09	1·517	0·1519	−0·2370	1·435	0·1451	0·0831			
15·65	1·638	0·1737	−0·2450	1·563	0·1659	0·0482			
17·21	1·766	0·1998	−0·2321	1·677	0·1880	+0·0222			
18·75	1·855	0·2288	−0·2180	1·798	0·2202	−0·0042			
20·27	1·901	0·2611	−0·1779	1·865	0·2528	+0·0039			
21·78	1·899	0·2940	−0·1337	1·862	0·2842	0·0167			
23·28	1·897	0·3321	−0·0942	1·882	0·3269	0·0017			
			Flat nacelles with auxiliary surfaces 8·1 degrees nose down relative to body						
6·18	0·614	0·0731	−0·0704	0·511	0·0761	0·3044			
7·76	0·780	0·0804	−0·0886	0·688	0·0819	0·2483			
9·33	0·947	0·0901	−0·1068	0·869	0·0894	0·1895			
10·90	1·100	0·1021	−0·1174	1·038	0·1014	0·1490			
12·47	1·257	0·1183	−0·1262	1·204	0·1168	0·1103			
14·04	1·398	0·1368	−0·1288	1·362	0·1360	0·0715			
15·60	1·540	0·1592	−0·1289	1·494	0·1552	0·0390			
17·16	1·669	0·1816	−0·1321	1·618	0·1761	+0·0026			
18·71	1·762	0·2078	−0·1174	1·737	0·2049	−0·0209			
20·23	1·811	0·2375	−0·0840	1·809	0·2383	−0·0071			
21·74	1·818	0·2709	−0·0445	1·809	0·2693	+0·0036			
23·25	1·823	0·3070	−0·0126	1·845	0·3115	−0·0160			

TABLE 10

Low Wing with Slats 25 Degrees and Flaps 40 Degrees

	No tailplane			$\eta_B = -5$ degrees			$\eta_B = 0$ degrees		
α_{deg}	C_L	C_D	C_m	C_L	C_D	C_m	C_L	C_D	C_m
				No nacelles					
−2·93	0·362	0·1144	−0·3474	0·135	0·1301	0·3409	0·219	0·1164	+0·0676
−1·25	0·770	0·1173	−0·4806	0·552	0·1248	0·1732	0·648	0·1156	−0·1120
+0·36	1·003	0·1273	−0·5154	0·811	0·1313	0·0998	0·896	0·1247	−0·1913
1·94	1·186	0·1416	−0·5244	1·018	0·1416	0·0454	1·098	0·1384	−0·2502
3·51	1·330	0·1558	−0·5166	1·182	0·1534	+0·0021	1·263	0·1526	−0·2949
5·06	1·451	0·1691	−0·5070	1·337	0·1666	−0·0368	1·413	0·1668	−0·3461
6·62	1·581	0·1871	−0·4955	1·461	0·1795	−0·0814	1·559	0·1850	−0·3931
8·19	1·719	0·2070	−0·4829	1·611	0·1991	−0·1291	1·709	0·2067	−0·4379
9·74	1·834	0·2265	−0·4636	1·761	0·2199	−0·1785	1·849	0·2287	− 0·4748
11·30	1·957	0·2491	−0·4502	1·890	0·2414	−0·2157	1·989	0·2537	−0·5094
12·85	2·076	0·2715	−0·4319	2·030	0·2679	−0·2585	2·117	0·2801	−0·5425
14·40	2·180	0·2982	−0·4135	2·158	0·2950	−0·2937	2·246	0·3095	−0·5721
15·94	2·272	0·3254	−0·3859	2·259	0·3240	−0·3055	2·333	0·3384	−0·5737
17·45	2·271	0·3522	−0·3057	2·236	0·3486	−0·2383	2·317	0·3657	−0·5005
18·93	2·231	0·3796	−0·2222	2·220	0·3788	−0·1594	2·301	0·4015	−0·4159
20·42	2·174	0·4184	−0·1519						
				Round nacelles parallel to body					
−2·99	0·247	0·1309	−0·2473	0·037	0·1440	0·3646	0·126	0·1409	+0·0827
−1·29	0·667	0·1286	−0·3930	0·453	0·1362	0·1915	0·583	0·1389	−0·1197
+0·32	0·911	0·1382	−0·4425	0·739	0·1403	0·0938	0·861	0·1425	−0·2107
1·91	1·107	0 1512	−0·4622	0·955	0·1498	+0·0306	1·074	0·1540	−0·2771
3·48	1·261	0·1648	−0·4686	1·120	0·1618	−0·0182	1·247	0·1677	−0·3285
5·04	1·401	0·1784	−0·4666	1·279	0·1729	−0·0675	1·410	0·1827	−0·3800
6·60	1·535	0·1939	−0·4640	1·426	0·1875	−0·1196	1·563	0·1999	−0·4324
8·16	1·671	0·2132	−0·4602	1·584	0·2074	−0·1701	1·712	0·2208	−0·4804
9·73	1·804	0·2338	−0·4552	1·734	0·2273	−0·2177	1·864	0·2441	−0·5194
11·28	1·925	0·2548	−0·4488	1·872	0·2498	−0·2621	2·005	0·2676	−0·5574
12·84	2·048	0·2788	−0·4421	2·011	0·2739	−0·3038	2·141	0·2950	−0·5991
14·39	2·166	0·3057	−0·4348	2·142	0·3027	−0·3441	2·261	0·3235	−0·6259
15·94	2·261	0·3331	−0·4102	2·263	0·3330	−0·3639	2·357	0·3548	−0·6341
17·44	2·256	0·3602	−0·3345	2·266	0·3615	−0·3024	2·342	0·3833	−0·5668
18·94	2·237	0·3919	−0·2596	2·237	0·3902	−0·2213	2·280	0·4158	−0·4789
20·42	2·181	0·4266	−0·1906	2·157	0·4209	−0·1022	2·201	0·4476	−0·3901

TABLE 10 (continued)

	No tailplane			$\eta_B = -5$ degrees			$\eta_B = 0$ degrees		
α_{deg}	C_L	C_D	C_m	C_L	C_D	C_m	C_L	C_D	C_m
				Flat nacelles parallel to body					
−3·03	0·158	0·1306	−0·1929	−0·051	0·1498	+0·3068	0·049	0·1362	+0·0375
−1·34	0·575	0·1262	−0·3463	+0·412	0·1366	+0·1162	0·466	0·1272	−0·1307
+0·29	0·854	0·1336	−0·4160	0·721	0·1406	+0·0185	0·798	0·1338	−0·2516
1·89	1·069	0·1469	−0·4485	0·936	0·1485	−0·0373	1·022	0·1451	−0·3072
3·46	1·224	0·1588	−0·4582	1·102	0·1577	−0·0814	1·201	0·1592	−0·3482
5·03	1·369	0·1725	−0·4626	1·263	0·1687	−0·1198	1·341	0·1713	−0·3817
6·59				1·407	0·1827	−0·1569	1·486	0·1860	−0·4205
8·15	1·639	0·2050	−0·4623	1·560	0·2000	−0·1950	1·646	0·2069	−0·4689
9·71	1·766	0·2246	−0·4535	1·682	0·2166	−0·2198	1·785	0·2272	−0·5103
11·27	1·898	0·2479	−0·4502	1·850	0·2422	−0·2714	1·939	0·2539	−0·5596
12·83	2·024	0·2719	−0·4456	1·986	0·2676	−0·3060	2·077	0·2803	−0·5844
14·38	2·142	0·2992	−0·4373				2·218	0·3109	−0·6134
15·93	2·248	0·3275	−0·4209	2·228	0·3674	−0·3630	2·313	0·3399	−0·6248
17·43	2·242	0·3515	−0·3459	2·240	0·3514	−0·3016	2·304	0·3706	−0·5429
18·93	2·212	0·3838	−0·2769	2·198	0·3822	−0·2053	2·274	0·4039	−0·4587
20·41	2·170	0·4202	−0·2108	2·146	0·4100	−0·1074	2·211	0·4333	−0·3440
				Flat nacelles 4·2 degrees nose down relative to body					
−3·08	0·054	0·1429	−0·1116	−0·080	0·1540	0·2856	0·019	0·1410	+0·0247
−1·39	0·470	0·1334	−0·2690	+0·311	0·1408	0·1309	0·359	0·1314	−0·1177
+0·26	0·781	0·1400	−0·3558	0·663	0·1438	+0·0100	0·768	0·1372	−0·2696
1·85	0·990	0·1508	−0·3892	0·889	0·1514	−0·0442	0·982	0·1473	−0·3246
3·43	1·159	0·1627	−0·4034	1·060	0·1602	−0·0824	1·168	0·1608	−0·3668
5·00	1·303	0·1737	−0·4043	1·216	0·1697	−0·1185	1·319	0·1722	−0·4066
6·56	1·438	0·1865	−0·4061	1·362	0·1825	−0·1561	1·450	0·1850	−0·4348
8·12	1·582	0·2030	−0·4093	1·519	0·1990	−0·1992	1·609	0·2042	−0·4873
9·69	1·720	0·2223	−0·4085	1·666	0·2170	−0·2358	1·761	0·2259	−0·5233
11·25	1·857	0·2431	−0·4140	1·815	0·2397	−0·2702	1·908	0·2502	−0·5578
12·81	1·978	0·2662	−0·4139	1·958	0·2630	−0·3093	2·031	0·2732	−0·5763
14·36	2·098	0·2921	−0·4062	2·080	0·2879	−0·3374	2·131	0·2941	−0·5964
15·91	2·202	0·3174	−0·3909	2·207	0·3191	−0·3618	2·289	0·3337	−0·6290
17·42	2·215	0·3452	−0·3202	2·214	0·3468	−0·3003	2·285	0·3608	−0·5638
18·90	2·167	0·3733	−0·2447	2·189	0·3760	−0·2076	2·268	0·3976	−0·4667
20·40	2·139	0·4072	−0·1732	2·133	0·4054	−0·1070	2·194	0·4261	−0·3470
				Flat nacelles 8·1 degrees nose down relative to body					
−3·12	−0·039	0·1601	−0·0338	−0·135	0·1663	+0·2497	−0·055	0·1527	+0·0178
−1·46	+0·310	0·1485	−0·1581	+0·214	0·1510	+0·1166	+0·293	0·2203	−0·1331
+0·21	0·667	0·1518	−0·2725	0·605	0·1529	−0·0298	0·691	0·1446	−0·2754
1·81	0·891	0·1615	−0·3120	0·840	0·1593	−0·0876	0·915	0·1547	−0·3328
3·39	1·065	0·1729	−0·3260	1·010	0·1689	−0·1181	1·099	0·1657	−0·3706
4·96	1·214	0·1819	−0·3270	1·162	0·1768	−0·1449	1·254	0·1754	−0·4015
6·52	1·346	0·1914	−0·3261	1·305	0·1868	−0·1747	1·402	0·1889	−0·4398
8·08	1·491	0·2064	−0·3338	1·459	0·2016	−0·2100	1·558	0·2058	−0·4821
9·65	1·630	0·2232	−0·3363	1·610	0·2182	−0·2427	1·708	0·2262	−0·5201

TABLE 10 (continued)

α_{deg}	No tailplane			$\eta_B = -5$ degrees			$\eta_B = 0$ degrees		
	C_L	C_D	C_m	C_L	C_D	C_m	C_L	C_D	C_m
				Flat nacelles 8·1 degrees nose down relative to body (concluded)					
11·21	1·767	0·2430	−0·3371	1·759	0·2388	−0·2762	1·856	0·2479	−0·5558
12·77	1·902	0·2643	−0·3362	1·898	0·2609	−0·3130	2·004	0·2737	−0·5956
14·33	2·034	0·2874	−0·3353	2·035	0·2869	−0·3468	2·139	0·3007	−0·6318
15·88	2·139	0·3115	−0·3232	2·159	0·3140	−0·3741	2·260	0·3302	−0·6498
17·39	2·160	0·3369	−0·2609	2·185	0·3397	−0·3250	2·266	0·3589	−0·5857
18·88	2·115	0·3629	−0·1921	2·151	0·3652	−0·2377	2·244	0·3888	−0·4980
20·38	2·099	0·3933	−0·1146	2·102	0·3941	−0·1228	2·195	0·4175	−0·3805
				Flat nacelles with auxiliary surfaces parallel to body					
−3·04	0·140	0·1359	−0·1693	−0·036	0·1530	+0·3143	0·074	0·1381	+0·0352
−1·35	0·558	0·1300	−0·3345	+0·386	0·1399	+0·1372	0·495	0·1308	−0·1454
+0·29	0·853	0·1375	−0·4128	0·727	0·1433	+0·0183	0·823	0·1373	−0·2578
1·89	1·073	0·1505	−0·4442	0·945	0·1516	−0·0360	1·039	0·1492	−0·3148
3·46	1·233	0·1637	−0·4607	1·117	0·1614	−0·0867	1·214	0·1626	−0·3636
5·03	1·380	0·1769	−0·4679	1·280	0·1733	−0·1267	1·370	0·1761	−0·4043
6·60	1·523	0·1931	−0·4741	1·424	0·1872	−0·1621	1·527	0·1931	−0·4458
8·16	1·659	0·2111	−0·4733	1·572	0·2051	−0·2050	1·667	0·2118	−0·4872
9·72	1·790	0·2309	−0·4694	1·717	0·2252	−0·2417	1·816	0·2343	−0·5276
11·27	1·912	0·2520	−0·4634	1·866	0·2483	−0·2848	1·963	0·2599	−0·5755
12·83	2·039	0·2765	−0·4616	2·003	0·2732	−0·3203	2·108	0·2873	−0·6139
14·39	2·162	0·3032	−0·4538	2·142	0·3024	−0·3585	2·240	0·3185	−0·6394
15·94	2·268	0·3324	−0·4584	2·256	0·3317	−0·3785	2·354	0·3499	−0·6543
17·45	2·270	0·3608	−0·3748	2·263	0·3613	−0·3229	2·343	0·3801	−0·5858
18·94	2·249	0·3941	−0·3023	2·222	0·3919	−0·2333	2·309	0·4138	−0·4895
20·43	2·211	0·4264	−0·2316	2·184	0·4230	−0·1309	2·244	0·4471	−0·3722
				Flat nacelles with auxiliary surfaces 8·1 degrees nose down relative to body					
−3·13	−0·070	0·1682	+0·0355	−0·157	0·1770	+0·2904	−0·070	0·1617	+0·0452
−1·45	+0·318	0·1545	−0·1101	+0·220	0·1595	+0·1436	+0·281	0·1493	−0·0953
+0·20	0·664	0·1584	−0·2252	0·601	0·1610	−0·0004	0·676	0·1507	−0·2503
1·80	0·881	0·1667	−0·2664	0·838	0·1659	−0·0653	0·921	0·1602	−0·3179
3·38	1·057	0·1767	−0·2909	1·010	0·1740	−0·1036	1·107	0·1711	−0·3648
4·95	1·210	0·1860	−0·2987	1·187	0·1823	−0·1426	1·263	0·1821	−0·3984
6·52	1·364	0·1974	−0·3119	1·326	0·1927	−0·1665	1·414	0·1900	−0·4335
8·08	1·493	0·2103	−0·3174	1·479	0·2076	−0·2036	1·578	0·2127	−0·4843
9·65	1·647	0·2281	−0·3264	1·634	0·2245	−0·2456	1·724	0·2322	−0·5255
11·22	1·787	0·2459	−0·3332	1·788	0·2443	−0·2778	1·879	0·2546	−0·5595
12·78	1·924	0·2681	−0·3345	1·926	0·2667	−0·3175	2·028	0·2809	−0·6038
14·33	2·039	0·2902	−0·3298	2·071	0·2934	−0·3547	2·160	0·3072	−0·6398
15·89	2·158	0·3159	−0·3273	2·195	0·3198	−0·3802	2·289	0·3373	−0·6652
17·41	2·194	0·3377	−0·2847	2·210	0·3450	−0·3301	2·307	0·3679	−0·6146
18·89	2·137	0·3723	−0·1875	2·193	0·3749	−0·2458	2·282	0·3989	−0·5187
20·40	2·138	0·4034	−0·1290	2·139	0·4023	−0·1428	2·240	0·4278	−0·4206

TABLE 10 (continued)

	No tailplane			$\eta_B = -5$ degrees			$\eta_B = 0$ degrees		
α_{deg}	C_L	C_D	C_m	C_L	C_D	C_m	C_L	C_D	C_m
				(BLOCKED) Flat nacelles parallel to body					
−3·08	0·039	0·1680	−0·1564				0·004	0·1652	+0·0270
−1·42	0·389	0·1576	−0·2775	0·265	0·1624	+0·1272	0·358	0·1546	−0·1209
+0·24	0·746	0·1643	−0·3923	0·628	0·1658	−0·0164	0·724	0·1605	−0·2594
1·84	0·967	0·1750	−0·4285	0·859	0·1743	−0·0889	0·948	0·1717	−0·3227
3·42	1·135	0·1867	−0·4426	1·048	0·1848	−0·1367	1·129	0·1842	−0·3705
4·99	1·278	0·1982	−0·4467	1·204	0·1945	−0·1735	1·279	0·1958	−0·4060
6·55	1·419	0·2111	−0·4485	1·345	0·2070	−0·2099	1·425	0·2093	−0·4471
8·11	1·556	0·2269	−0·4545	1·501	0·2227	−0·2503	1·579	0·2273	−0·4909
9·67	1·685	0·2439	−0·4447	1·638	0·2391	−0·2809	1·724	0·2469	−0·5295
11·23	1·821	0·2641	−0·4589	1·789	0·2611	−0·3210	1·867	0·2704	−0·5655
12·79	1·951	0·2864	−0·4525	1·935	0·2853	−0·3630	2·019	0·2949	−0·6096
14·35	2·071	0·3110	−0·4449	2·069	0·3121	−0·3919	2·138	0·3225	−0·6409
15·89	2·166	0·3361	−0·4247	2·182	0·3386	−0·4174	2·255	0·3535	−0·6609
17·41	2·187	0·3575	−0·3657	2·195	0·3632	−0·3663	2·274	0·3808	−0·6056
18·90	2·150	0·3889	−0·2793	2·125	0·3884	−0·2895	2·223	0·4073	−0·5152
20·39	2·124	0·4210	−0·2199	2·137	0·4233	−0·2399	2·212	0·4417	−0·4575
				(BLOCKED) Flat nacelles with auxiliary surfaces parallel to body					
−3·06	0·092	0·1595	−0·2262	−0·069	0·1696	+0·2434	0·040	0·1601	−0·0195
−1·40	0·432	0·1521	−0·3411	+0·292	0·1565	+0·0816	0·364	0·1521	−0·1514
+0·26	0·779	0·1598	−0·4497	0·650	0·1611	−0·0568	0·738	0·1586	−0·3044
1·86	1·001	0·1716	−0·4886	0·898	0·1706	−0·1365	0·991	0·1710	−0·3760
3·44	1·176	0·1850	−0·5013	1·064	0·1808	−0·1777	1·148	0·1842	−0·4110
5·01	1·330	0·1999	−0·5120	1·231	0·1949	−0·2109	1·300	0·1983	−0·4419
6·56	1·449	0·2124	−0·5152	1·372	0·2080	−0·2533	1·452	0·2134	−0·4930
8·12	1·581	0·2288	−0·5116	1·525	0·2260	−0·2957	1·586	0·2303	−0·5261
9·68	1·712	0·2476	−0·5139	1·660	0·2422	−0·3236	1·744	0·2535	−0·5728
11·25	1·853	0·2708	−0·5167	1·813	0·2664	−0·3600	1·897	0·2790	−0·6088
12·81	1·978	0·2932	−0·5116	1·959	0·2936	−0·4022	2·035	0·3060	−0·6439
14·36	2·088	0·3171	−0·5002	2·088	0·3198	−0·4316	2·160	0·3341	−0·6719
15·91	2·197	0·3471	−0·4877	2·188	0·3469	−0·4460	2·268	0·3649	−0·6860
17·42	2·207	0·3729	−0·4173	2·211	0·3751	−0·3922	2·282	0·3974	−0·6204
18·90	2·161	0·3966	−0·3319	2·161	0·4007	−0·3157	2·240	0·4238	−0·5397
20·40	2·135	0·4273	−0·2711	2·145	0·4341	−0·2771	2·204	0·4570	−0·4828
	No tailplane			$\eta_B = -10$ degrees			$\eta_B = -2·5$ degrees		
				No nacelles					
3·51	1·330	0·1558	−0·5166	1·090	0·1684	0·2527			
5·06	1·451	0·1691	−0·5070	1·226	0·1739	0·2170			
6·62	1·581	0·1871	−0·4955	1·361	0·1836	0·1820	1·512	0·1871	−0·2398
8·19	1·719	0·2070	−0·4829	1·509	0·1979	0·1413	1·663	0·2078	−0·2897
9·74	1·834	0·2265	−0·4636	1·652	0·2140	0·0896	1·820	0·2313	−0·3333
11·30	1·957	0·2491	−0·4502	1·786	0·2342	+0·0427	1·945	0·2541	−0·3690
12·85	2·076	0·2715	−0·4319	1·921	0·2560	−0·0040	2·078	0·2796	−0·4072
14·40	2·180	0·2982	−0·4135	2·057	0·2824	−0·0386	2·215	0·3096	−0·4398
15·94	2·272	0·3254	−0·3859	2·169	0·3092	−0·0621	2·311	0·3373	−0·4475
17·45	2·271	0·3522	−0·3057	2·157	0·3339	+0·0095	2·296	0·3651	−0·3755
18·93	2·231	0·3796	−0·2222	2·133	0·3643	+0·0895	2·267	0·3958	−0·2936

TABLE 10 (concluded)

	No tailplane			$\eta_B = -10$ degrees			$\eta_B = +2{\cdot}5$ degrees		
α_{deg}	C_L	C_D	C_m	C_L	C_D	C_m	C_L	C_D	C_m
				No nacelles (concluded)					
−2·93	0·362	0·1144	−0·3474				0·264	0·1159	−0·0806
−1·25	0·770	0·1173	−0·4806				0·699	0·1154	−0·2693
+0·36	1·003	0·1273	−0·5154				0·947	0·1259	−0·3514
1·94	1·186	0·1416	−0·5244				1·152	0·1409	−0·4097
3·51	1·330	0·1558	−0·5166				1·309	0·1559	−0·4539
5·06	1·451	0·1691	−0·5070				1·461	0·1710	−0·5005
6·62	1·581	0·1871	−0·4955				1·604	0·1902	−0·5384
8·19	1·719	0·2070	−0·4829				1·751	0·2119	−0·5789
9·74	1·834	0·2265	−0·4636				1·893	0·2355	−0·6147
	No tailplane			$\eta_B = -10$ degrees			$\eta_B = -2{\cdot}5$ degrees		
				Round nacelles parallel to body					
3·48	1·261	0·1648	−0·4686	1·045	0·1745	0·2338			
5·04	1·401	0·1784	−0·4666	1·194	0·1820	0·1896			
6·60	1·535	0·1939	−0·4640	1·328	0·1913	0·1471	1·480	0·1897	−0·2701
8·16	1·671	0·2132	−0·4602	1·473	0·2040	0·1020	1·642	0·2108	−0·3269
9·73	1·804	0·2338	−0·4552	1·628	0·2214	+0·0435	1·796	0·2334	−0·3719
11·28	1·925	0·2548	−0·4488	1·763	0·2412	−0·0046	1·946	0·2587	−0·4150
12·84	2·048	0·2788	−0·4421	1·910	0·2644	−0·0581	2·079	0·2840	−0·4540
14·39	2·166	0·3057	−0·4348	2·050	0·2906	−0·0965	2·192	0·3114	−0·4868
15·94	2·261	0·3331	−0·4102	2·158	0·3182	−0·1137	2·300	0·3394	−0·4969
17·44	2·256	0·3602	−0·3345	2·158	0·3434	−0·0496	2·287	0·3689	−0·4324
18·94	2·237	0·3919	−0·2596	2·132	0·3741	+0·0179	2·258	0·4029	−0·3428
	No tailplane			$\eta_B = -10$ degrees			$\eta_B = +2{\cdot}5$ degrees		
−2·99	0·247	0·1309	−0·2473				0·194	0·1313	−0·0811
−1·29	0·667	0·1286	−0·3930				0·624	0·1282	−0·2734
+0·32	0·911	0·1382	−0·4425				0·897	0·1376	−0·3693
1·91	1·107	0·1512	−0·4622				1·104	0·1510	−0·4314
3·48	1·261	0·1648	−0·4686				1·275	0·1655	−0·4794
5·04	1·401	0·1784	−0·4666				1·430	0·1809	−0·5246
6·60	1·535	0·1939	−0·4640				1·579	0·1988	−0·5689
8·16	1·671	0·2132	−0·4602				1·729	0·2210	−0·6139
9·73	1·804	0·2338	−0·4552				1·882	0·2454	−0·6566

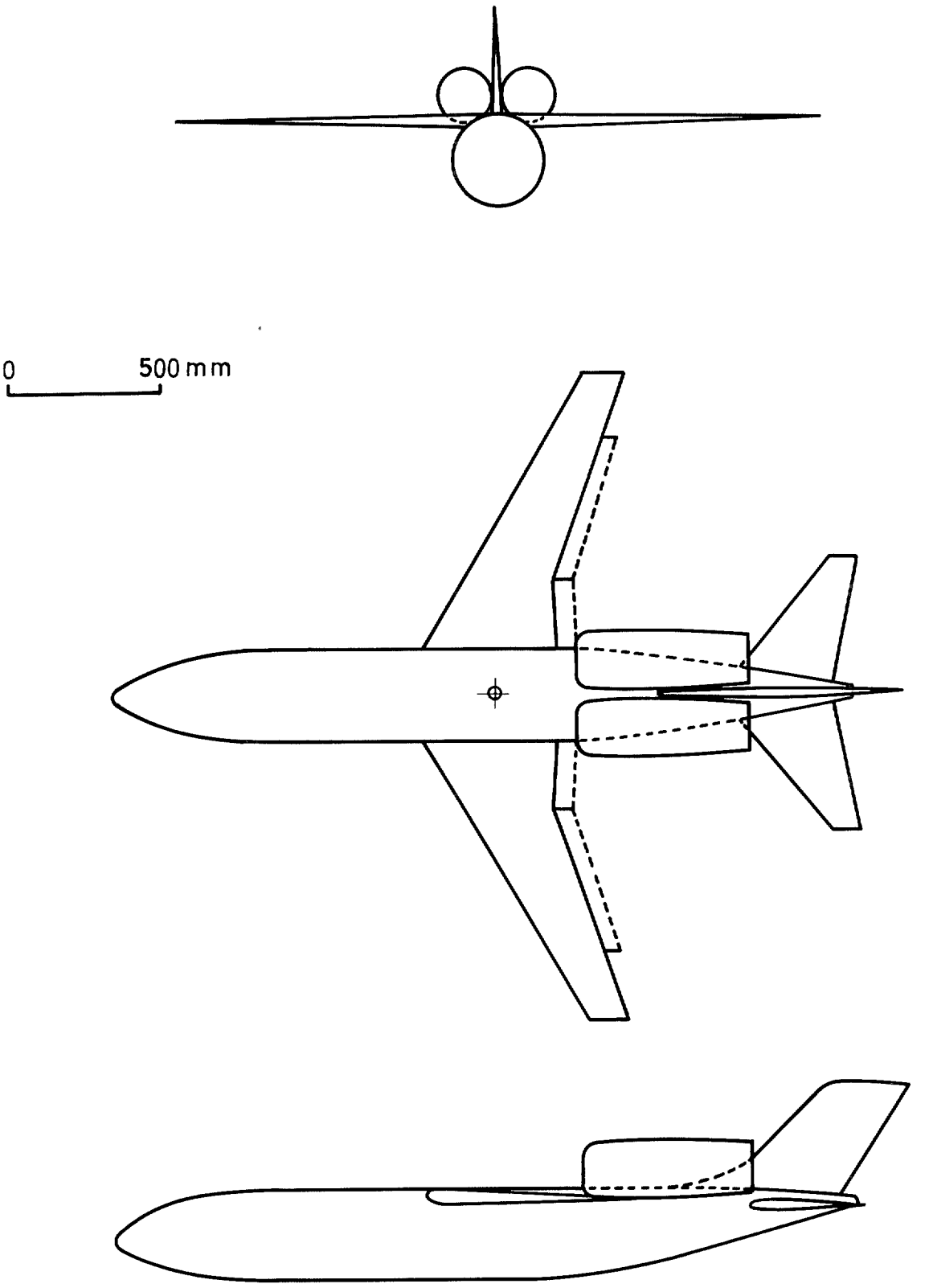

FIG. 1. G.A. of high-wing model.

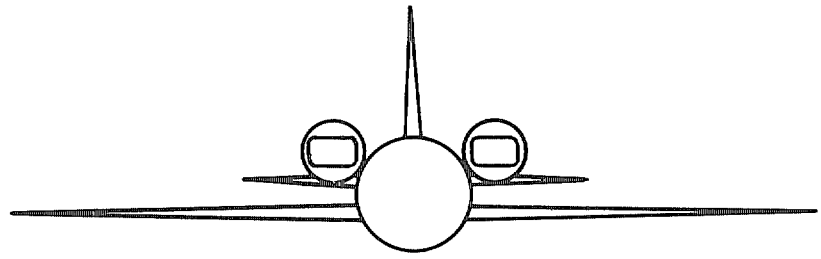

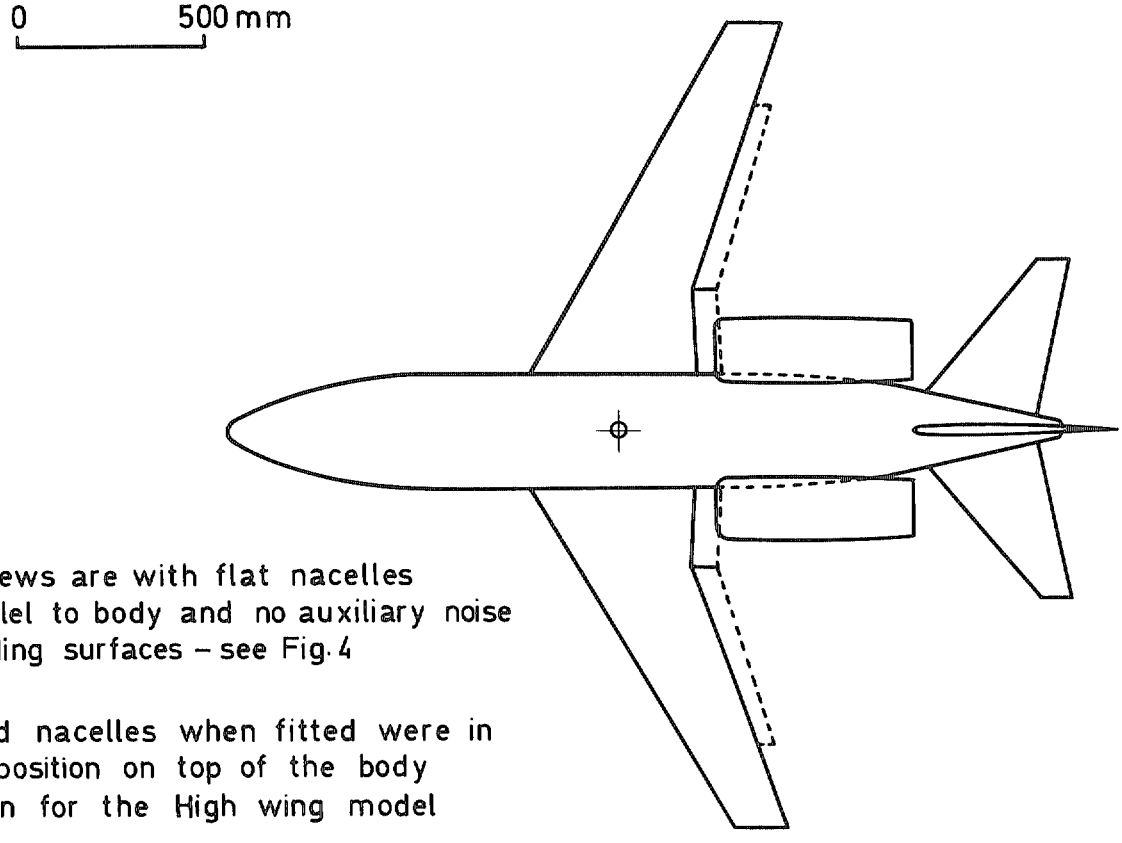

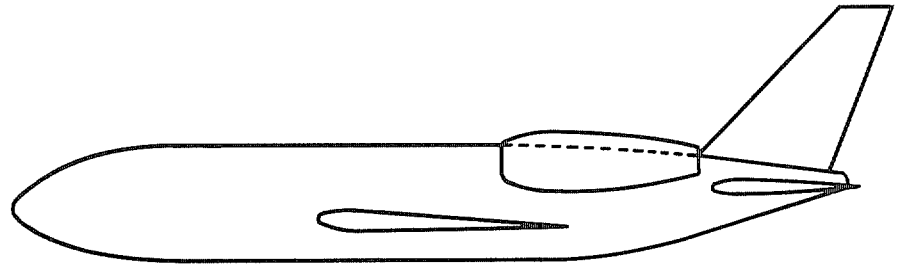

FIG. 2. G.A. of low-wing model.

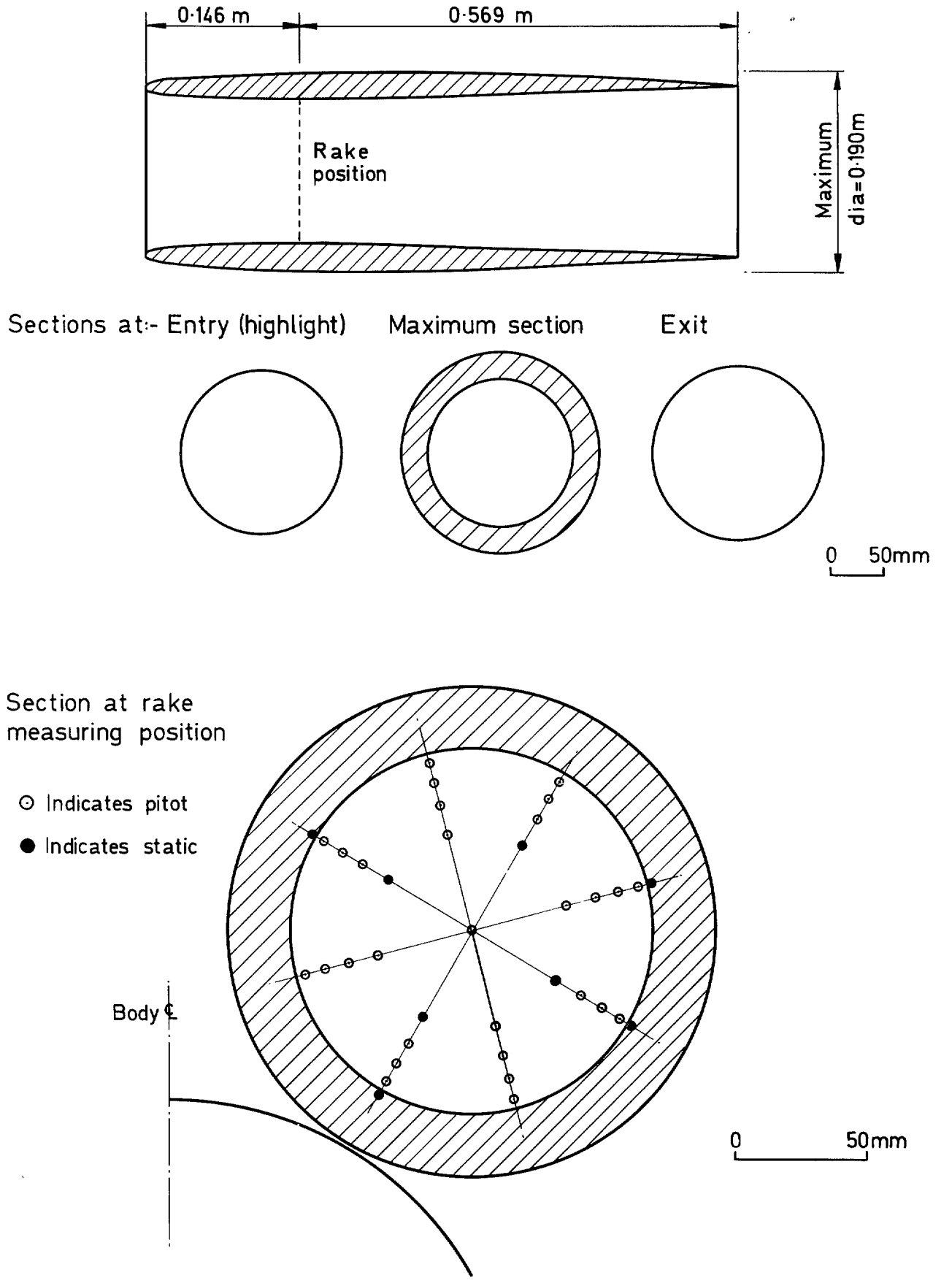

FIG. 3. Details of round nacelles and measuring rake.

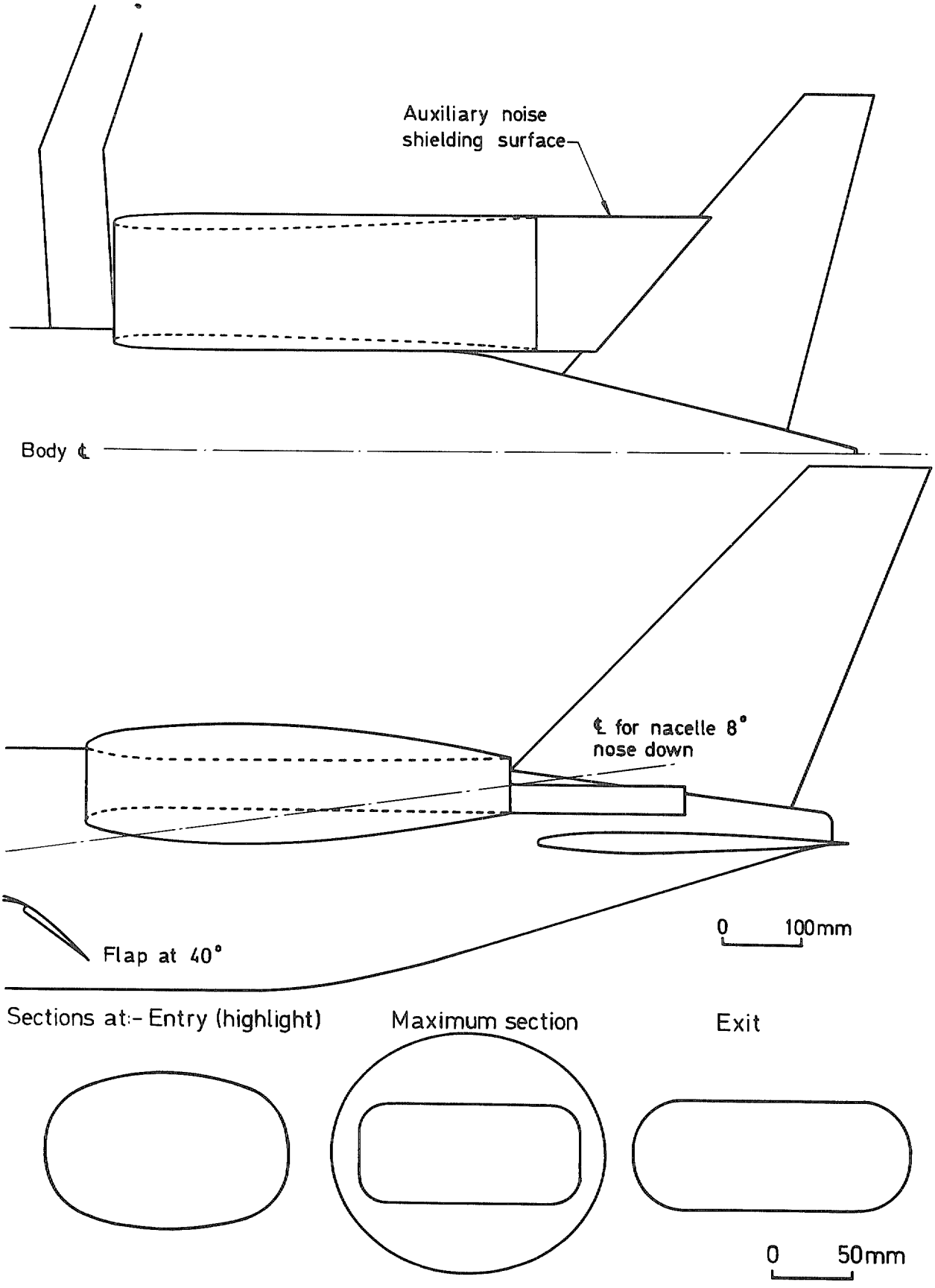

FIG. 4. Details of flat nacelles and auxiliary noise-shielding surfaces.

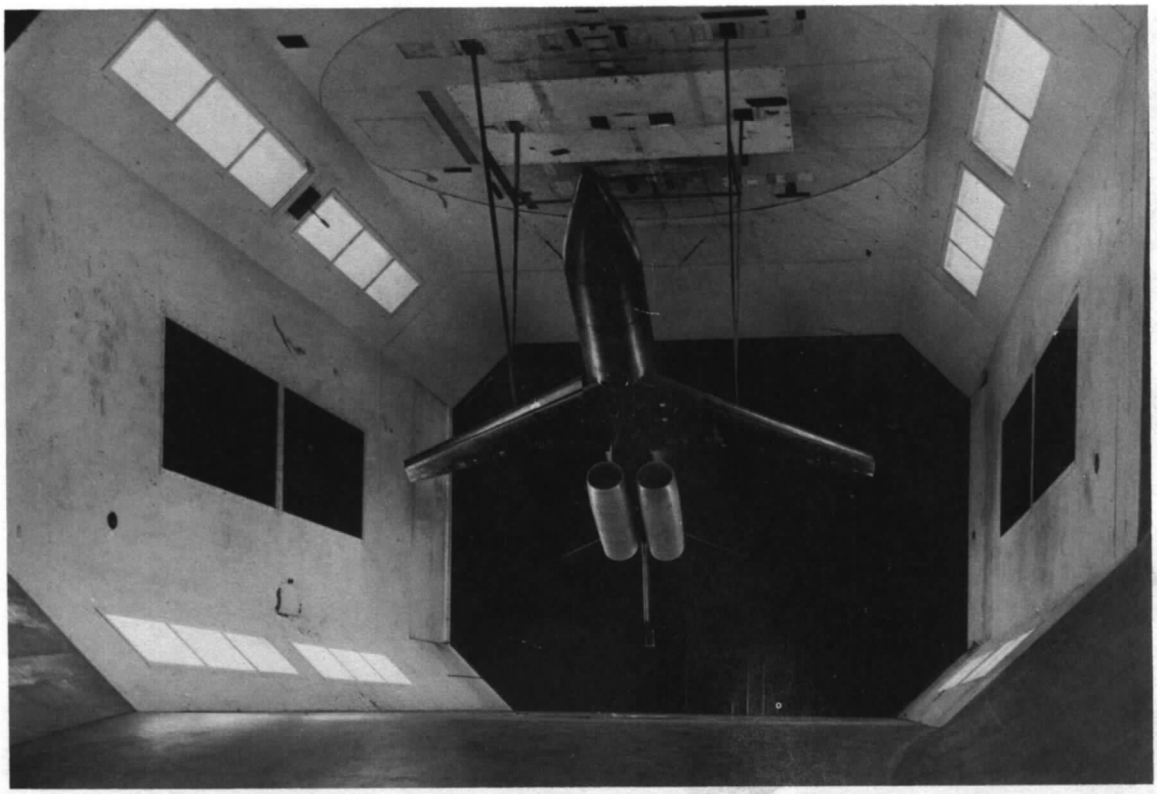

FIG. 5a. High-wing model with round nacelles in No. 1, $11\frac{1}{2}$ ft $\times$ $8\frac{1}{2}$ ft wind tunnel.

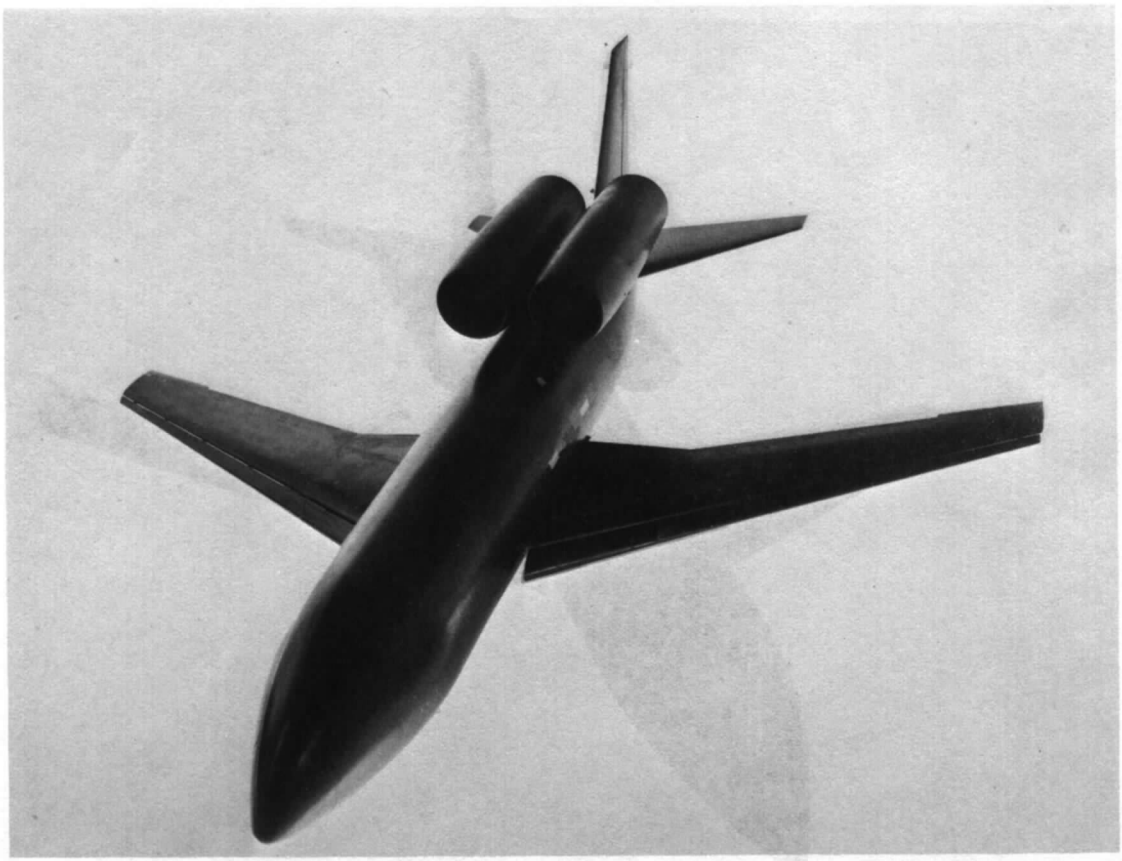

FIG. 5b. Low-wing model with round nacelles.

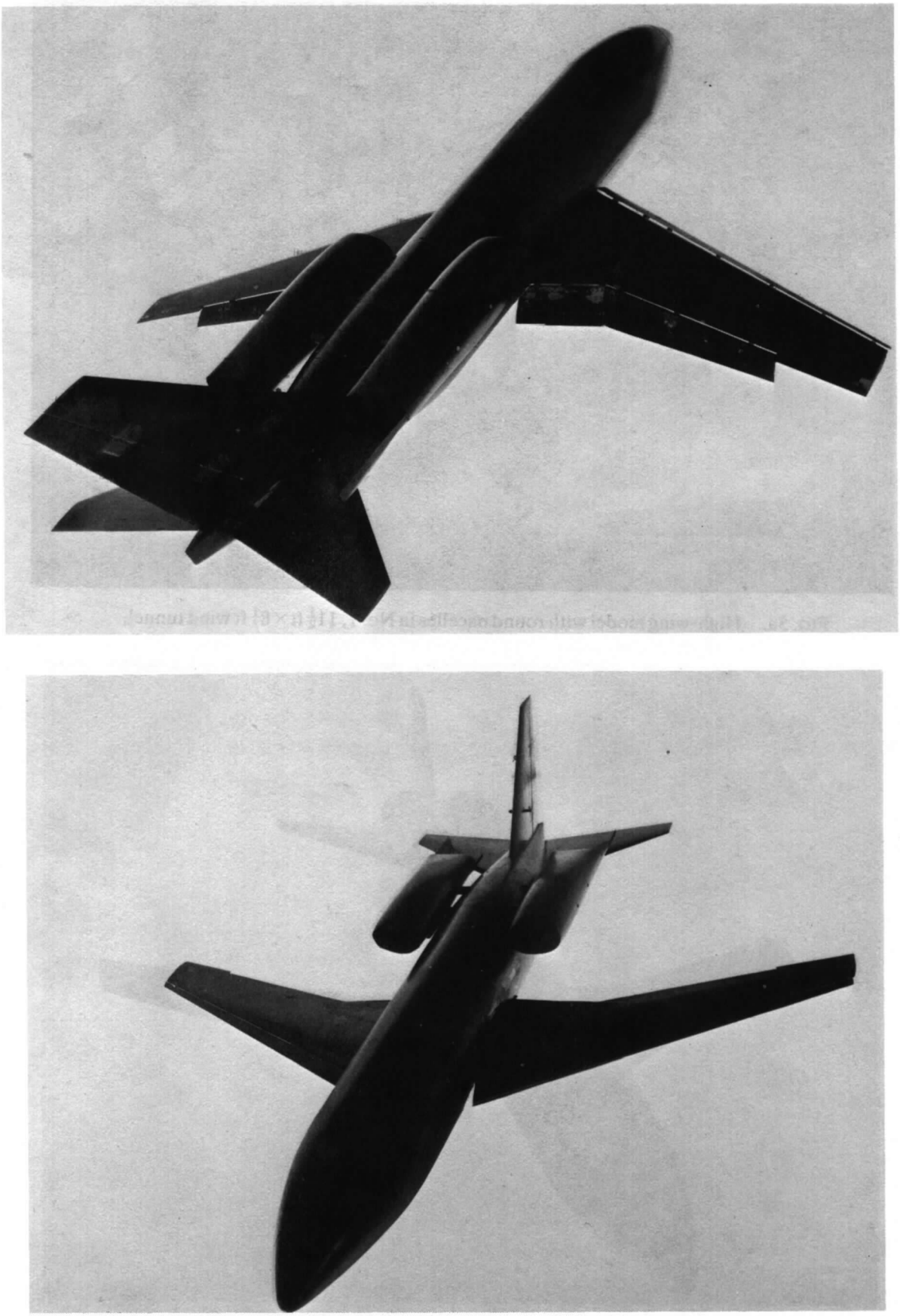

FIG. 6. Low-wing model with flat nacelles parallel to body—auxiliary noise-shielding surfaces fitted.

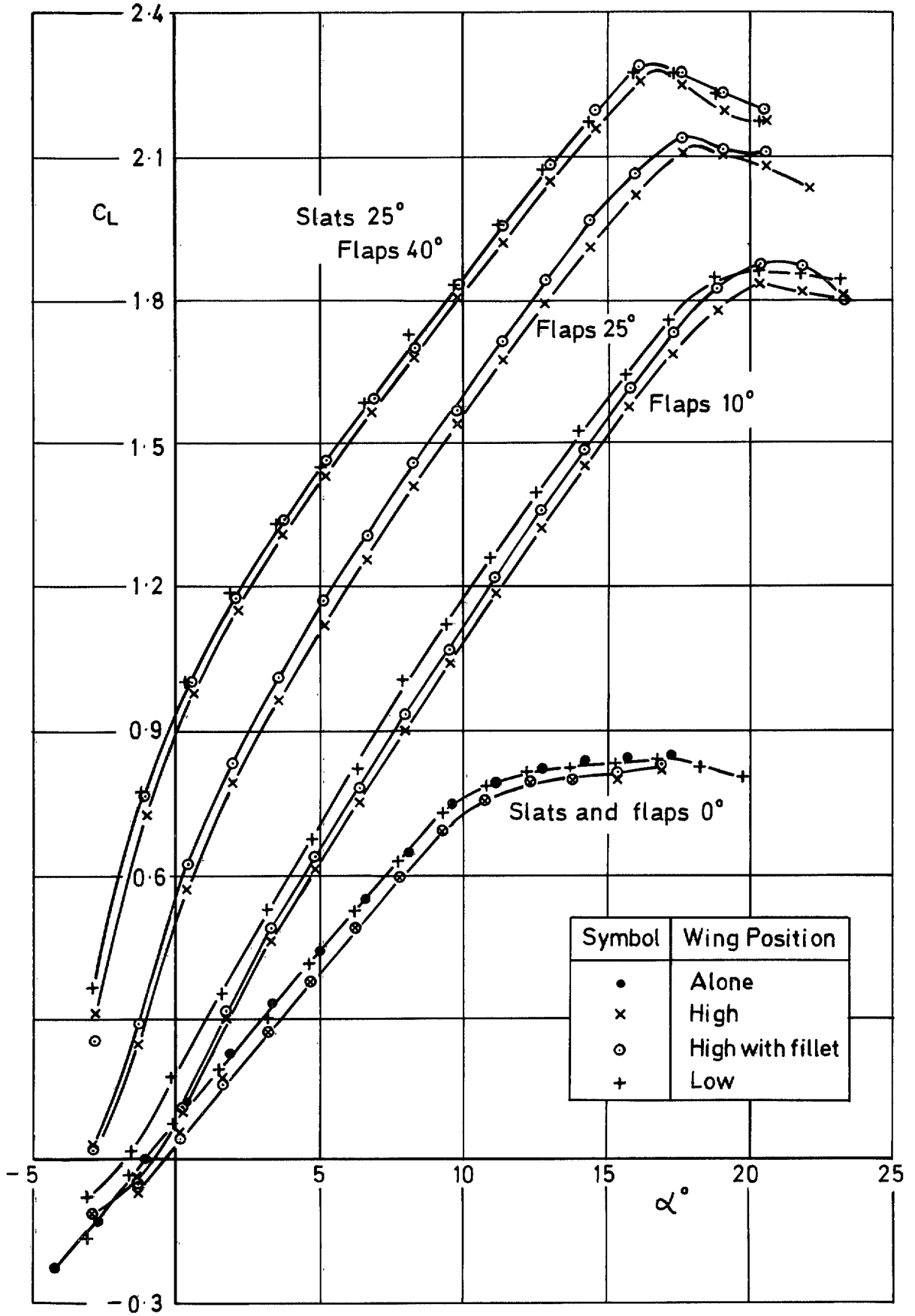

FIG. 7. Lift coefficient for various wing conditions.

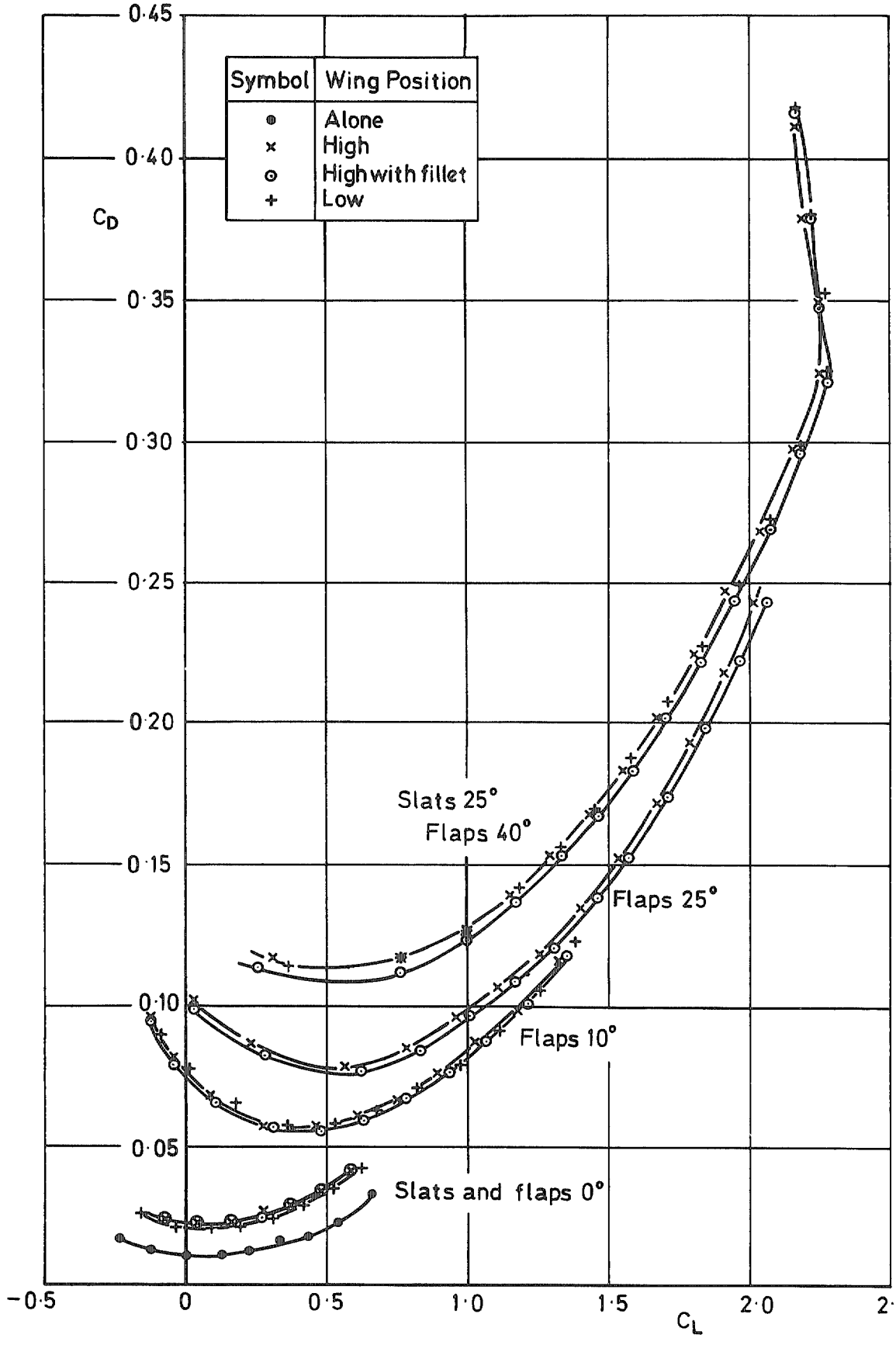

FIG. 8. Drag coefficient for various wing conditions.

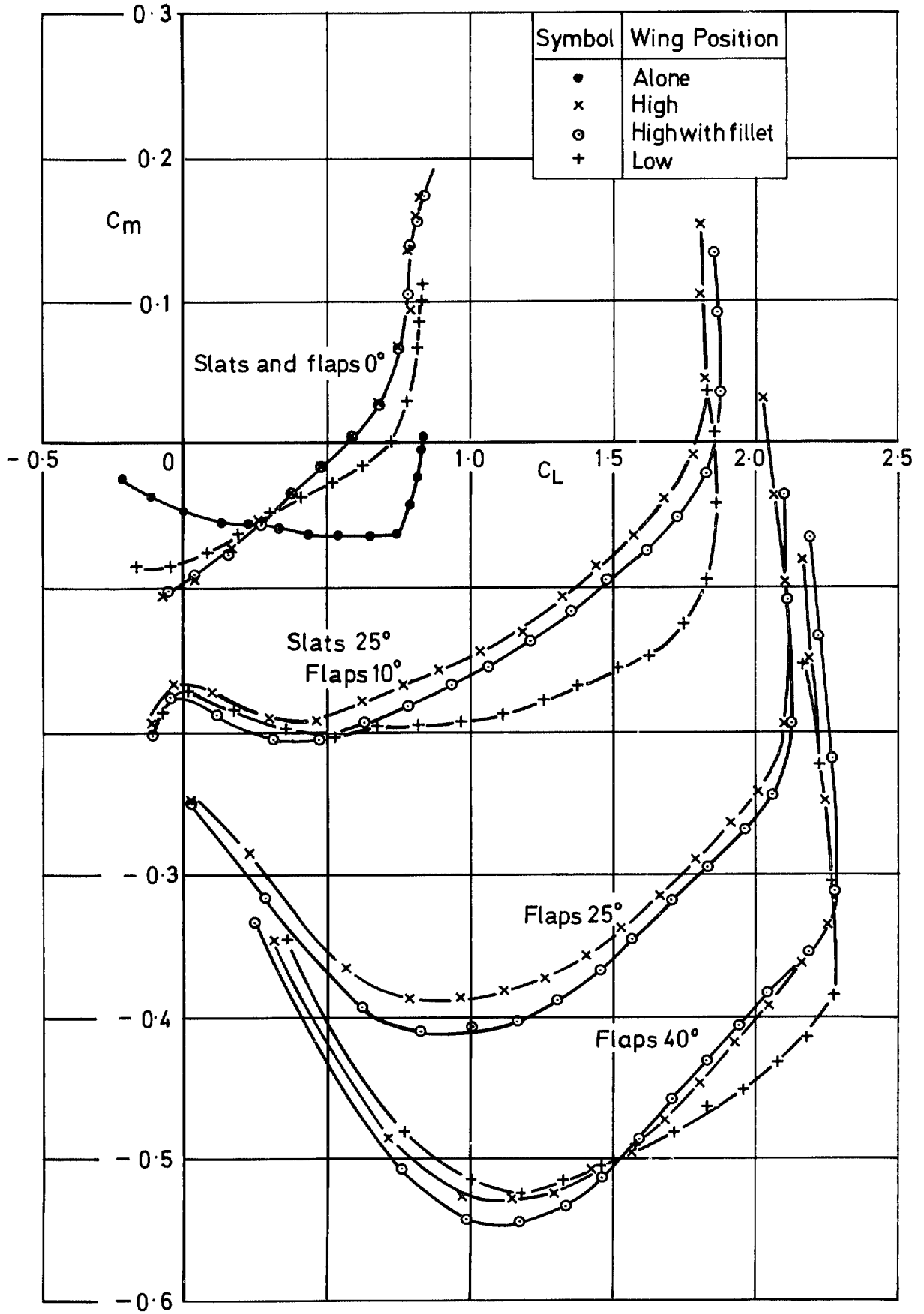

FIG. 9. Pitching moment coefficient for various wing conditions.

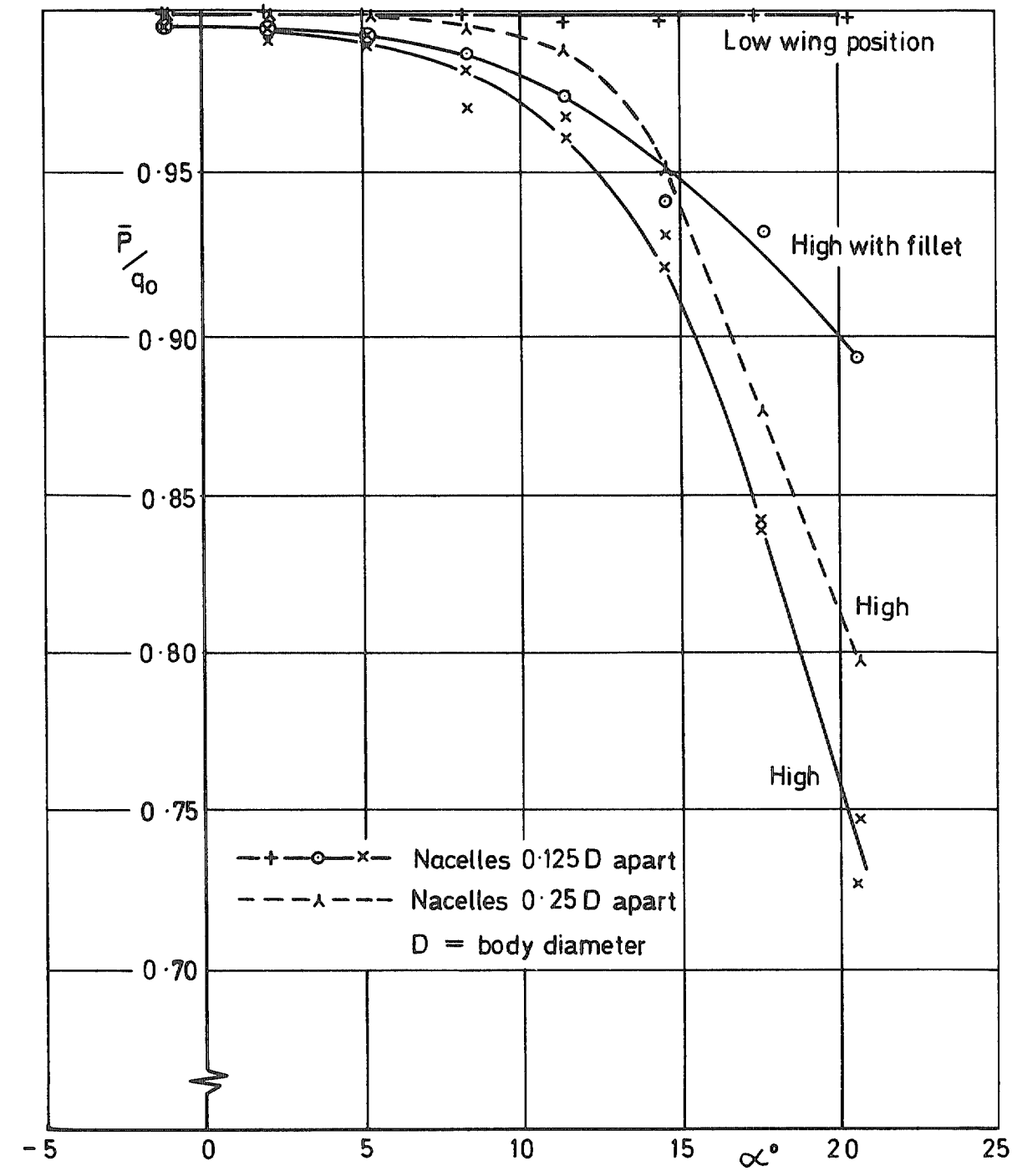

FIG. 10. Variation of mean total head at 'engine face' with incidence for round nacelles, slats 25° and flaps 40°.

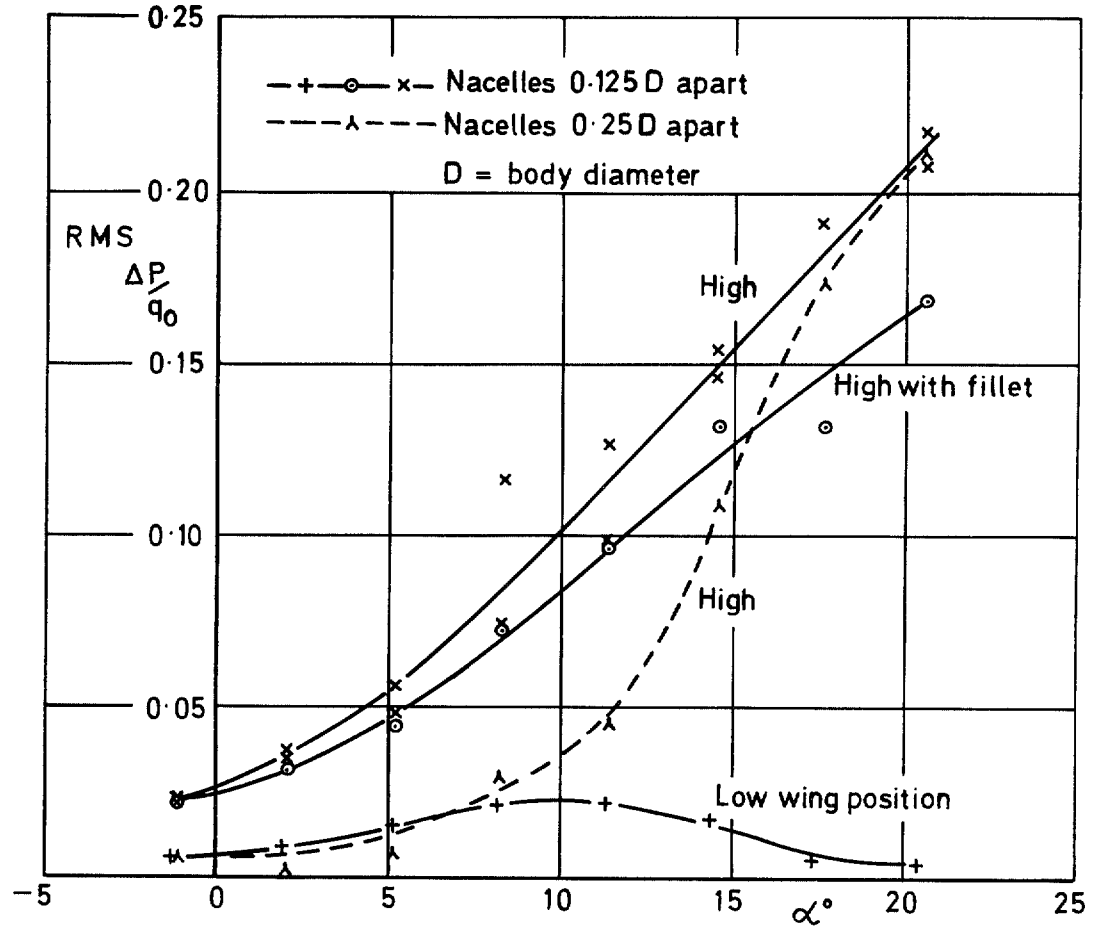

FIG. 11. Variation of distortion parameter at 'engine face' with incidence for round nacelles, slats 25° and flaps 40°.

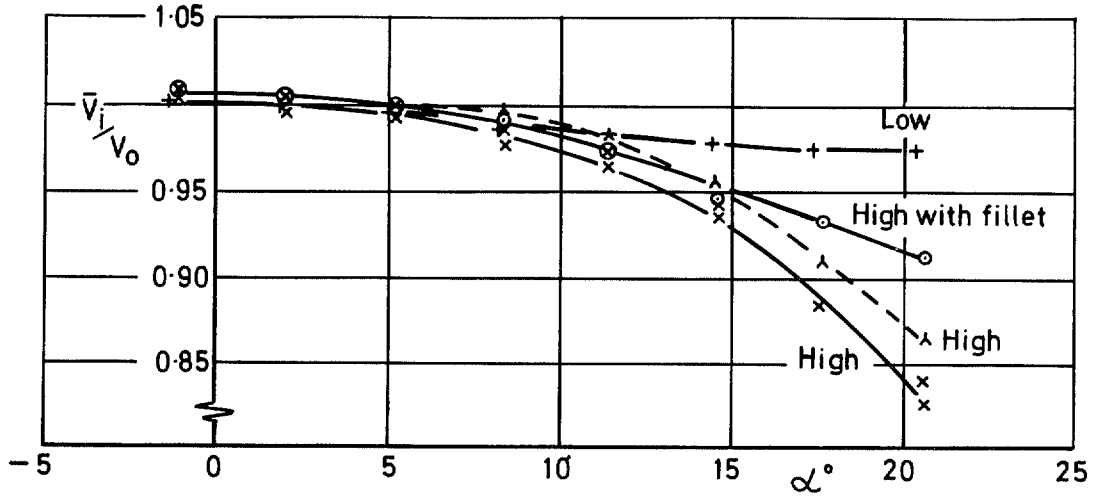

FIG. 12. Variation of entry velocity ratio with incidence for round nacelles, slats 25° and flaps 40°.

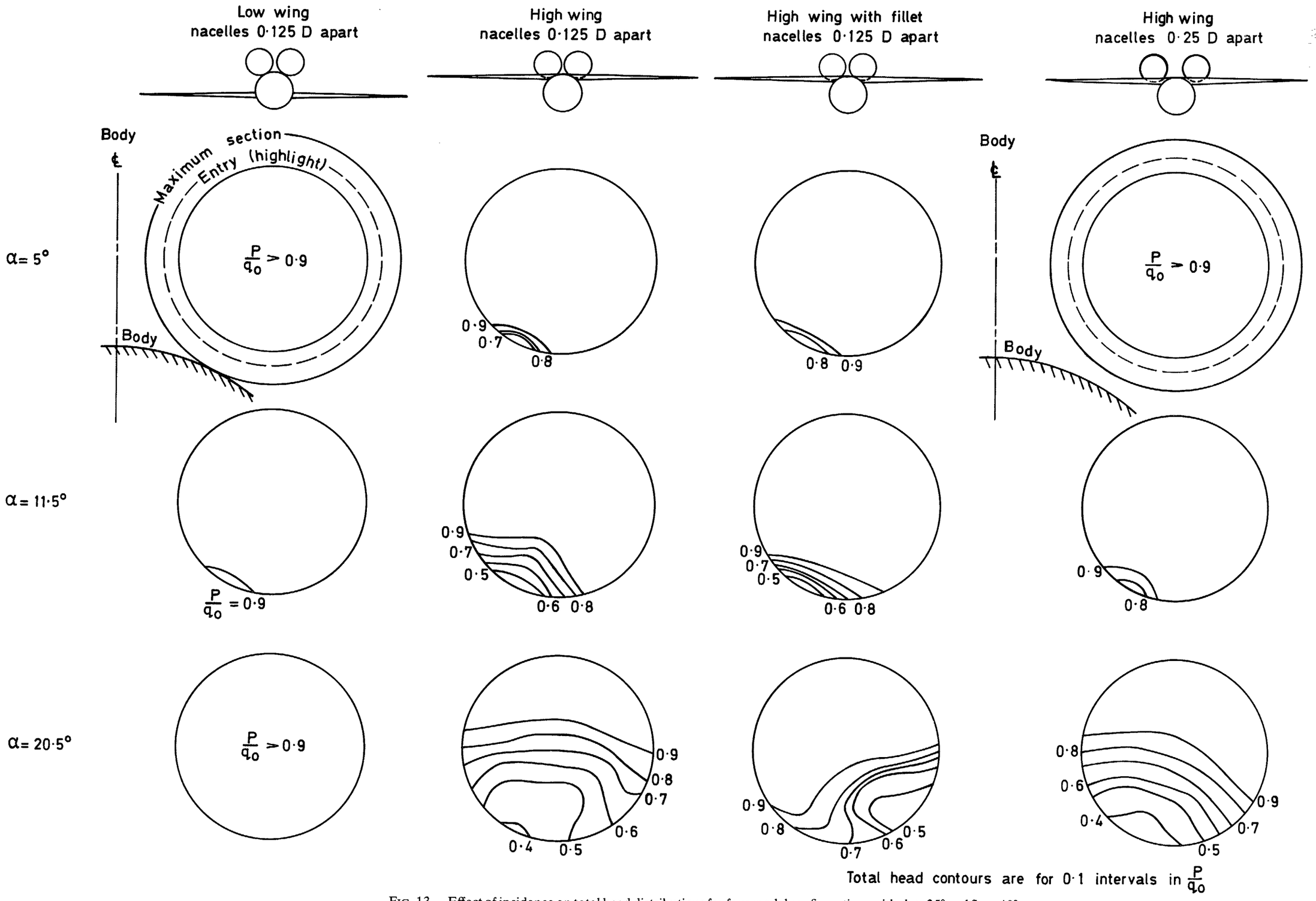

FIG. 13. Effect of incidence on total head distributions for four model configurations with slats 25° and flaps 40°.

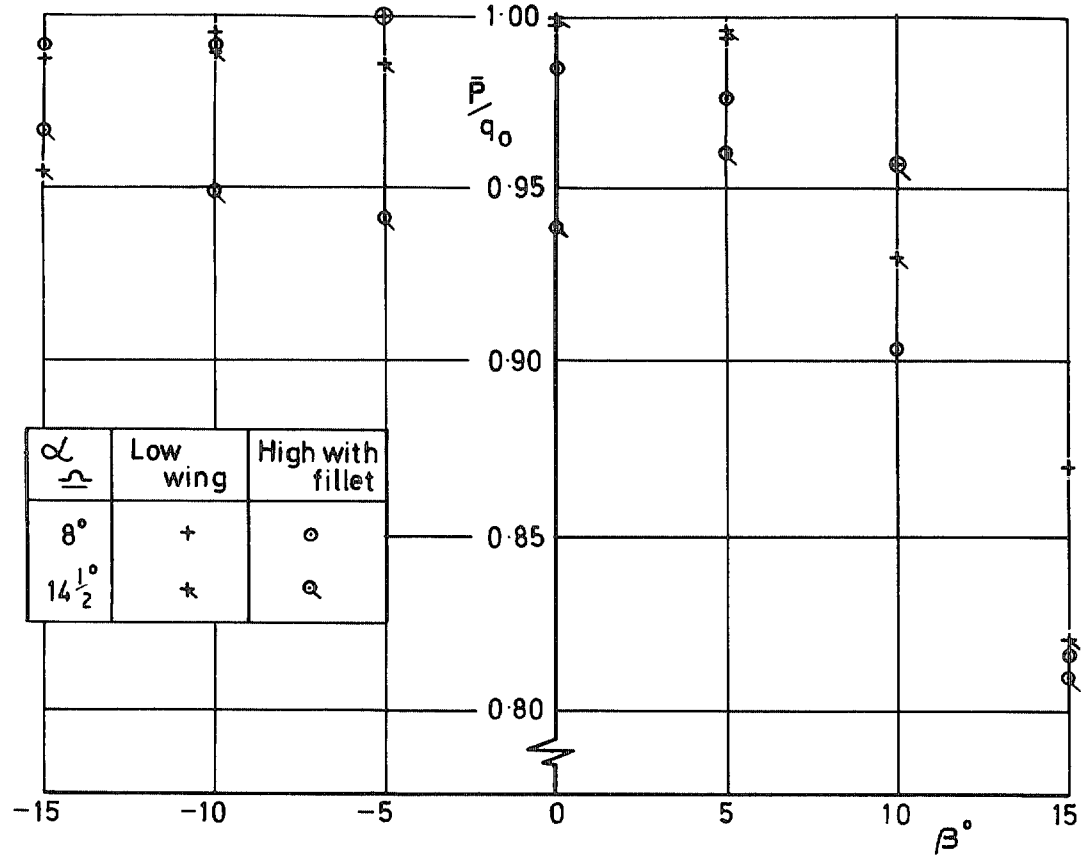

FIG. 14. Variations of total head at 'engine face' with sideslip for round nacelles, slats 25° and flaps 40°.

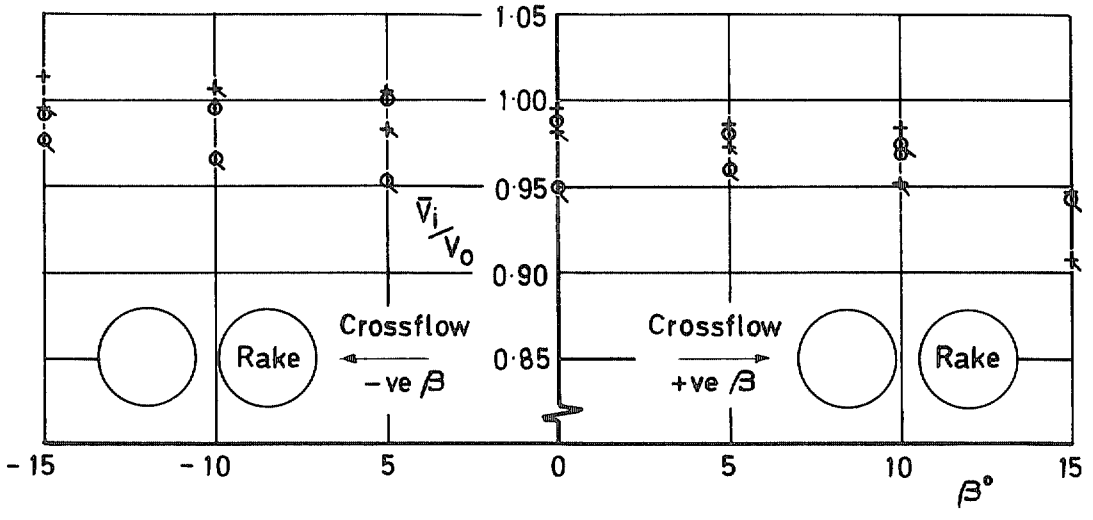

FIG. 15. Variation of entry velocity ratio with sideslip for round nacelles, slats 25° and flaps 40°.

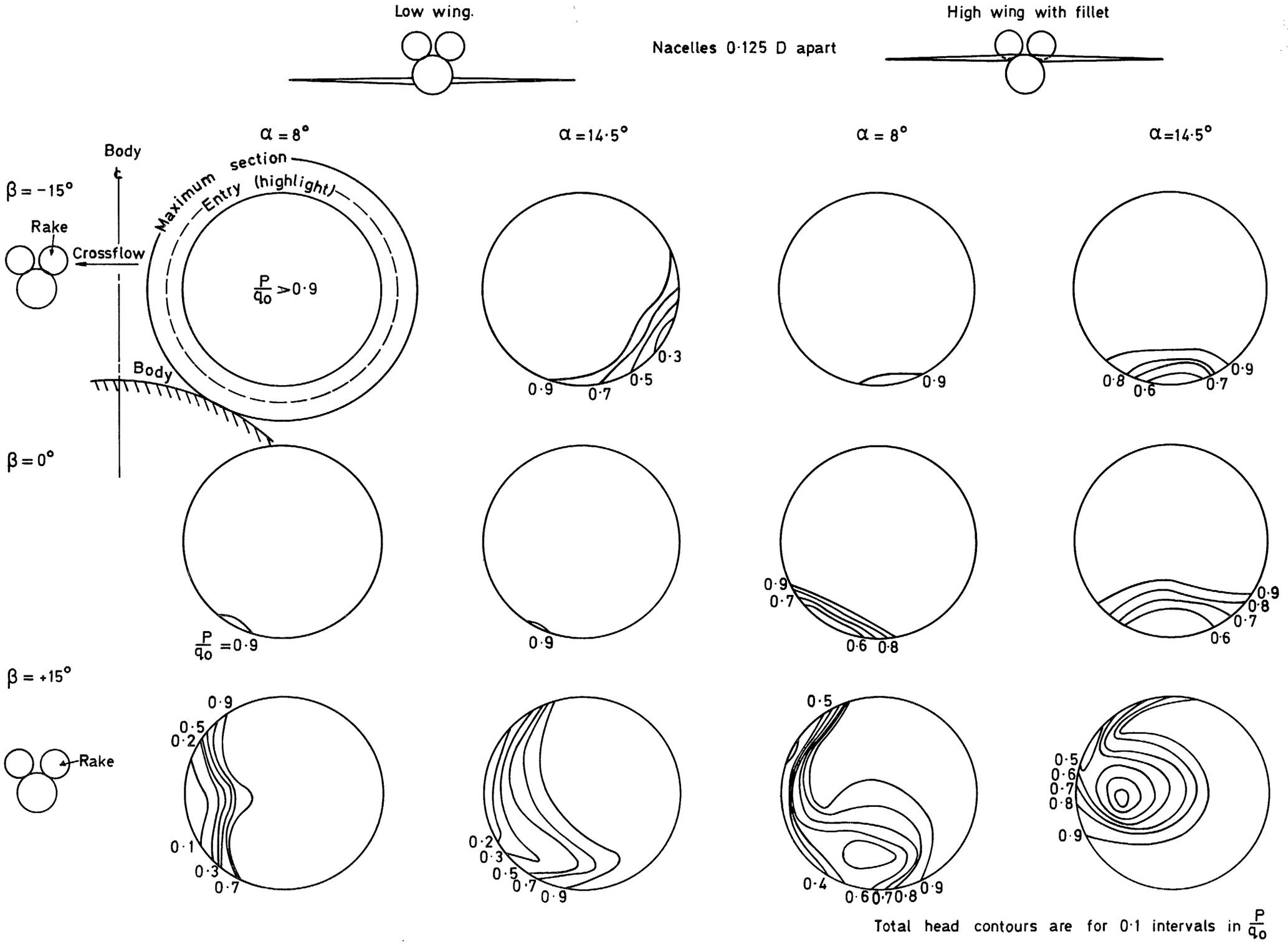

FIG. 16. Effect of sideslip on total head distributions for two model configurations with slats 25° and flaps 40°.

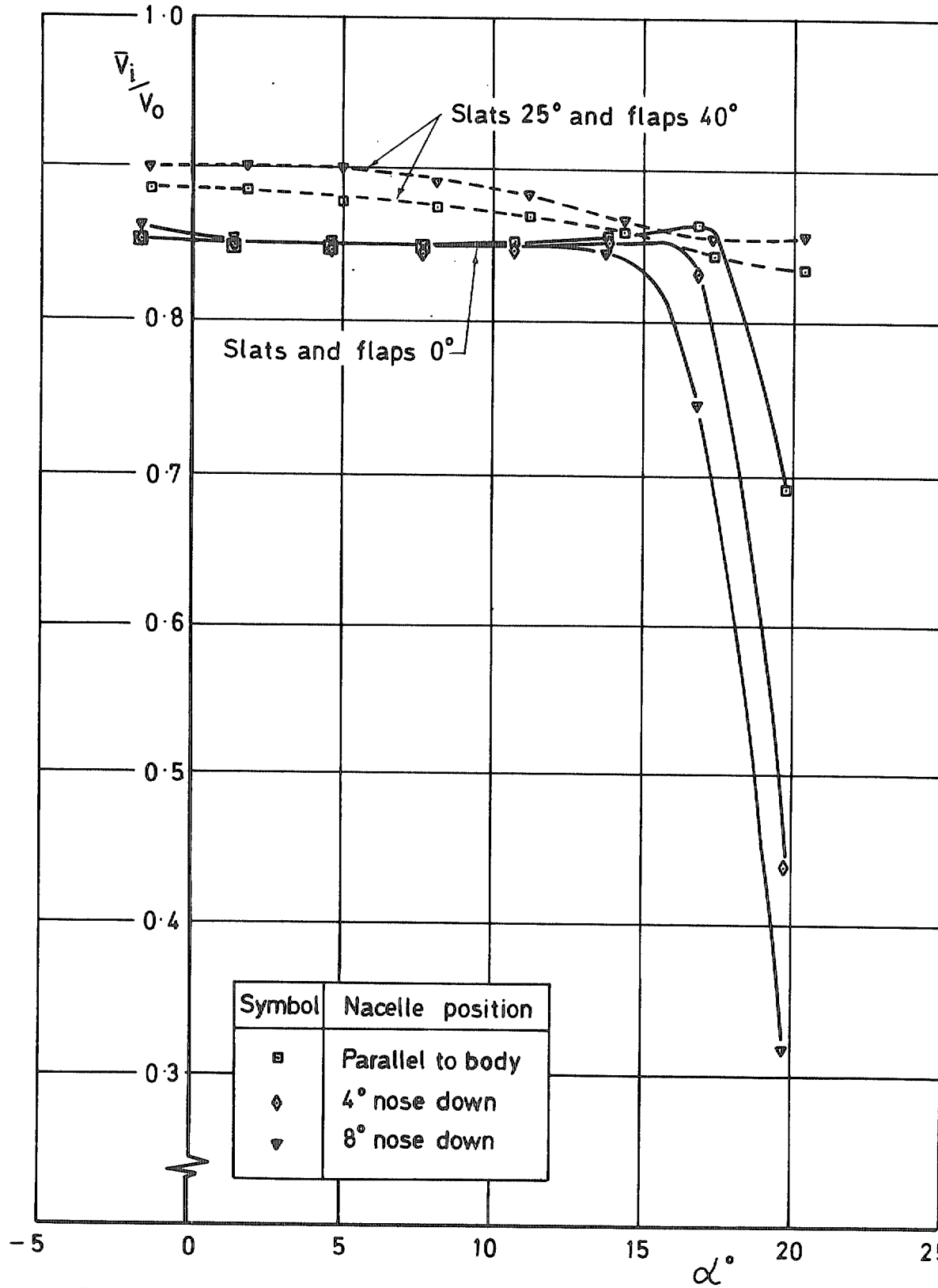

FIG. 17. Variation of entry velocity ratio with incidence for flat nacelles—low-wing model.

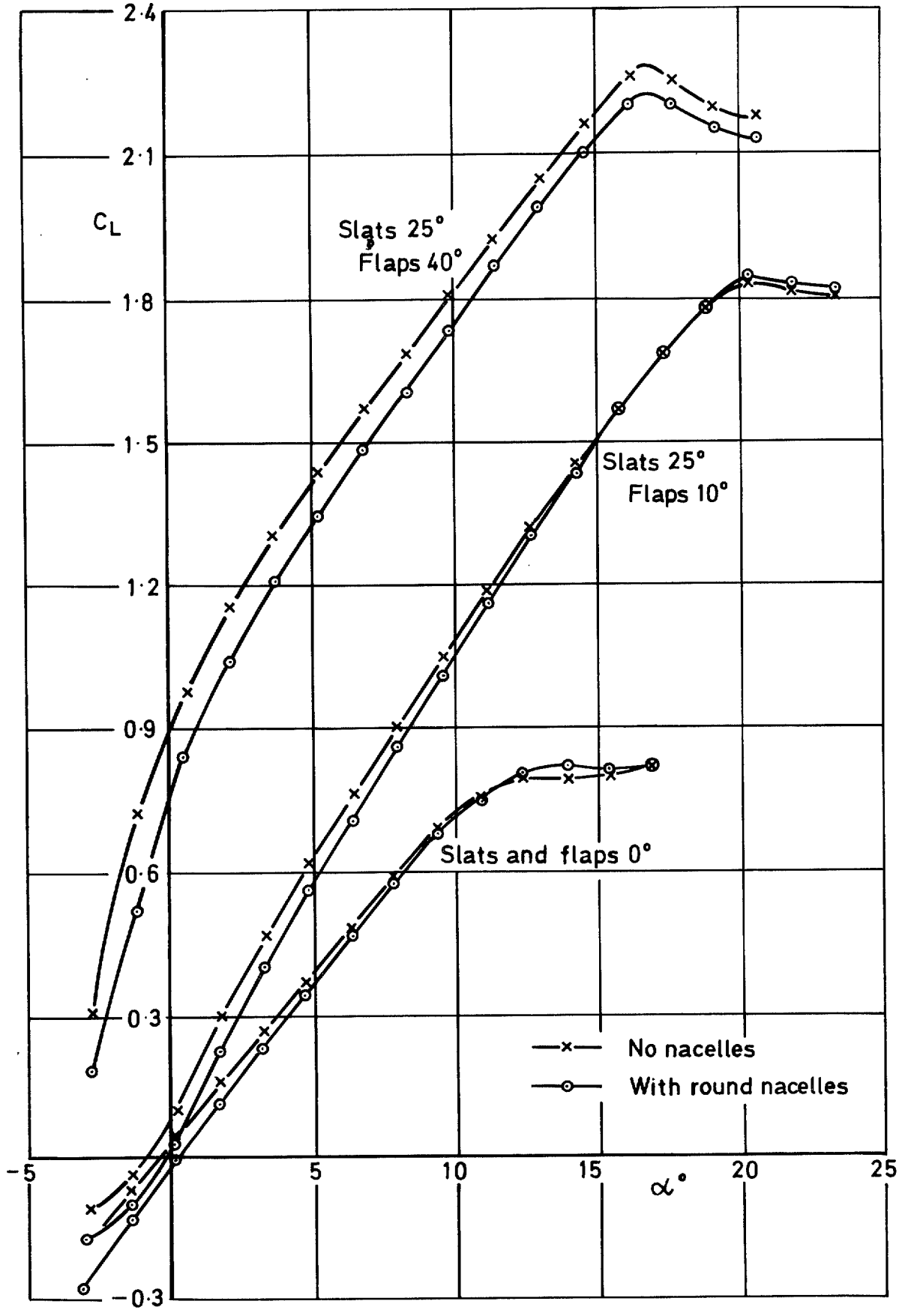

FIG. 18. Effect of round nacelles on lift coefficient of high-wing model without tailplane.

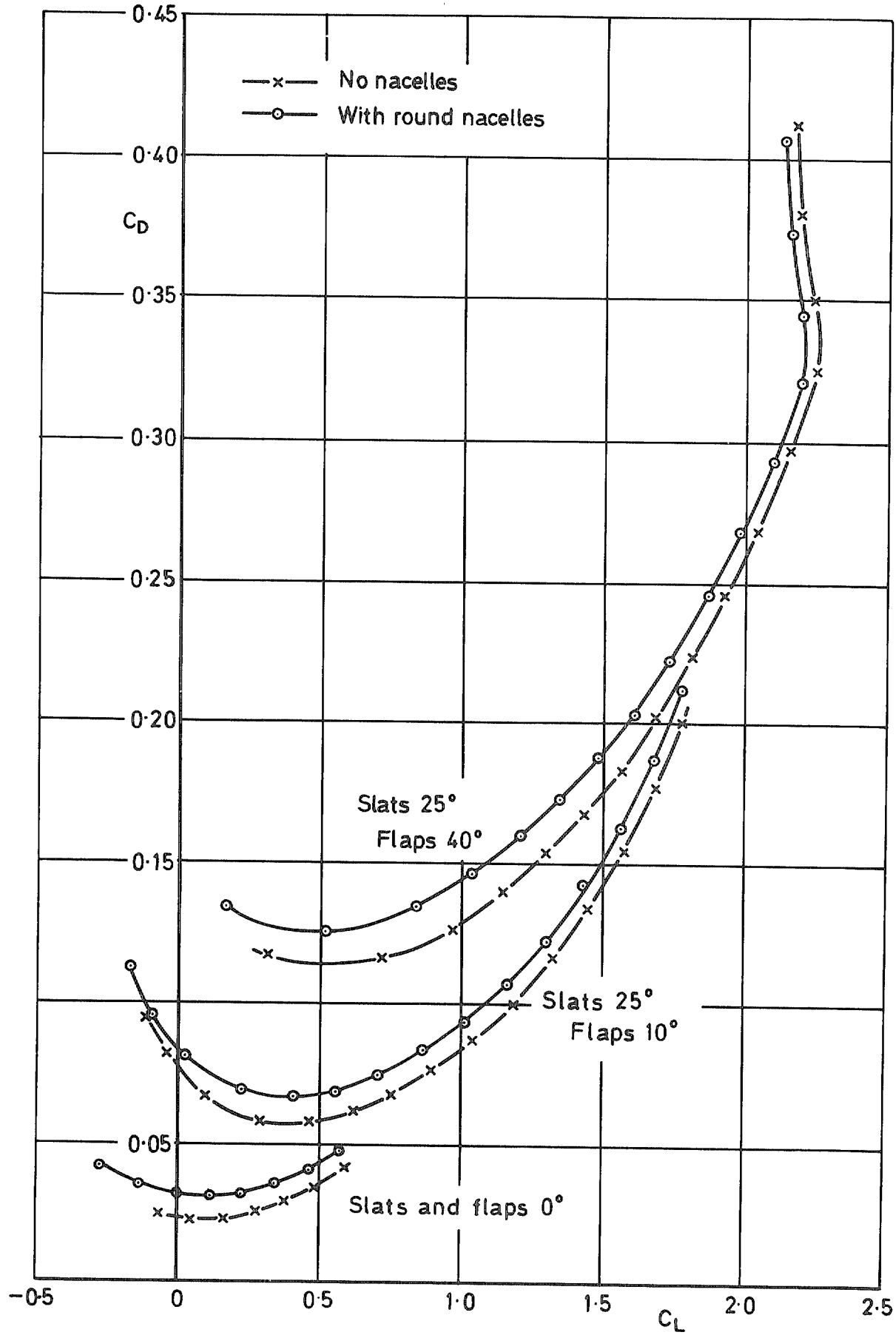

FIG. 19. Effect of round nacelles on drag coefficient of high-wing model without tailplane.

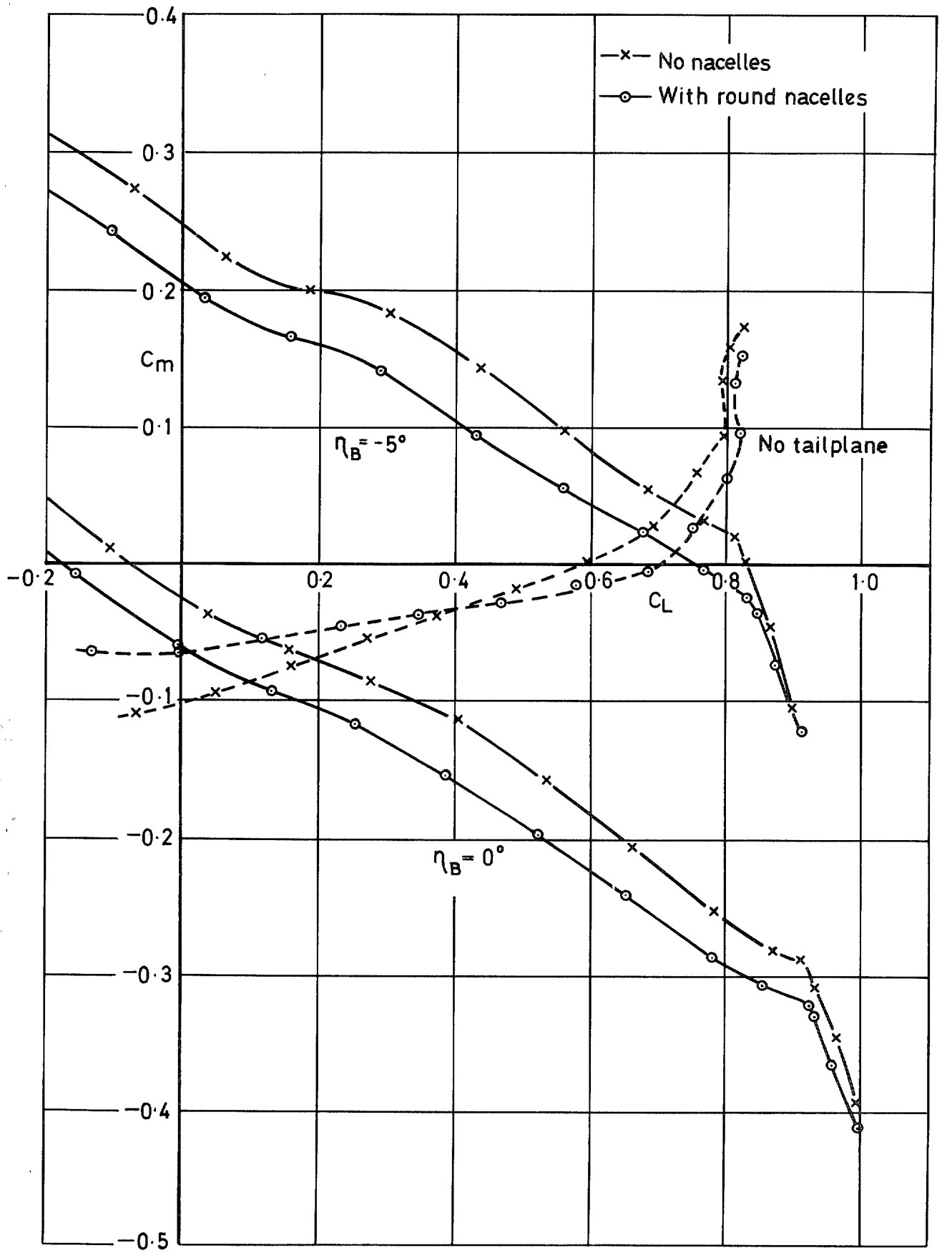

FIG. 20. Effect of round nacelles on pitching moment coefficient of high-wing model with slats and flaps 0°.

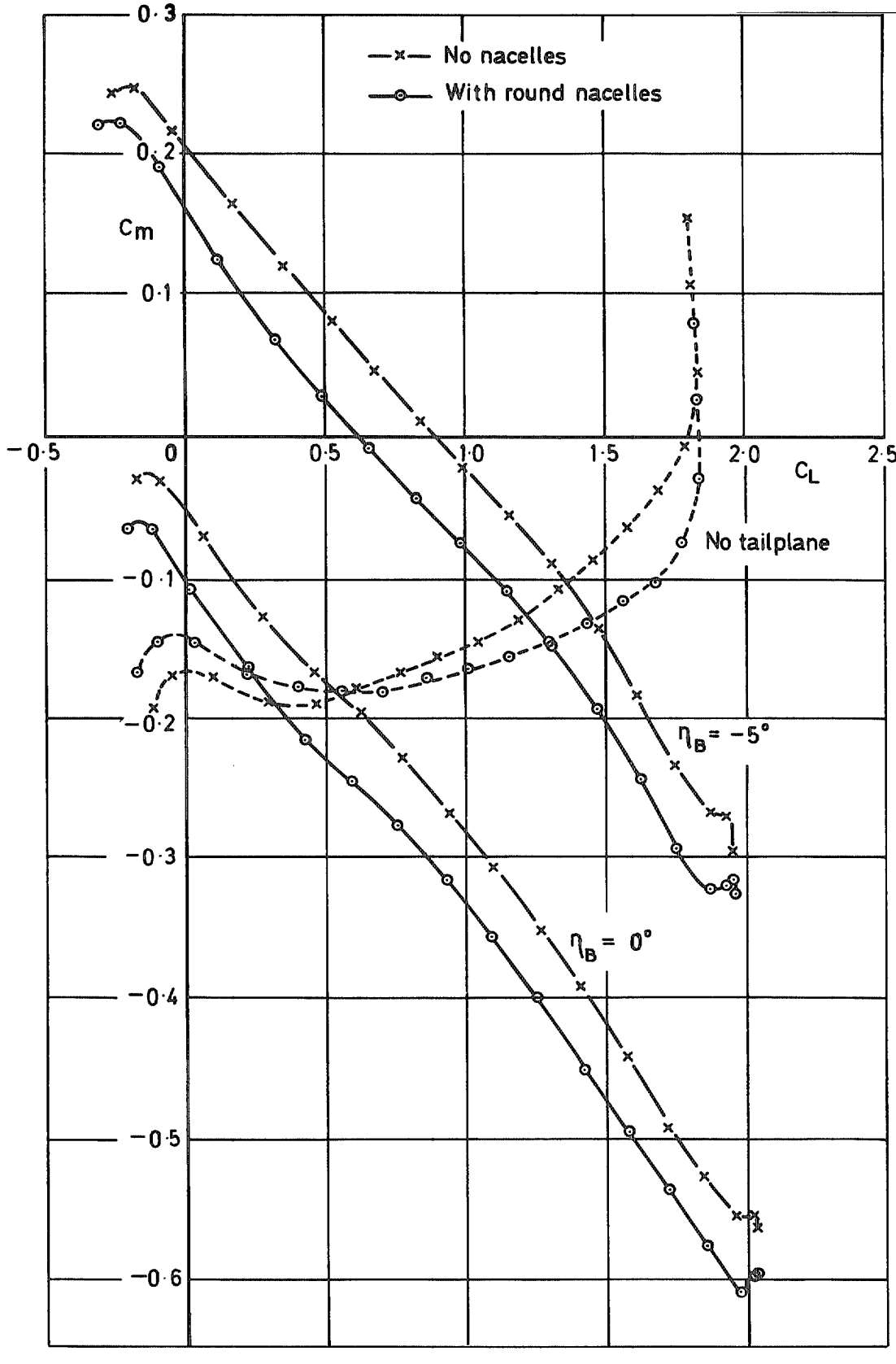

FIG. 21. Effect of round nacelles on pitching moment coefficient of high-wing model with slats 25° and flaps 10°.

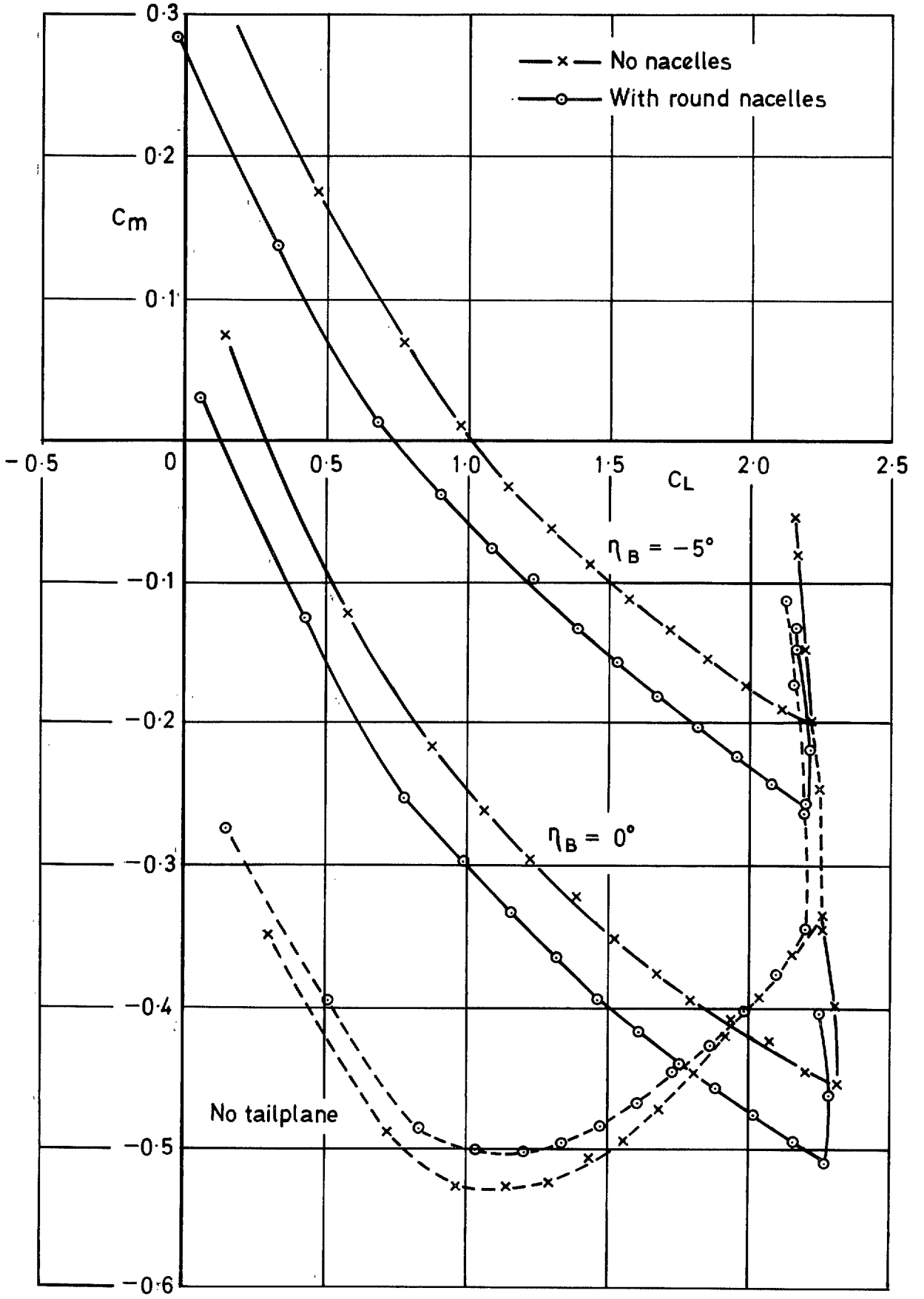

FIG. 22. Effect of round nacelles on pitching moment coefficient of high-wing model with slats 25° and flaps 40°.

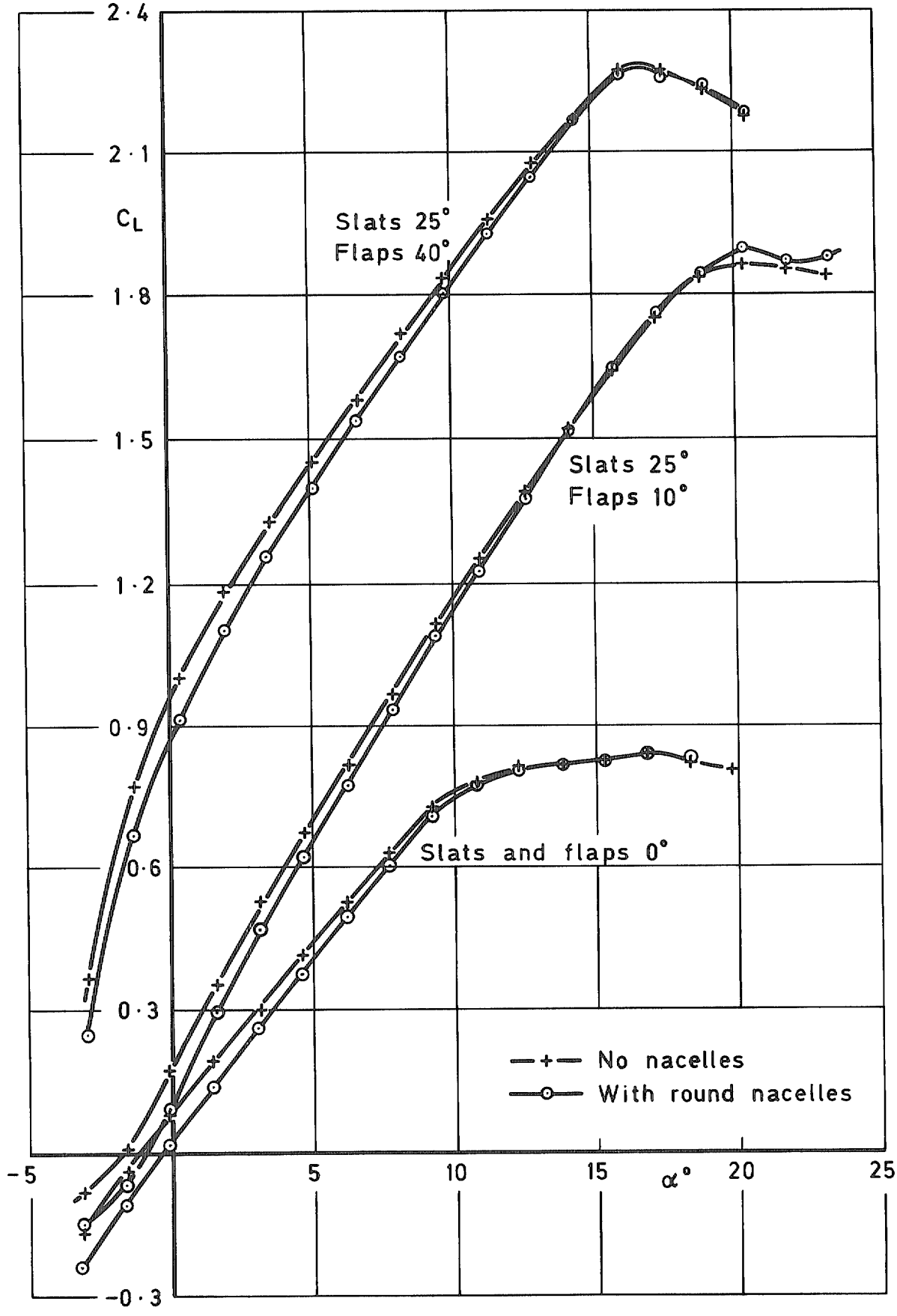

FIG. 23. Effect of round nacelles on lift coefficient of low-wing model without tailplane.

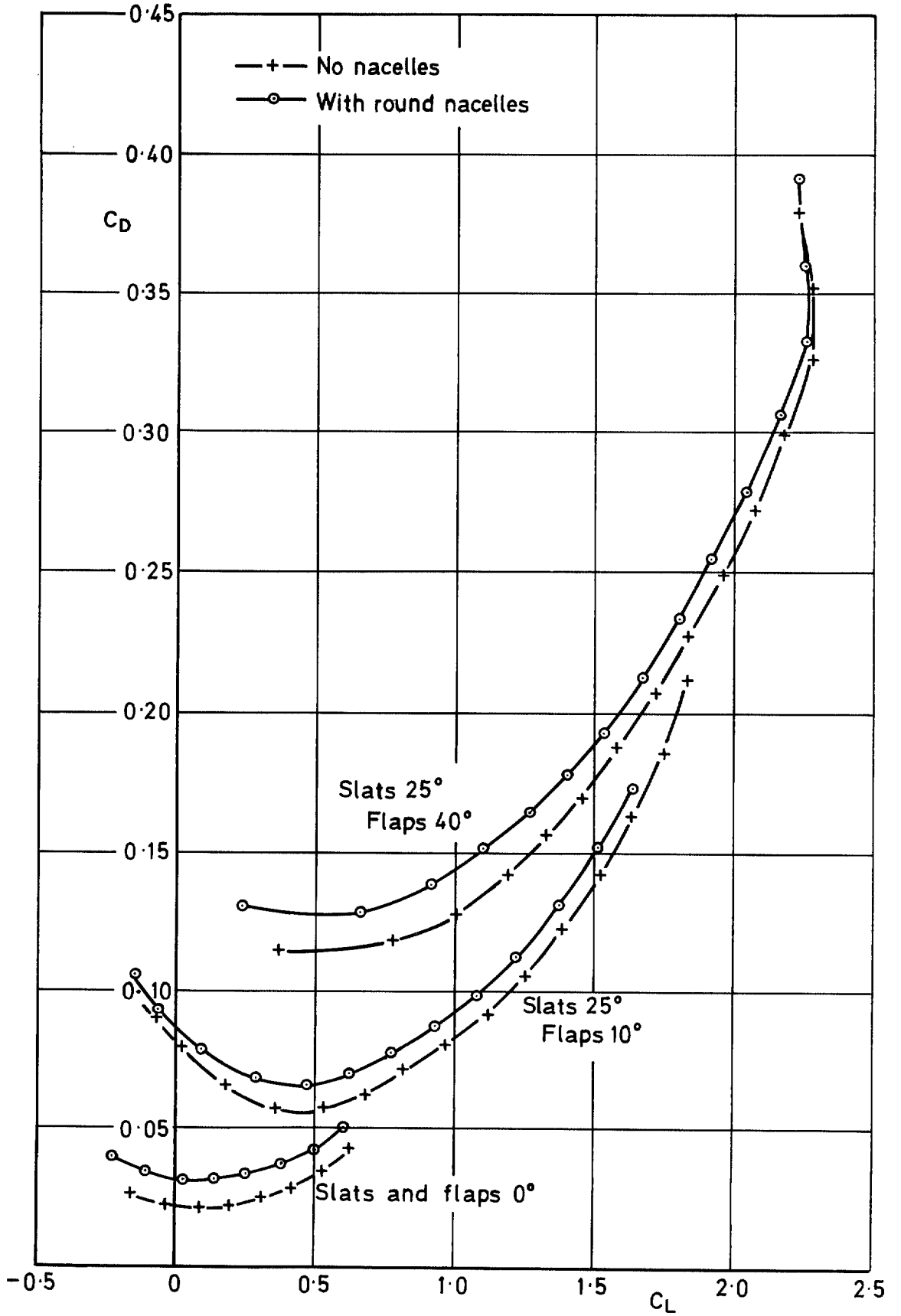

FIG. 24. Effect of round nacelles on drag coefficient of low-wing model without tailplane.

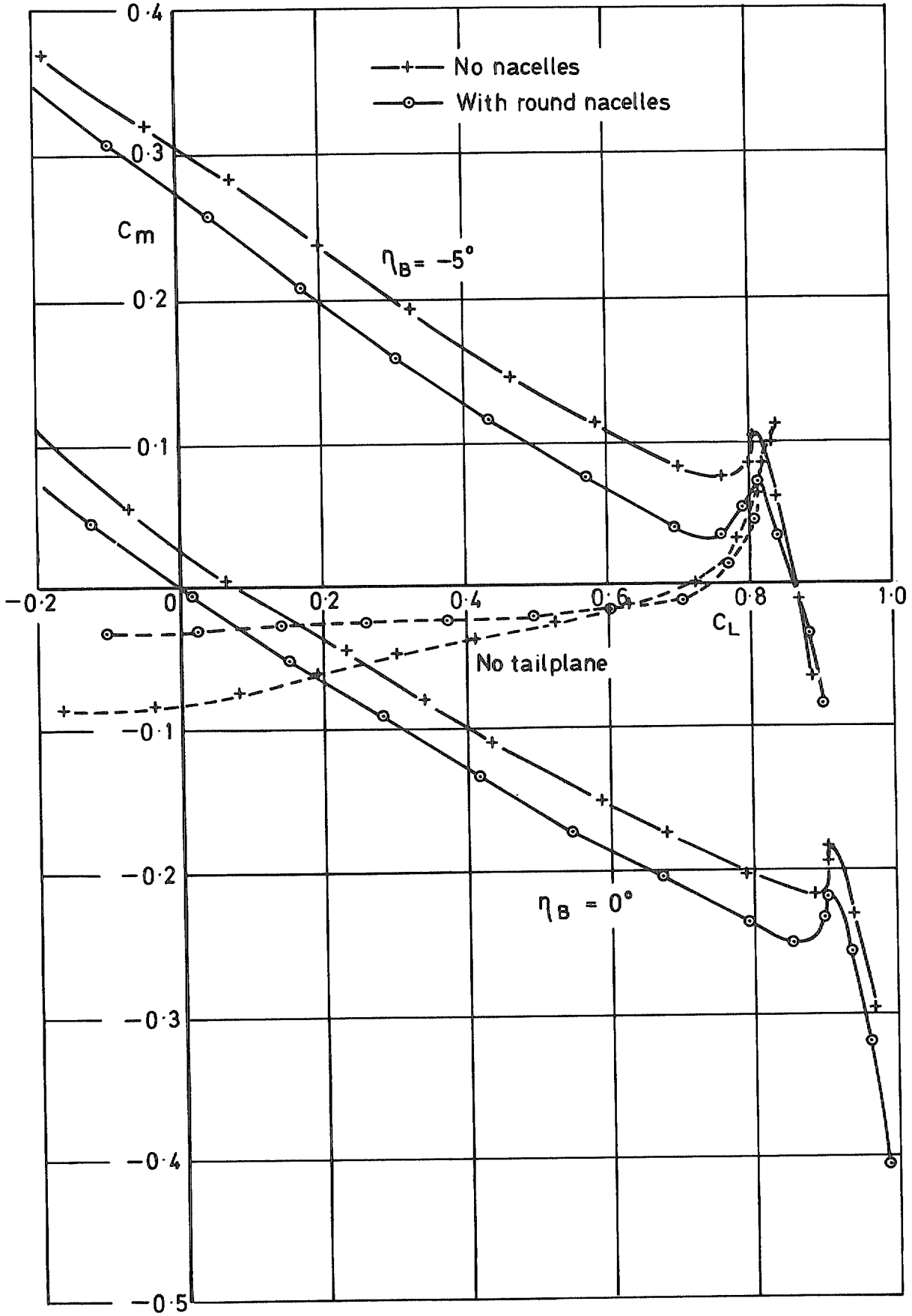

FIG. 25. Effect of round nacelles on pitching moment coefficient of low-wing model with slats and flaps 0°.

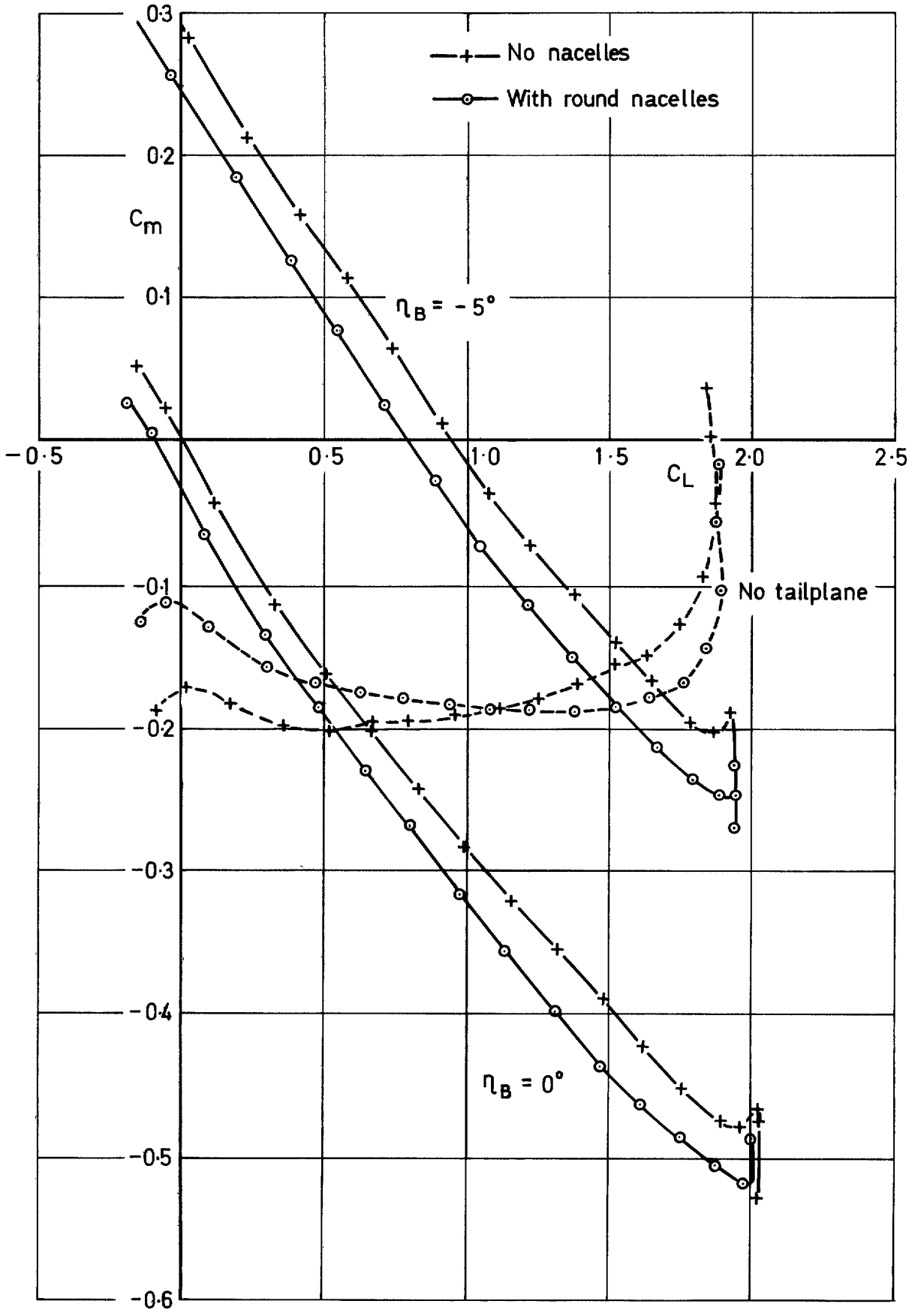

FIG. 26. Effect of round nacelles on pitching moment coefficient of low-wing model with slats 25° and flaps 10°.

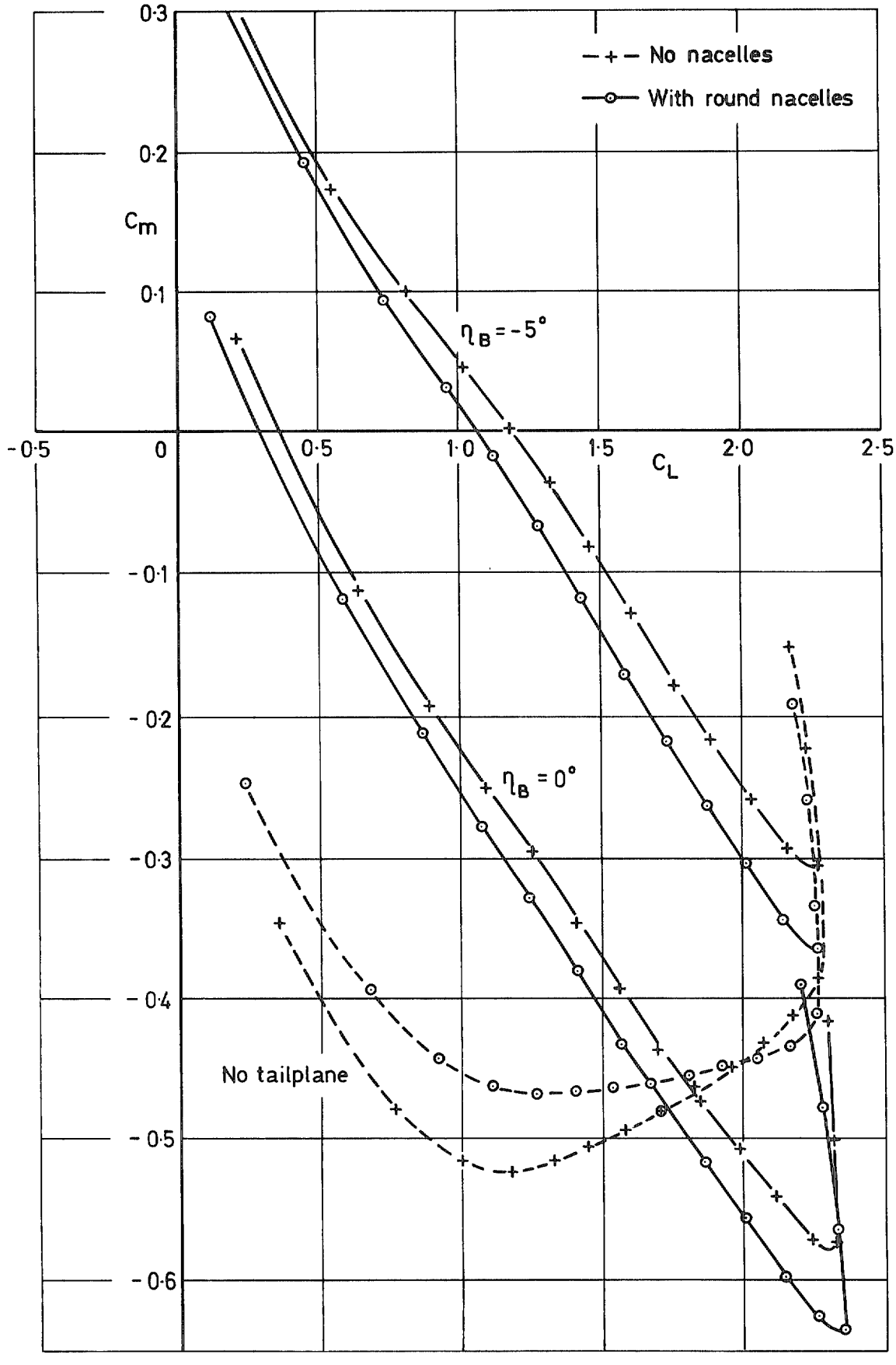

FIG. 27. Effect of round nacelles on pitching moment coefficient of low-wing model with slats 25° and flaps 40°.

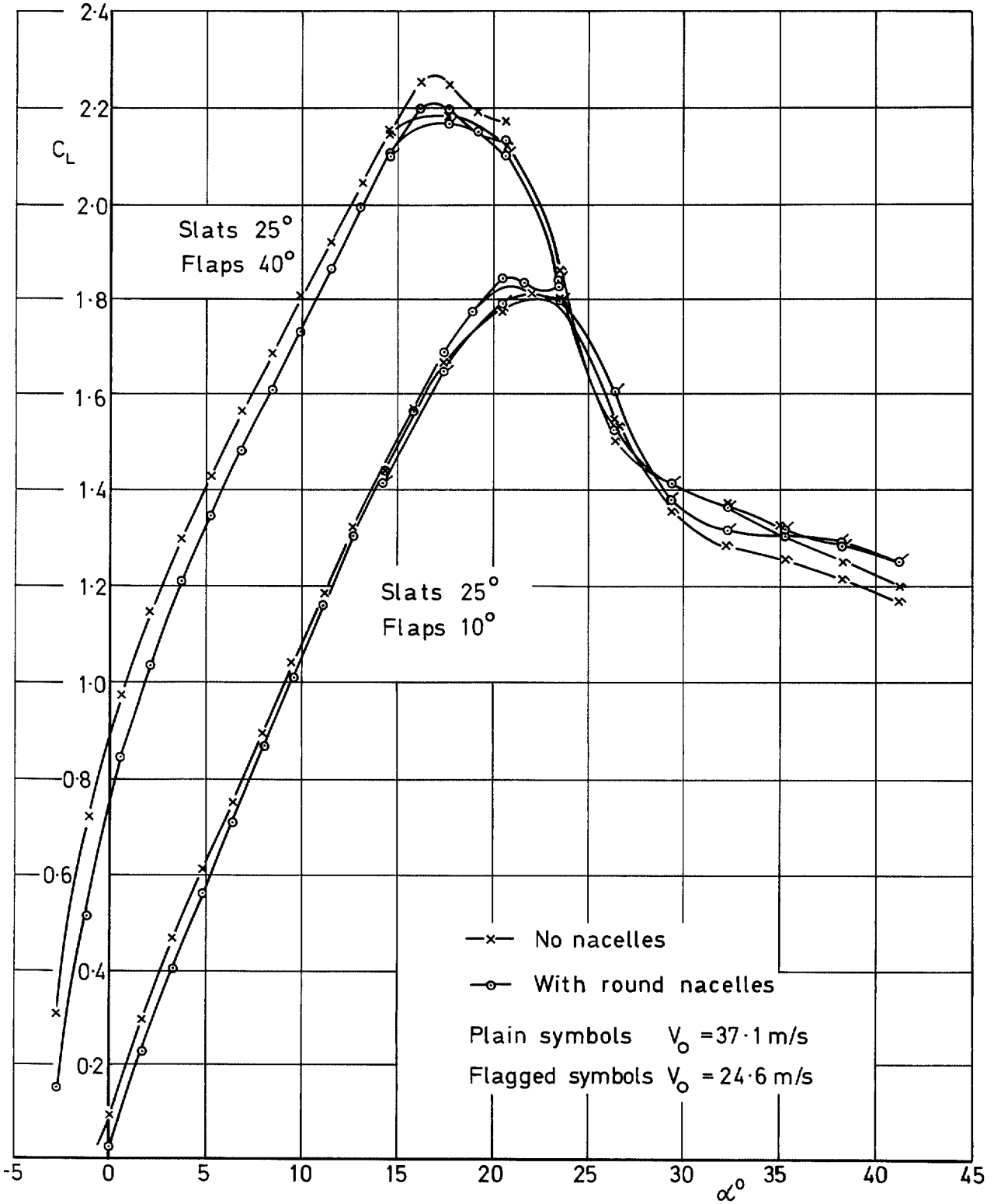

FIG. 28. High-wing, lift coefficient at high incidence.

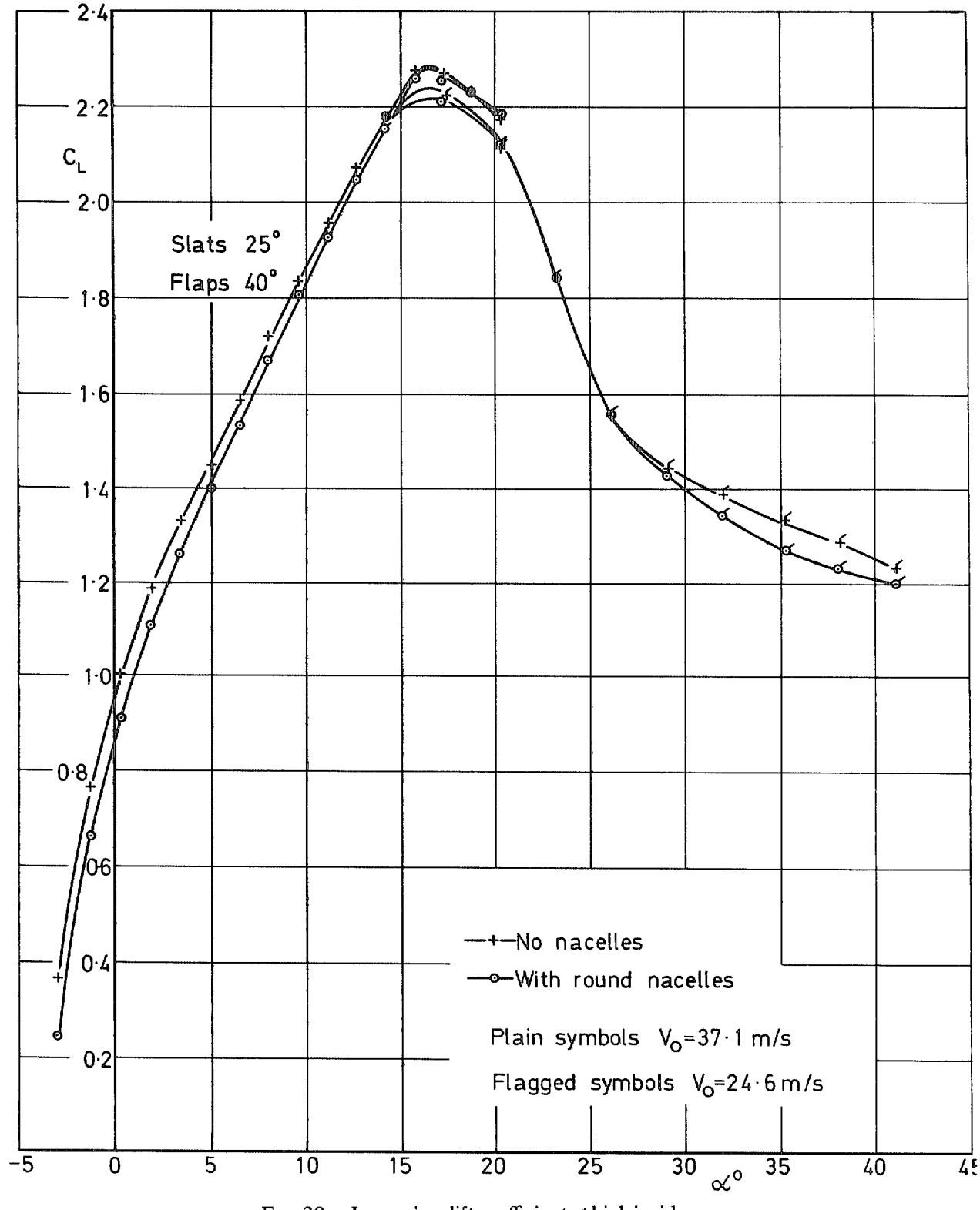

FIG. 29. Low-wing, lift coefficient at high incidence.

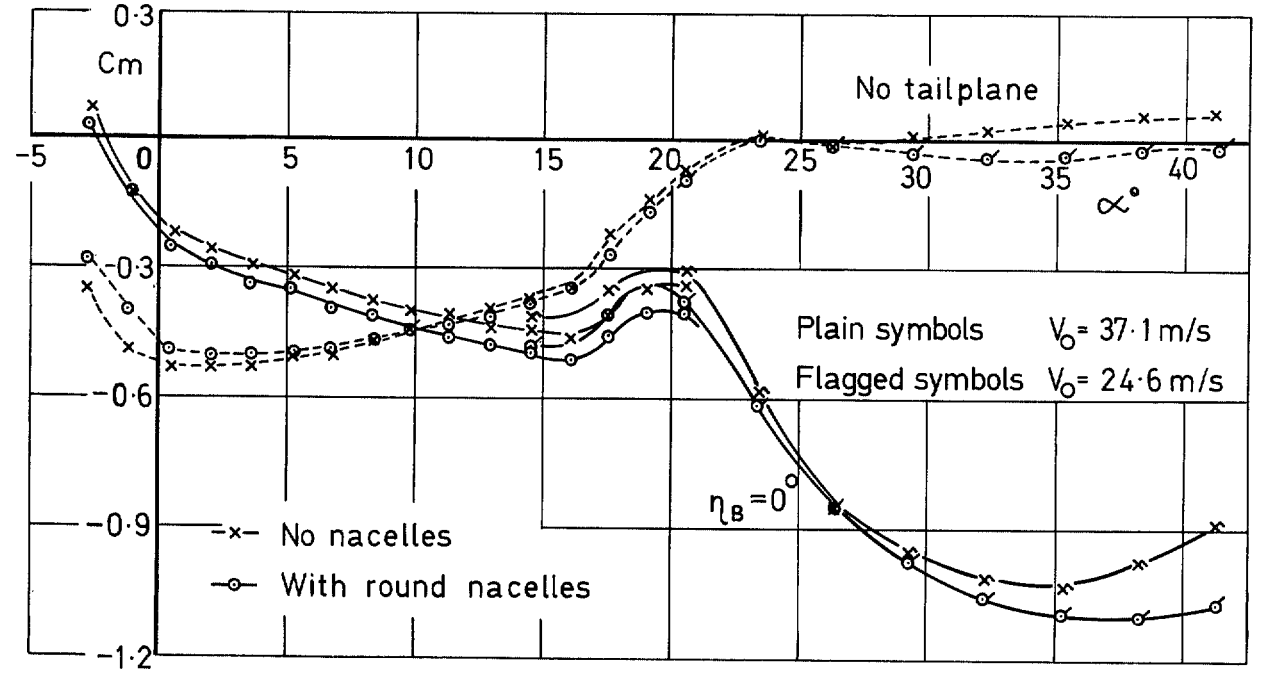

FIG. 30. High-wing, pitching moment coefficient at high incidence with slats 25° and flaps 40°.

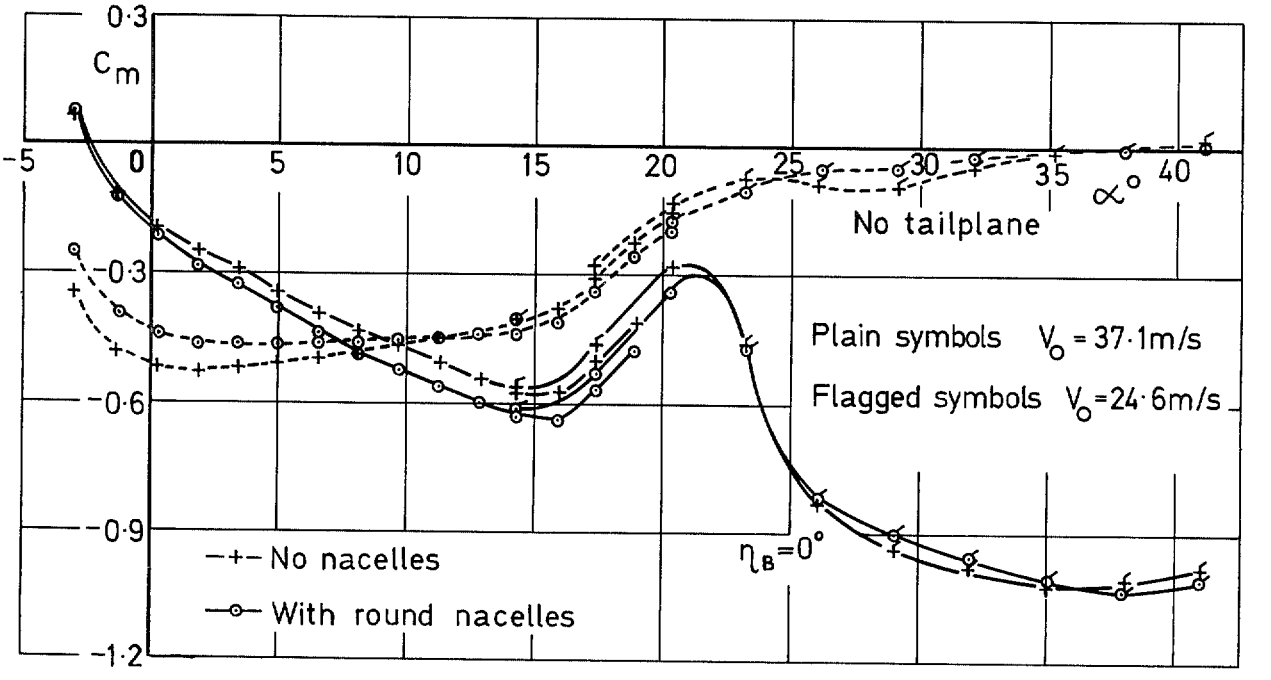

FIG. 31. Low-wing, pitching moment coefficient at high incidence with slats 25° and flaps 40°.

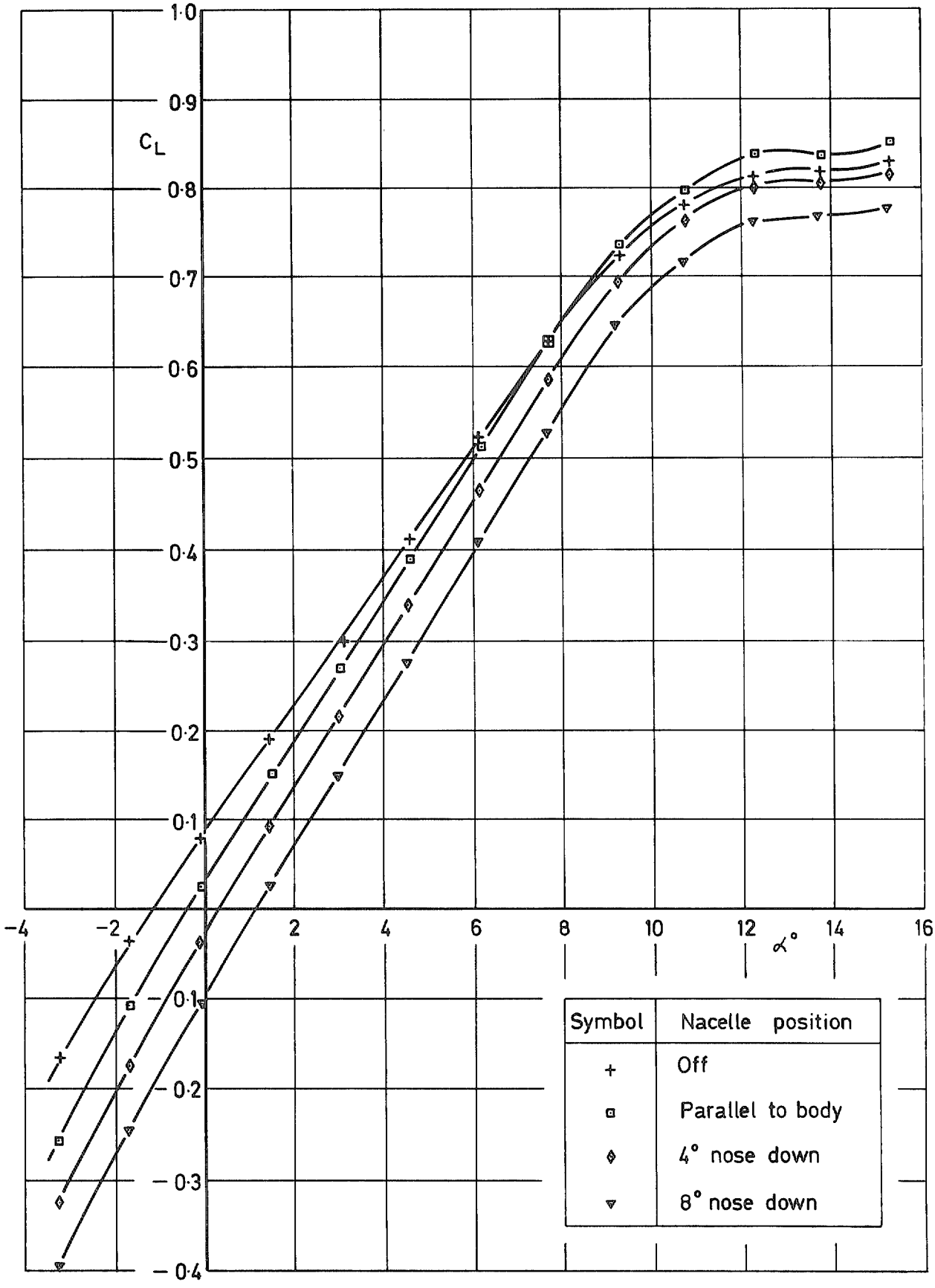

FIG. 32. Effect of flat nacelles on lift coefficient of low-wing model without tailplane, slats and flaps 0°.

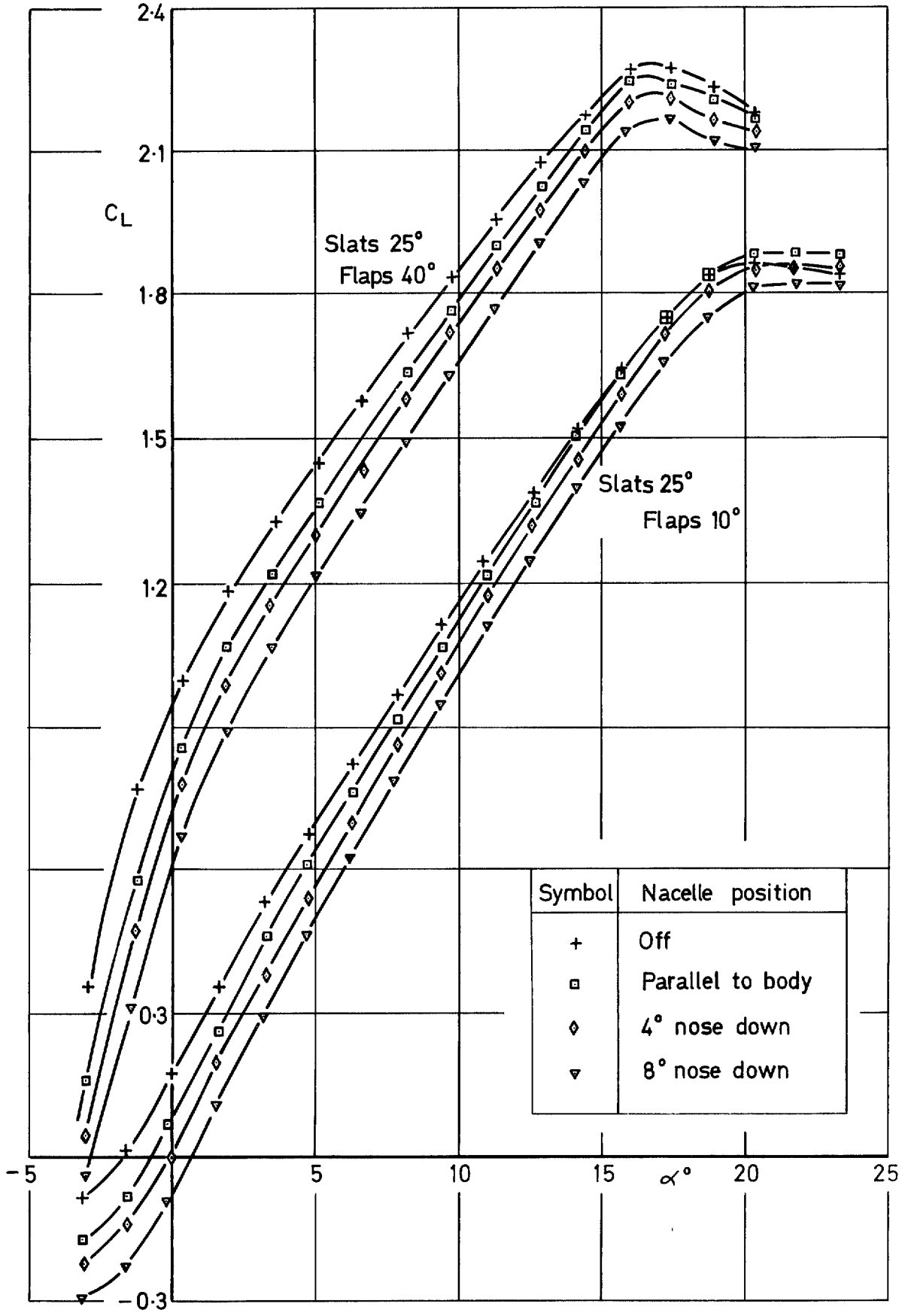

FIG. 33. Effect of flat nacelles on lift coefficient of low-wing model without tailplane, flaps 10° and 40°.

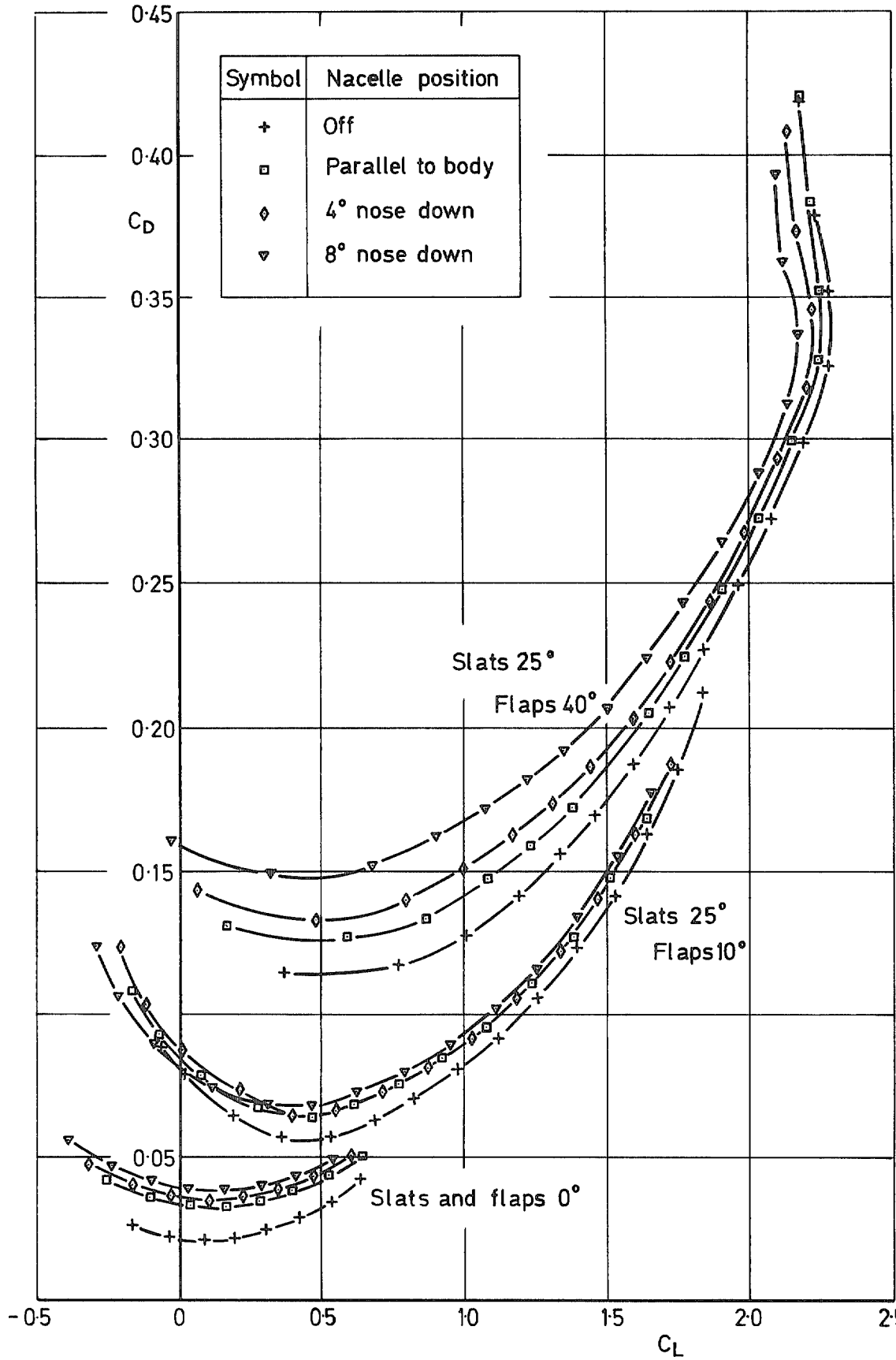

FIG. 34. Effect of flat nacelles on drag coefficient of low-wing model without tailplane.

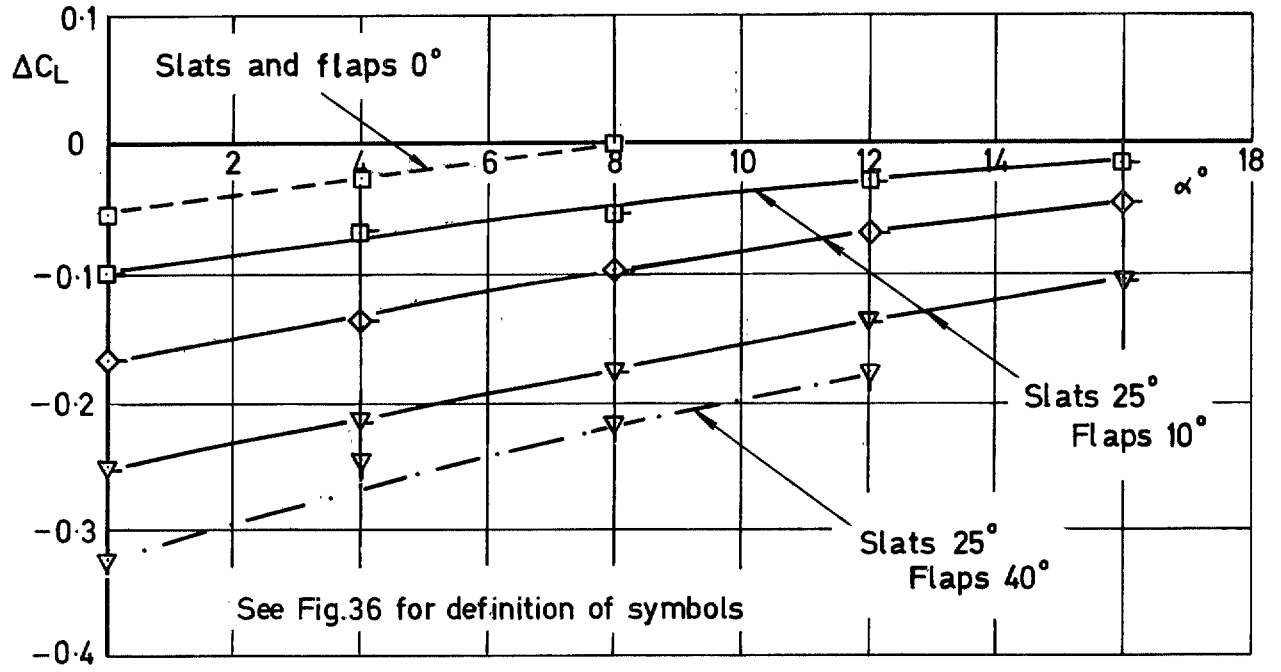

a Lift coefficient

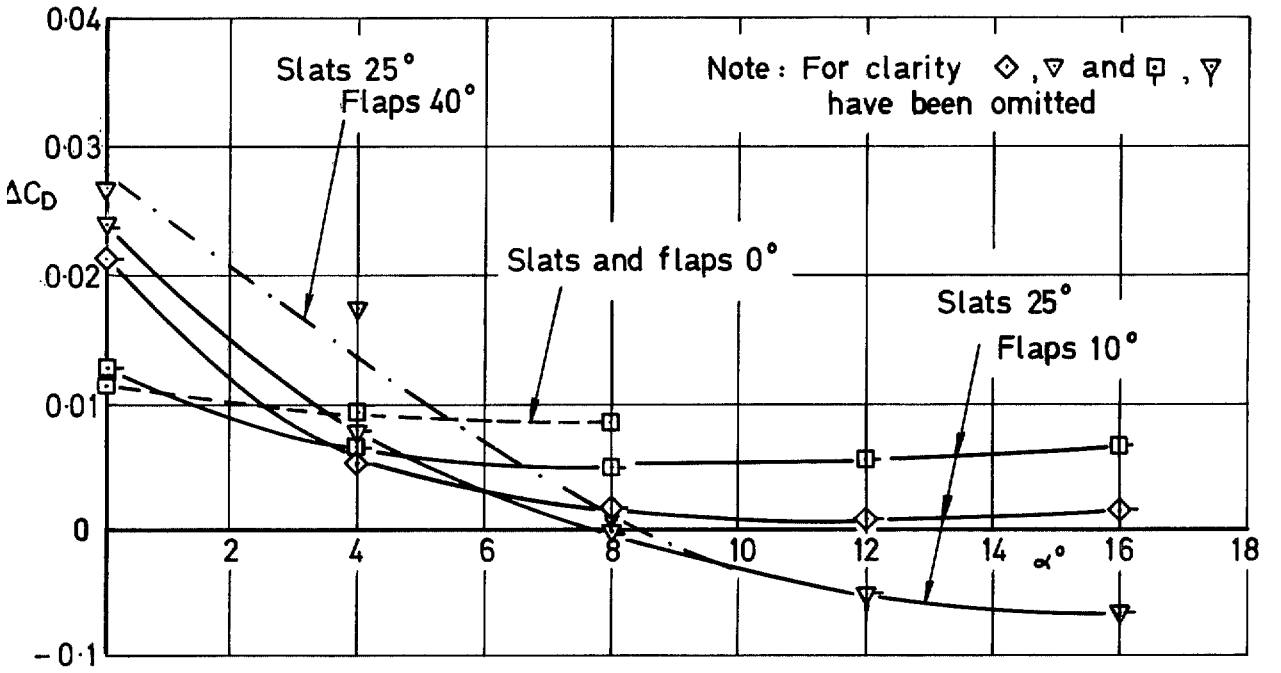

b Drag coefficient

FIG. 35 a and b. Changes in lift and drag coefficients caused by flat nacelles at constant wing incidence.

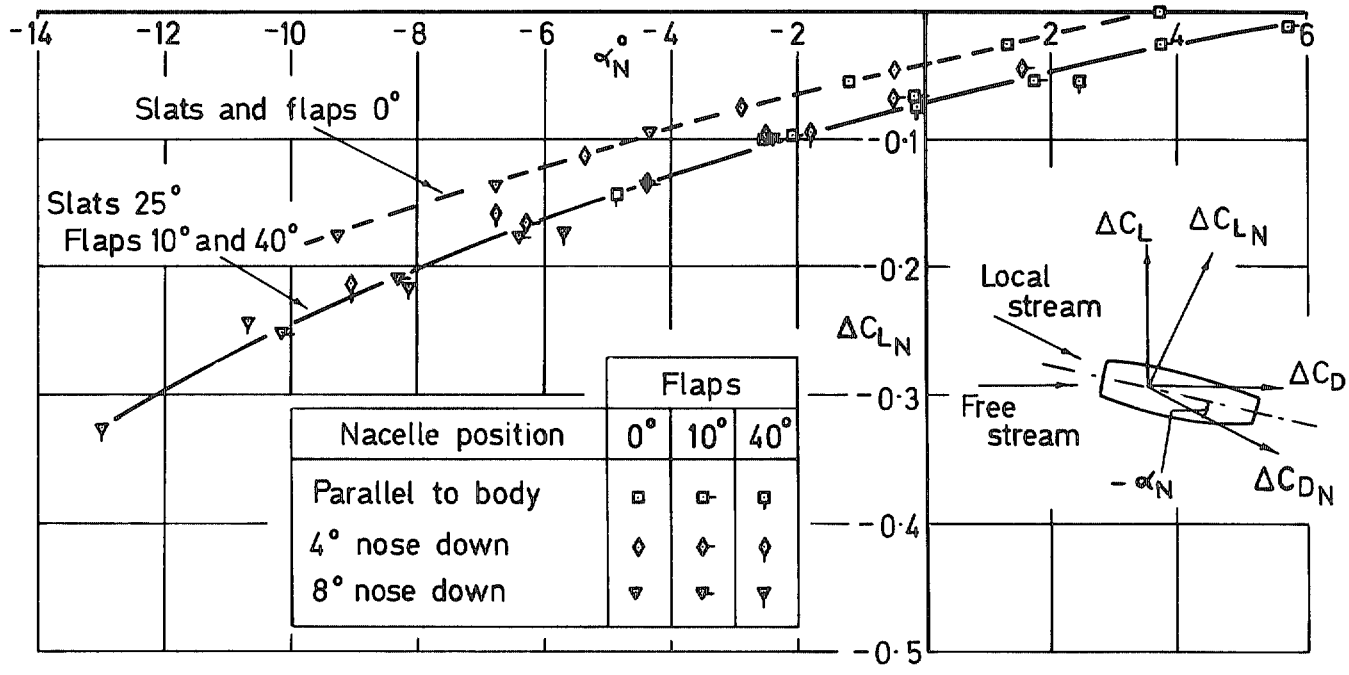

a Lift coefficient

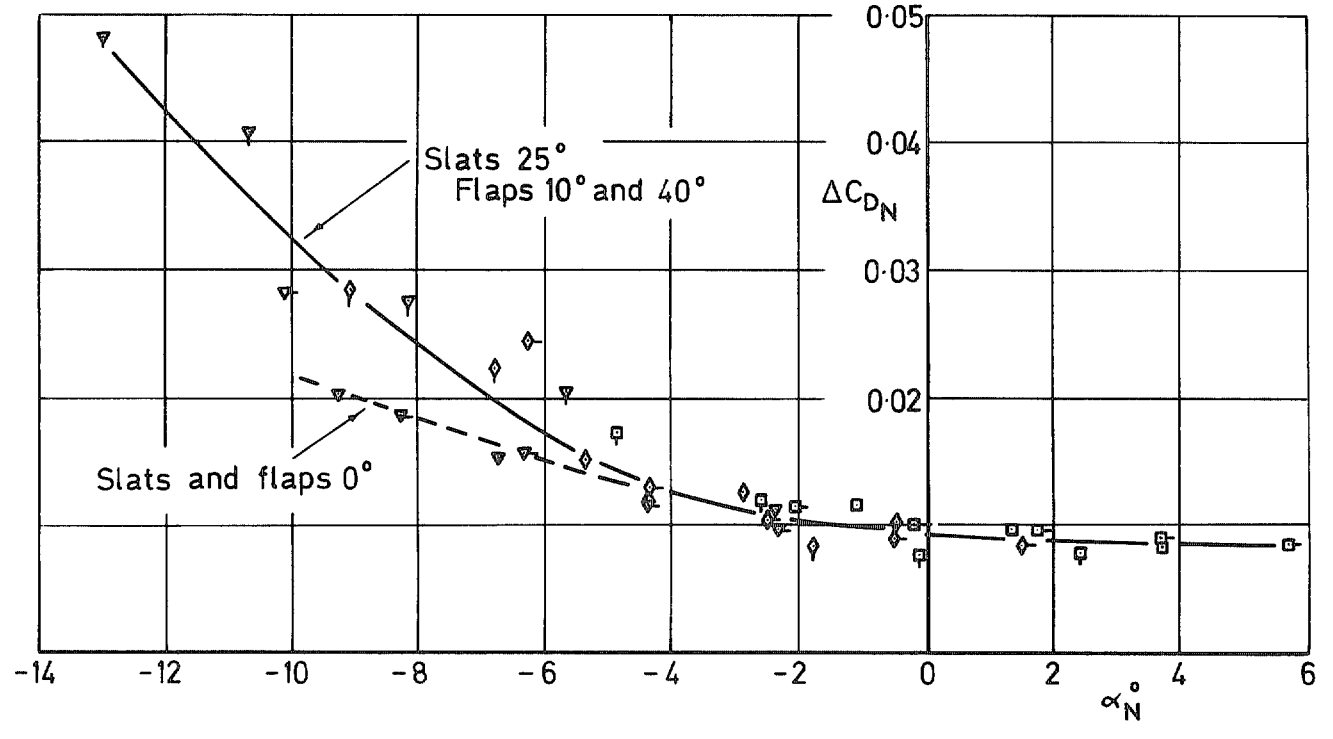

b Drag coefficient

FIG. 36 a and b. Changes in lift and drag coefficients caused by flat nacelles referred to mean local nacelle incidence.

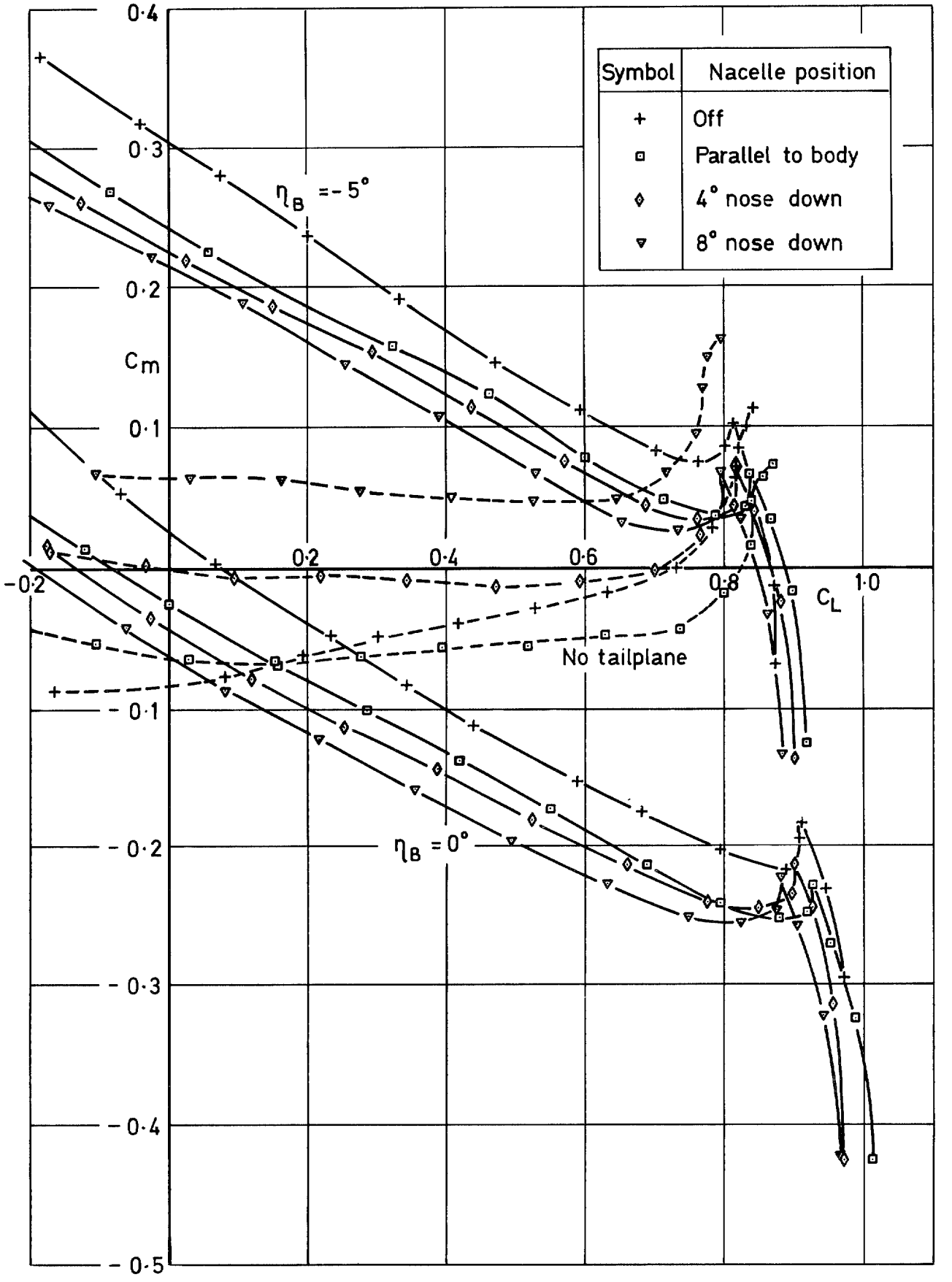

FIG. 37. Effect of flat nacelles on pitching moment coefficient of low-wing model with slats and flaps 0°.

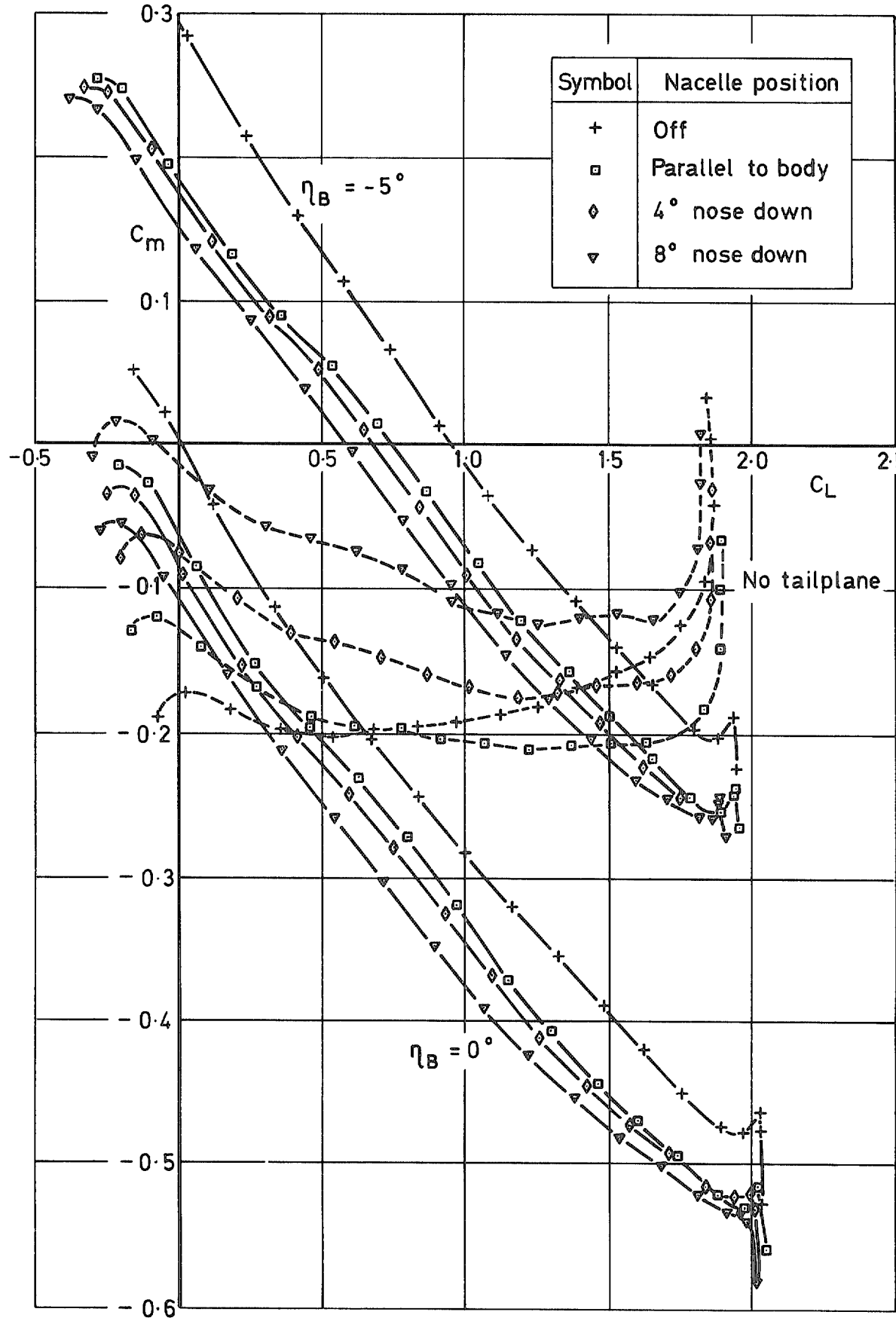

FIG. 38. Effect of flat nacelles on pitching moment coefficient of low-wing model with slats 25° and flaps 10°.

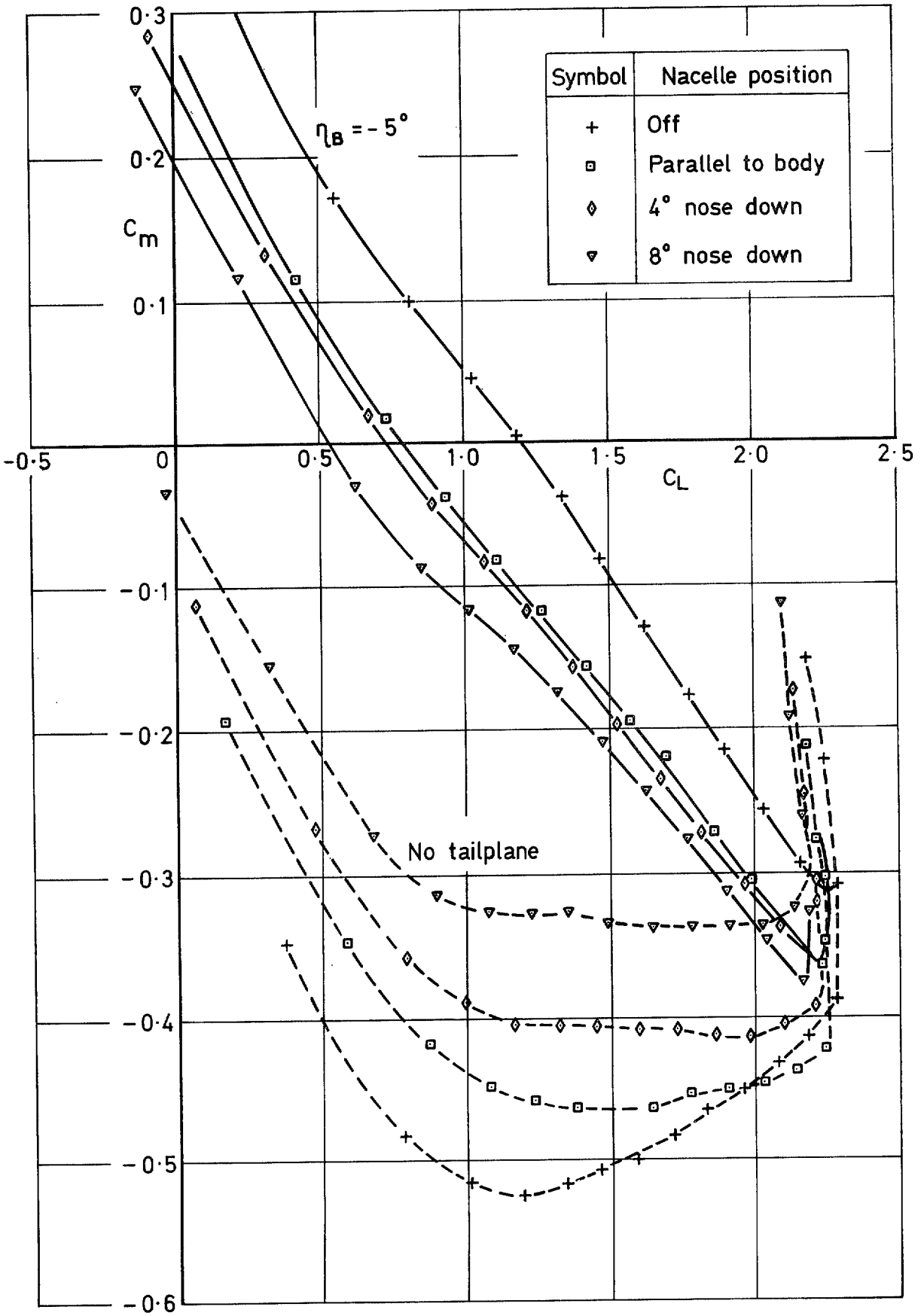

FIG. 39. Effect of flat nacelles on pitching moment coefficient of low-wing model with slats 25° and flaps 40°

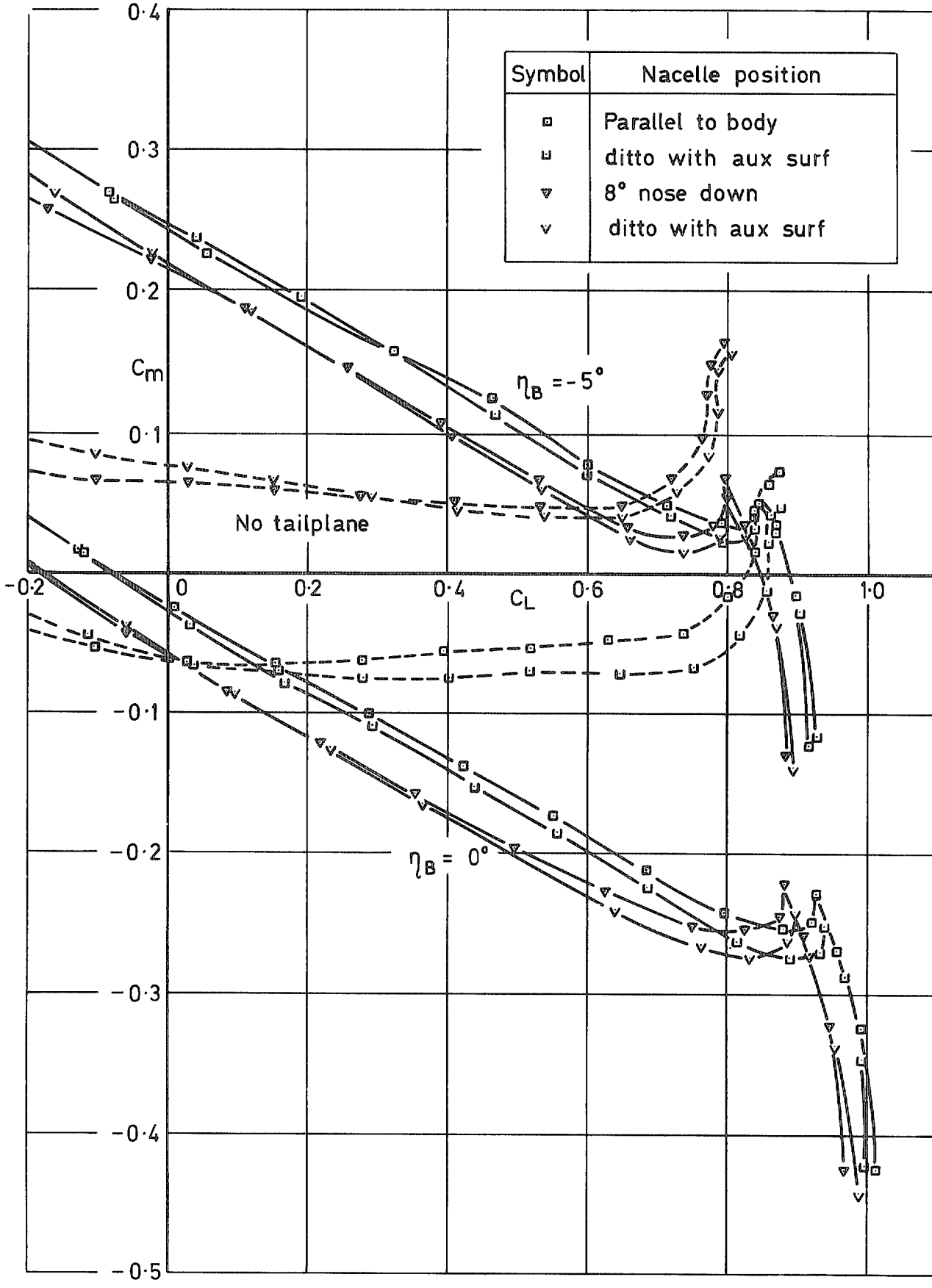

FIG. 40. Effect of adding auxiliary noise-shielding surfaces on pitching moment coefficient of low-wing model with flat nacelles, slats and flaps 0°.

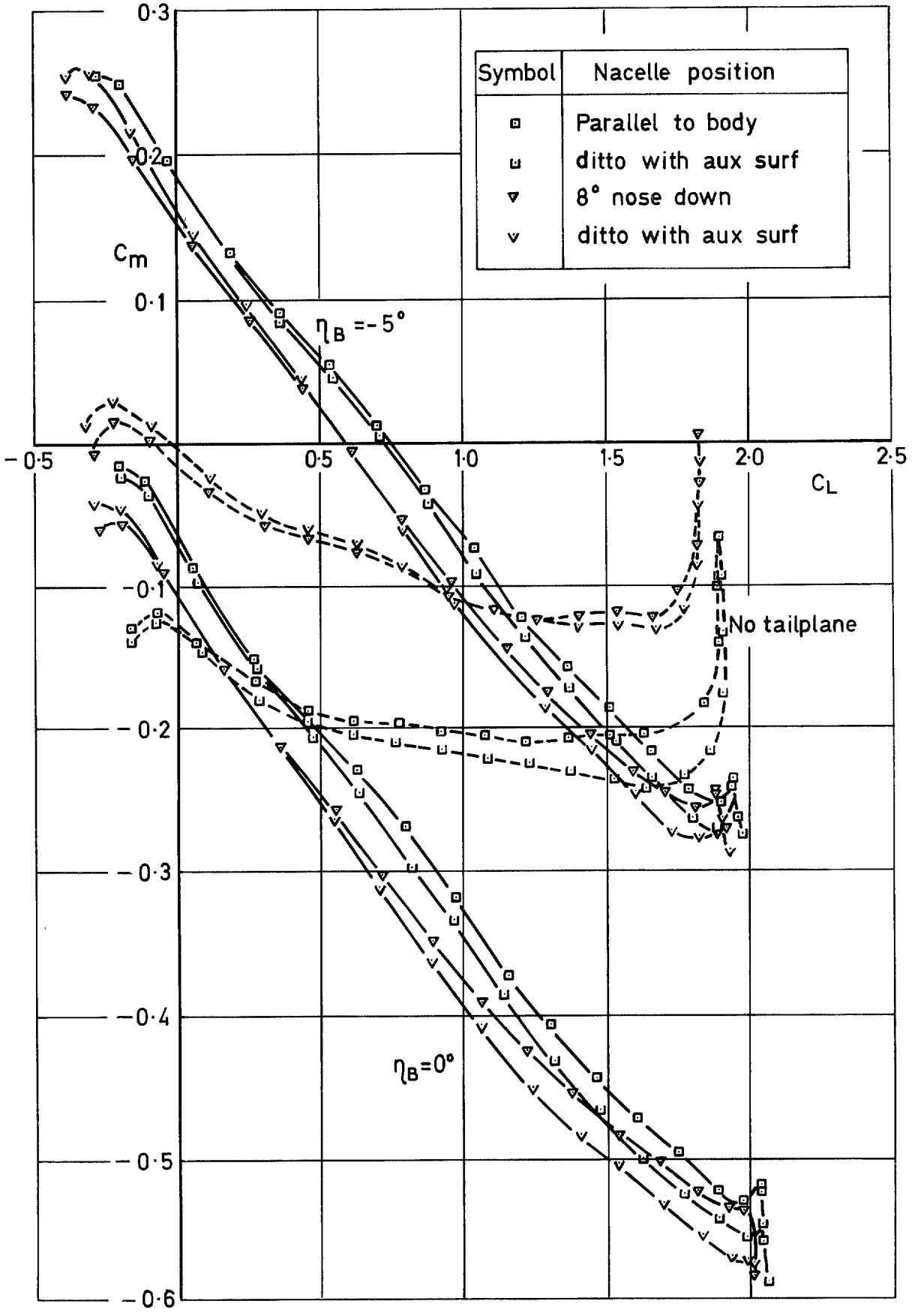

FIG. 41. Effect of adding auxiliary noise-shielding surfaces on pitching moment coefficient of low-wing model with flat nacelles, slats 25° and flaps 10°.

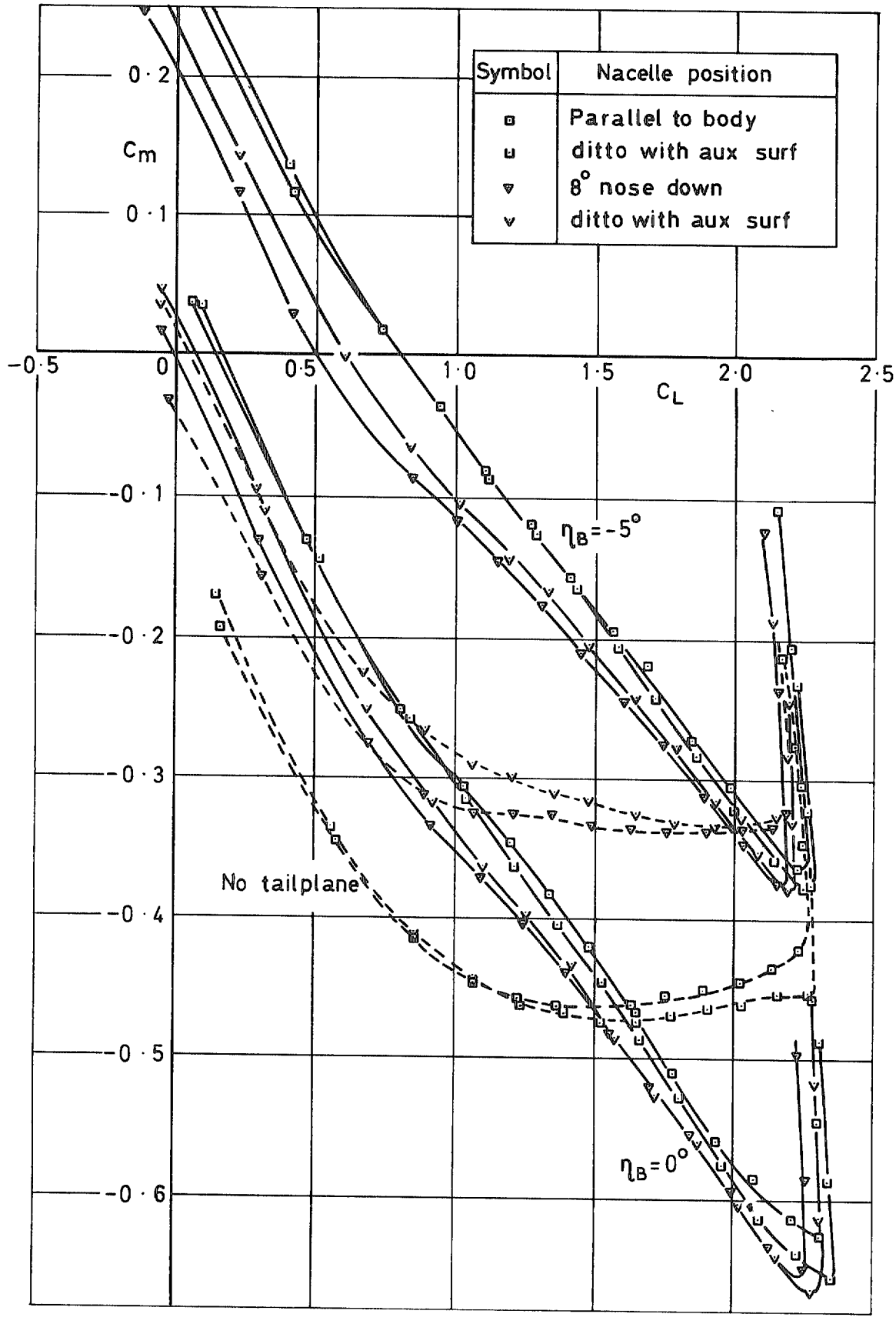

FIG. 42. Effect of adding auxiliary noise-shielding surfaces on pitching moment coefficient of low-wing model with flat nacelles, slats 25° and flaps 40°.

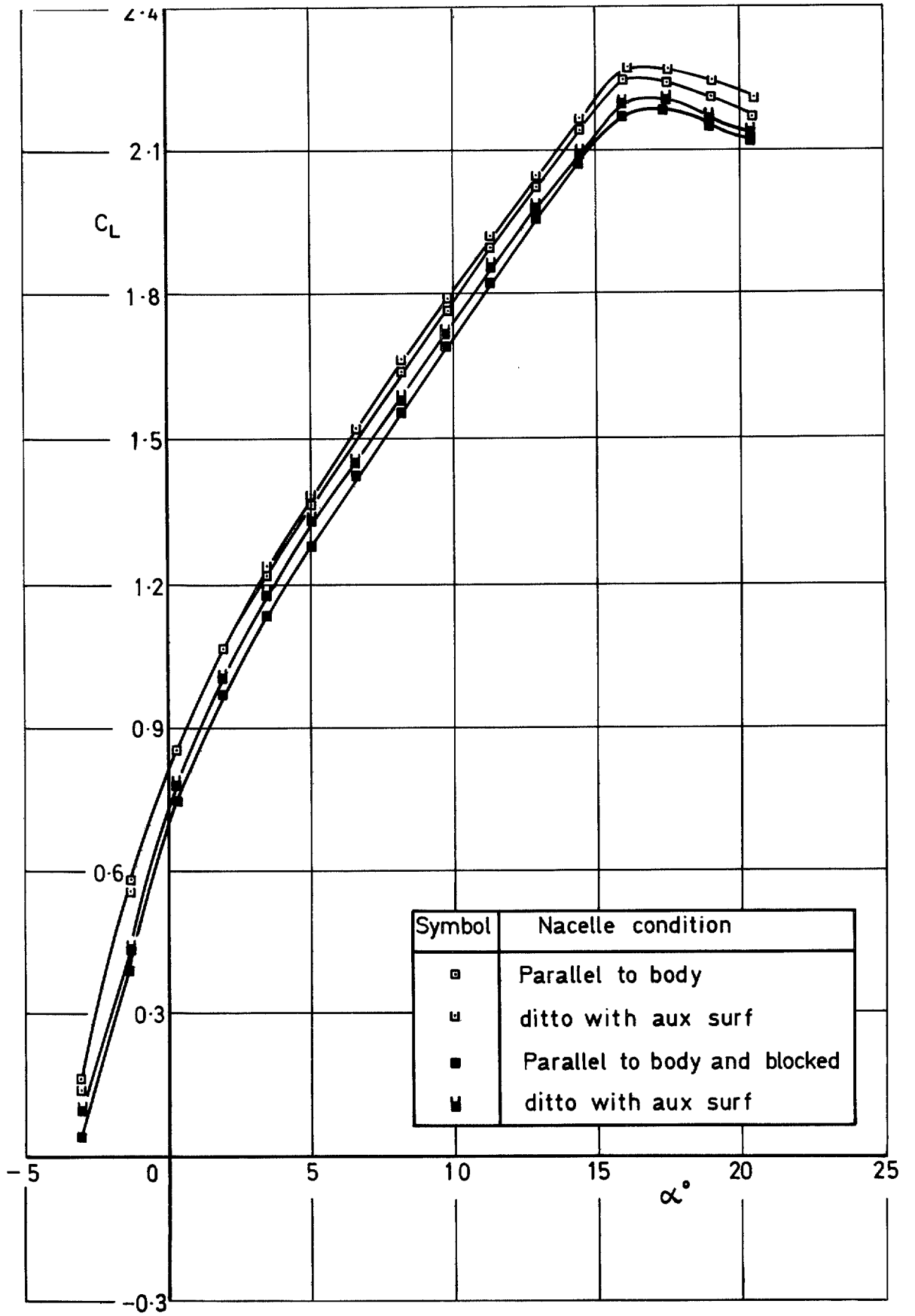

FIG. 43. Effect of blocking nacelles on lift coefficient of low-wing model with flat nacelles, slats 25° and flaps 40°.

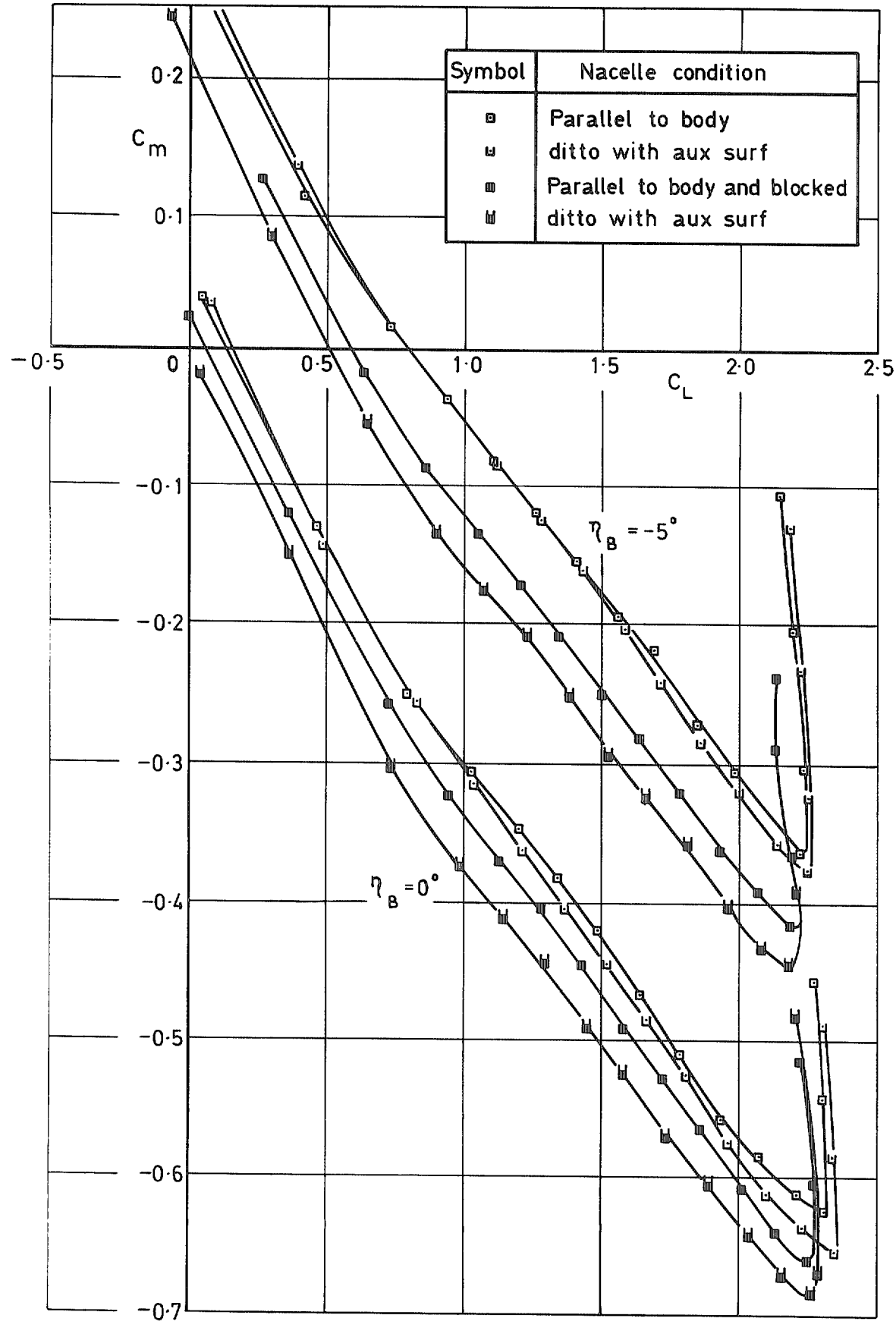

FIG. 44. Effect of blocking nacelles on pitching moment coefficient of low-wing model with flat nacelles, slats 25° and flaps 40°.

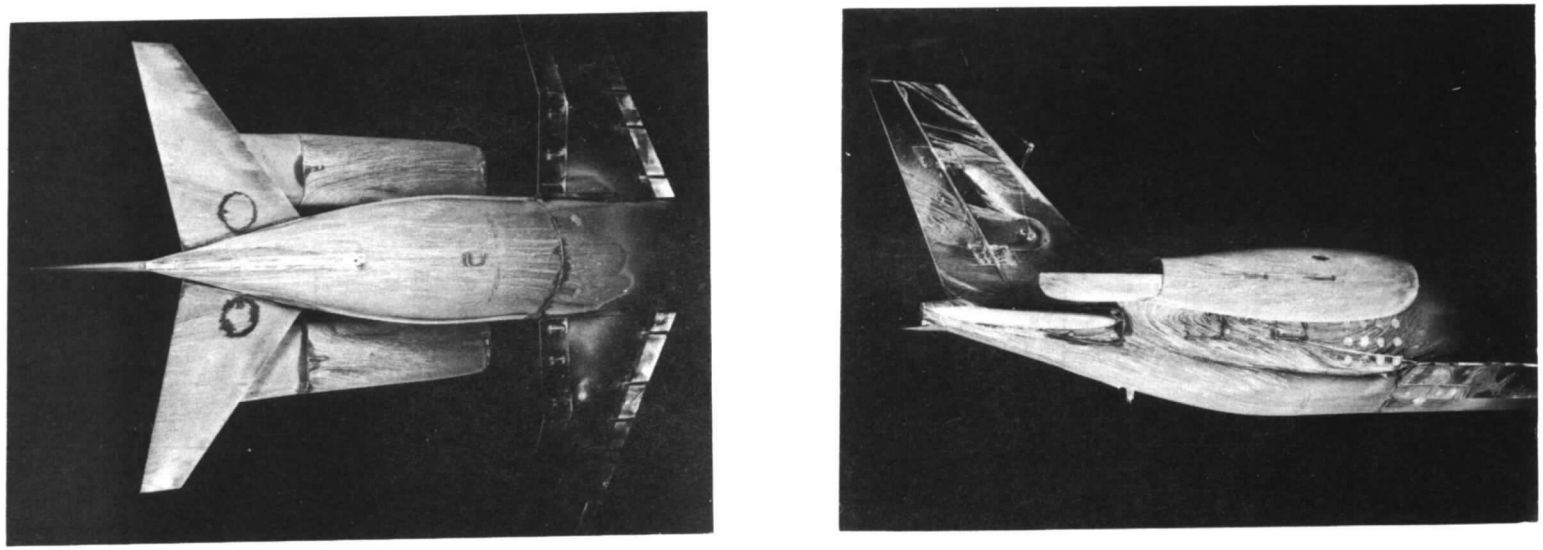

a. Nacelles parallel to body

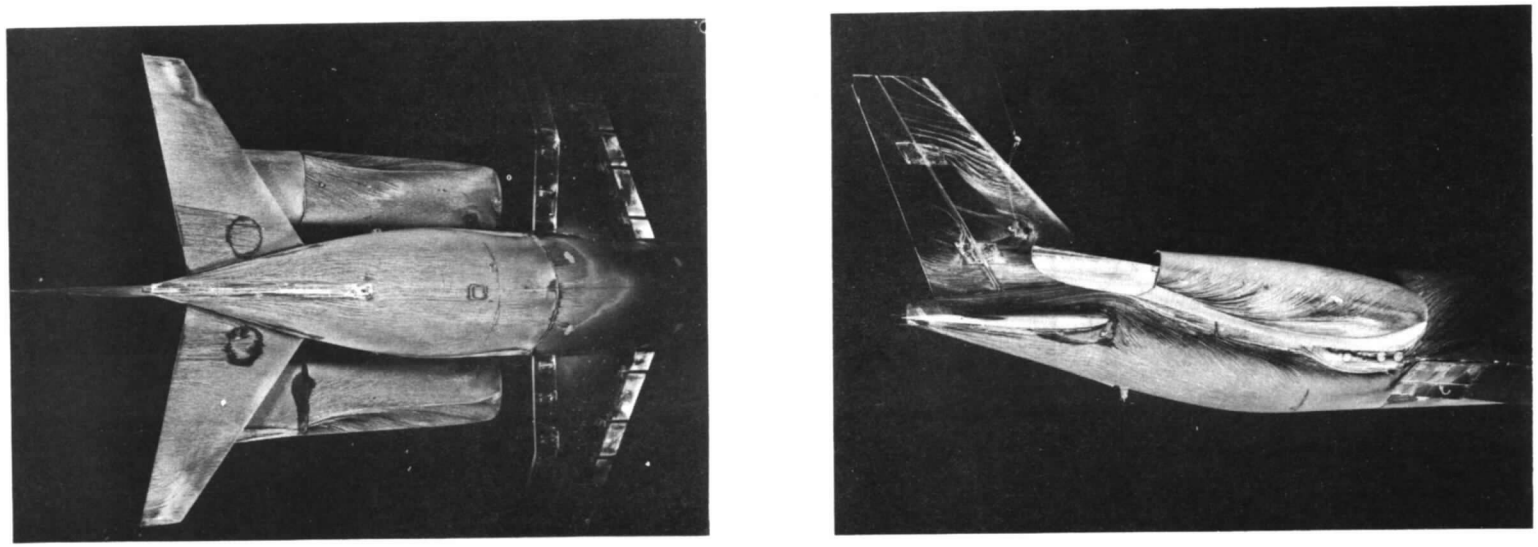

FIG. 45 a and b. Surface flow patterns at $\alpha = 10°$ on flat nacelles and adjacent surfaces, with low-wing model slats 25° and flaps 40°, $\eta_B = 0°$.

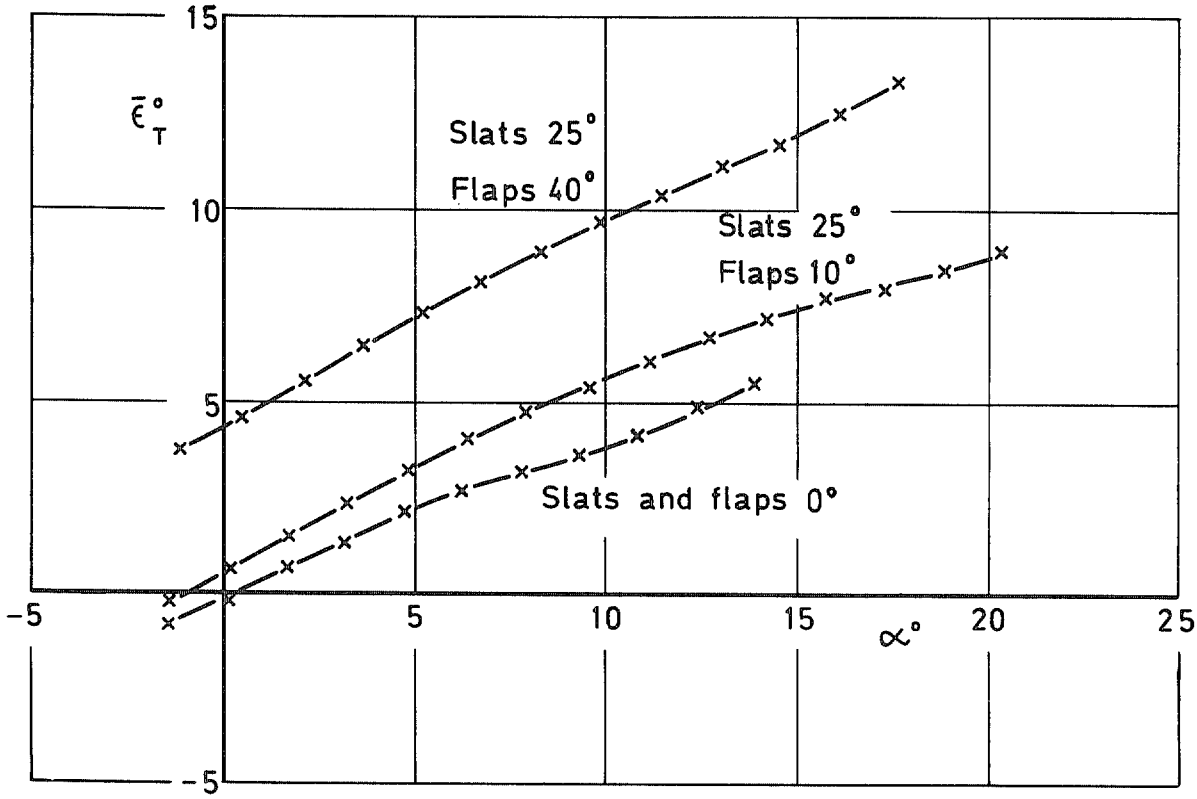

FIG. 46. Mean downwash angle at tailplane for high-wing model without nacelles.

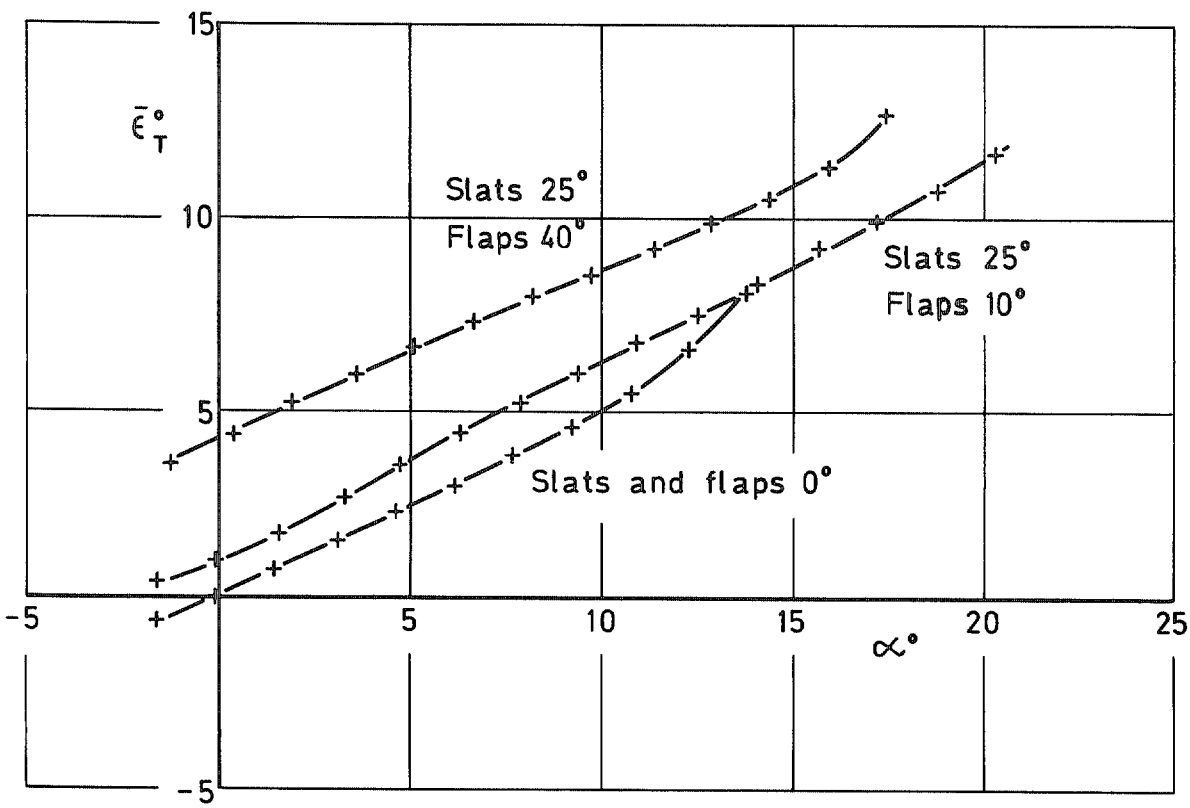

FIG. 47. Mean downwash angle at tailplane for low-wing model without nacelles.

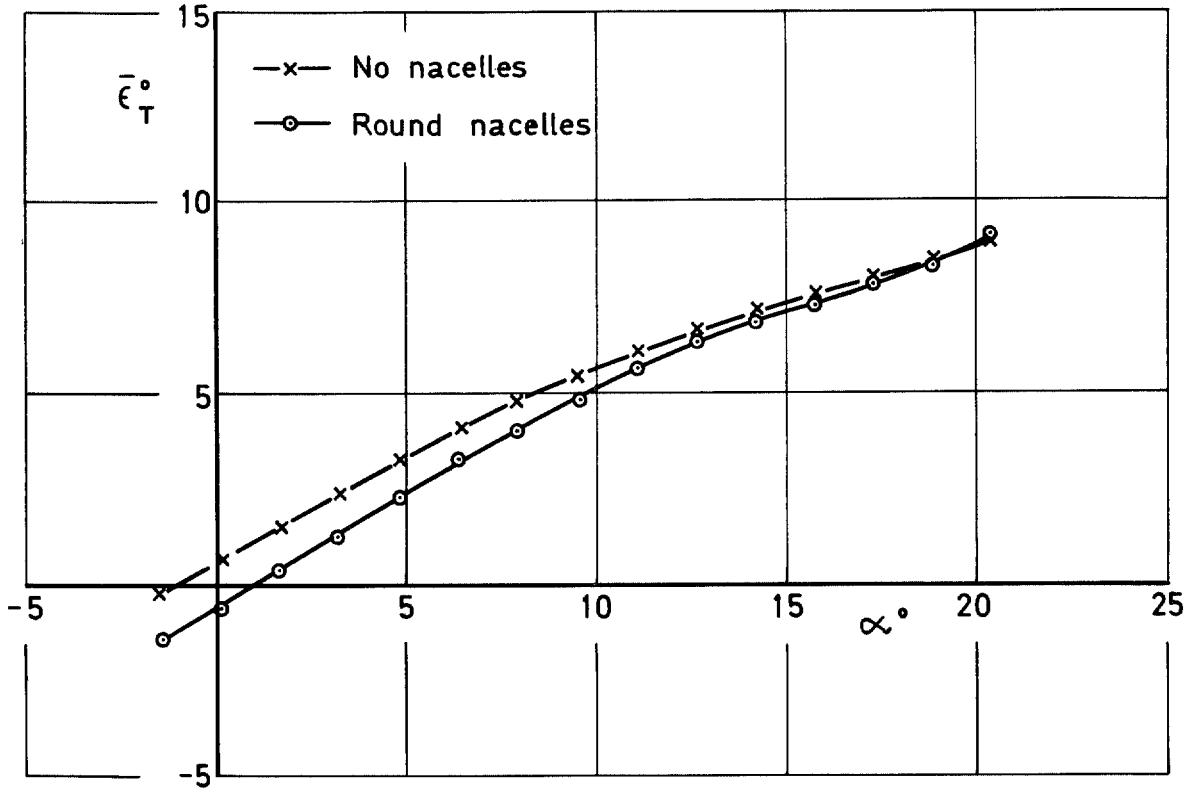

FIG. 48. Effect of nacelles on mean downwash angle at tailplane for high-wing model with slats 25° and flaps 10°.

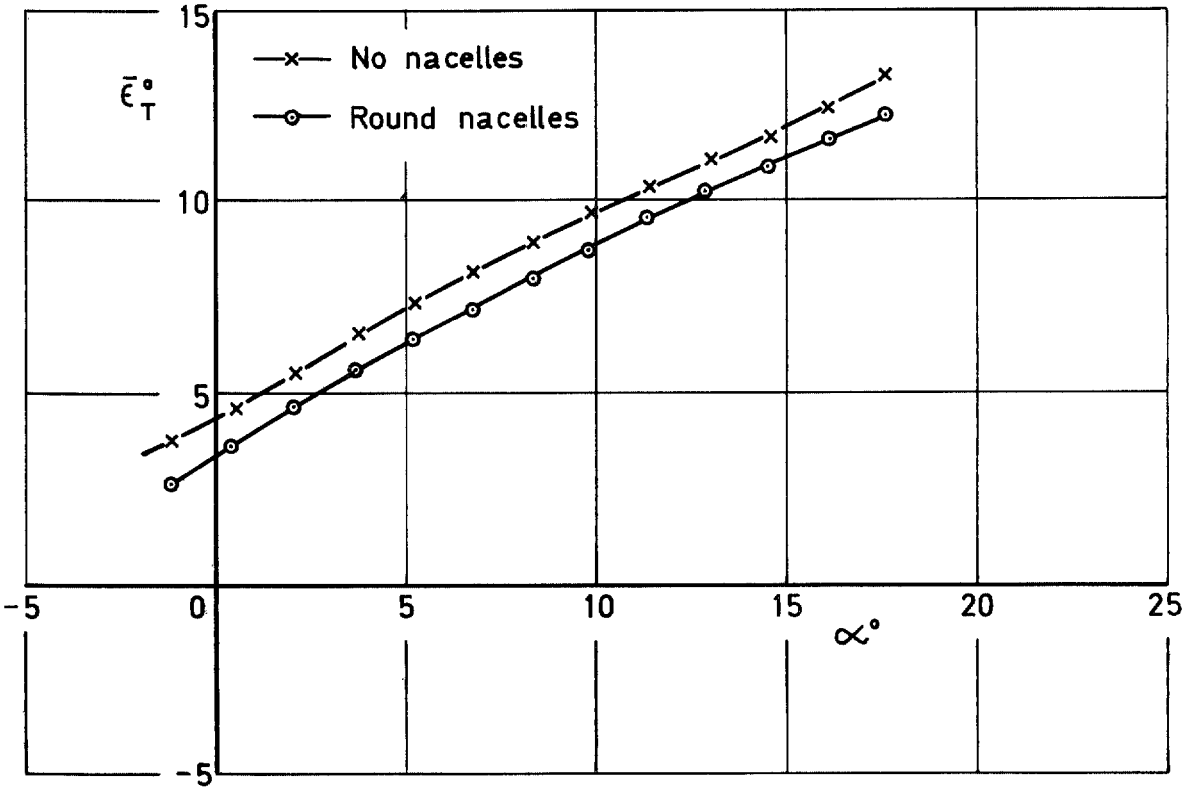

FIG. 49. Effect of nacelles on mean downwash angle at tailplane for high-wing model with slats 25° and flaps 40°.

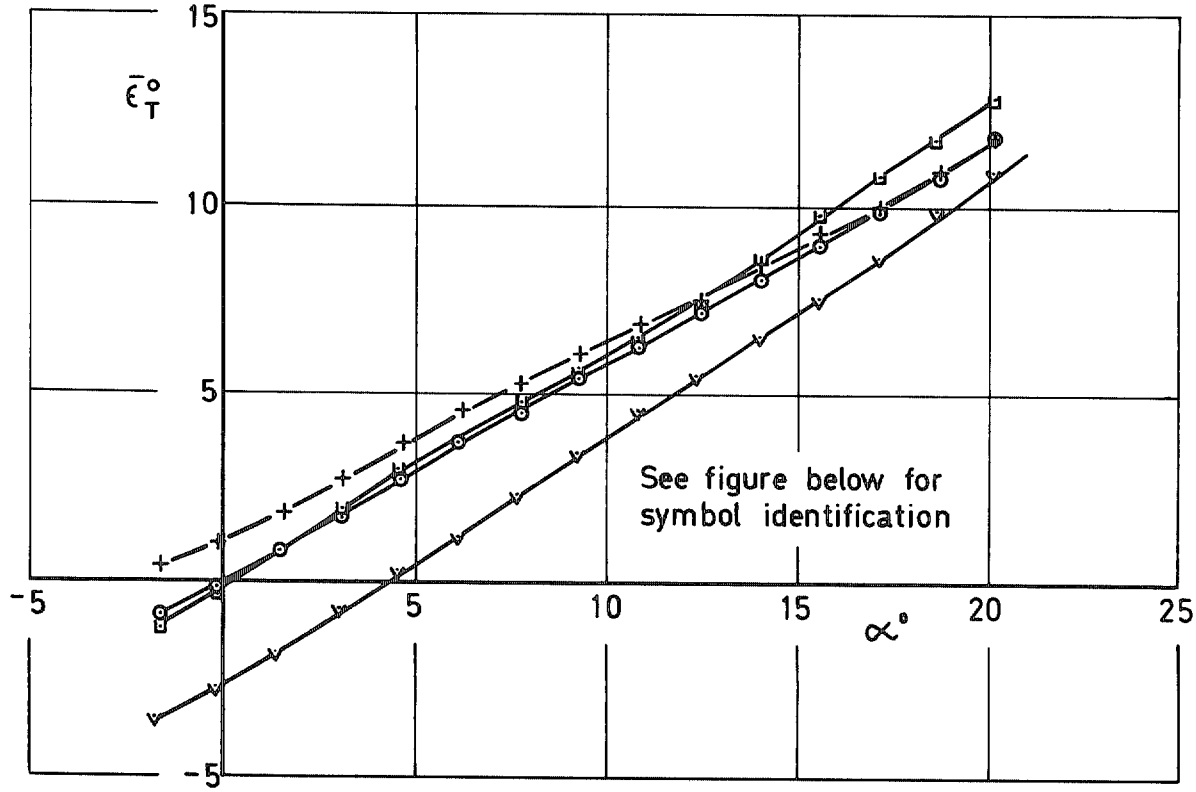

FIG. 50. Effect of nacelles on mean downwash angle at tailplane for low-wing model with slats 25° and flaps 10°.

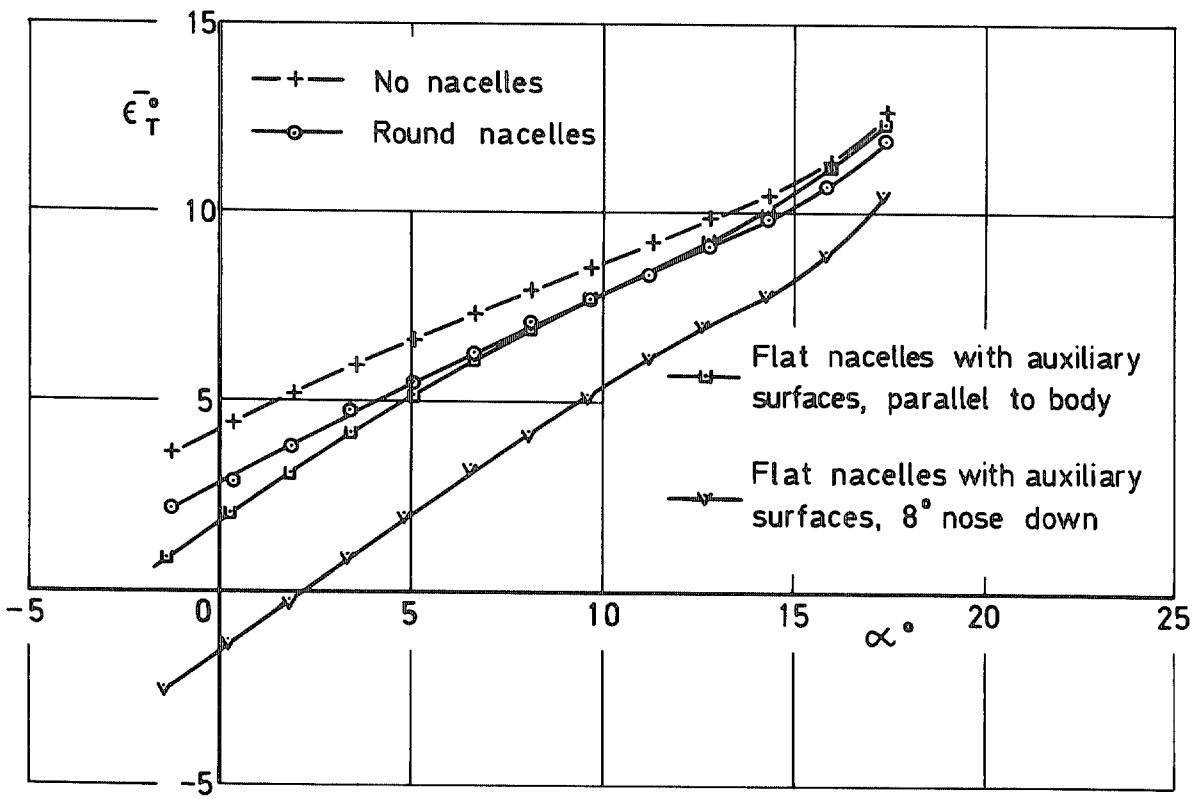

FIG. 51. Effect of nacelles on mean downwash angle at tailplane for low-wing model with slats 25° and flaps 40°.

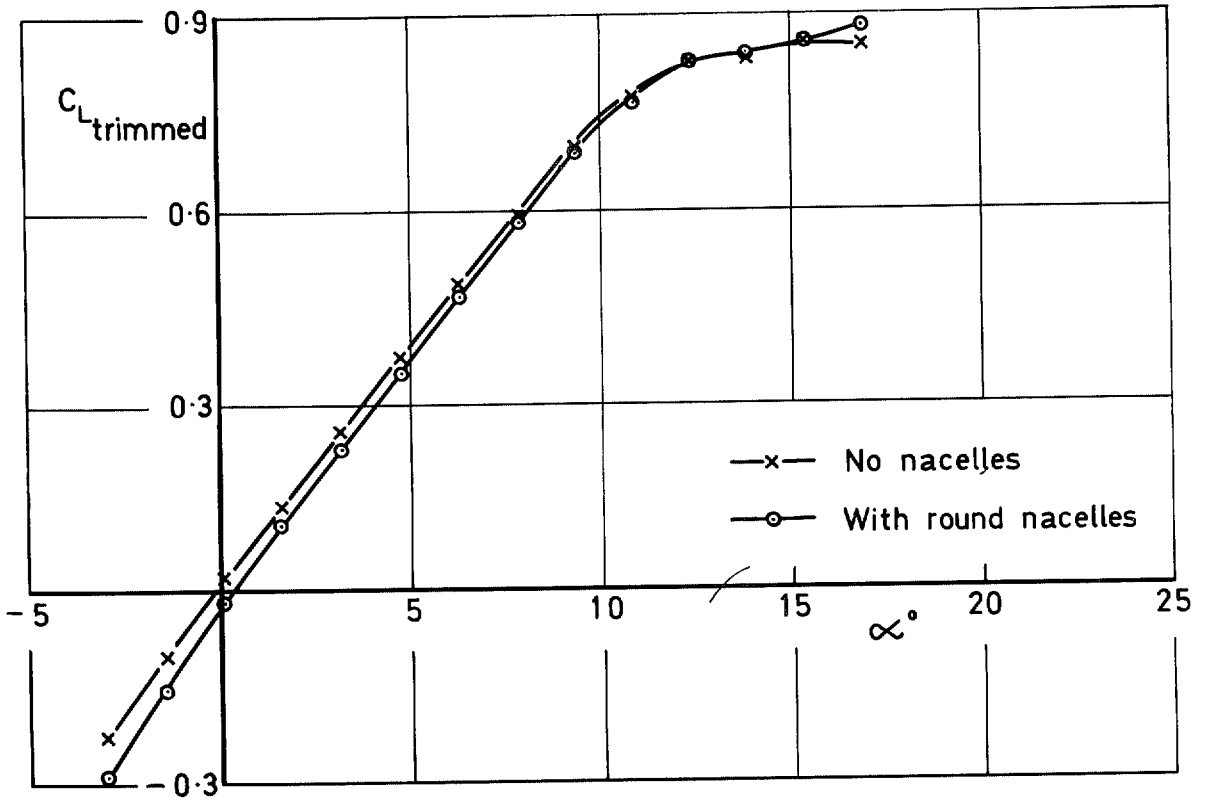

FIG. 52. Trimmed lift coefficient for high-wing model with slats and flaps 0°.

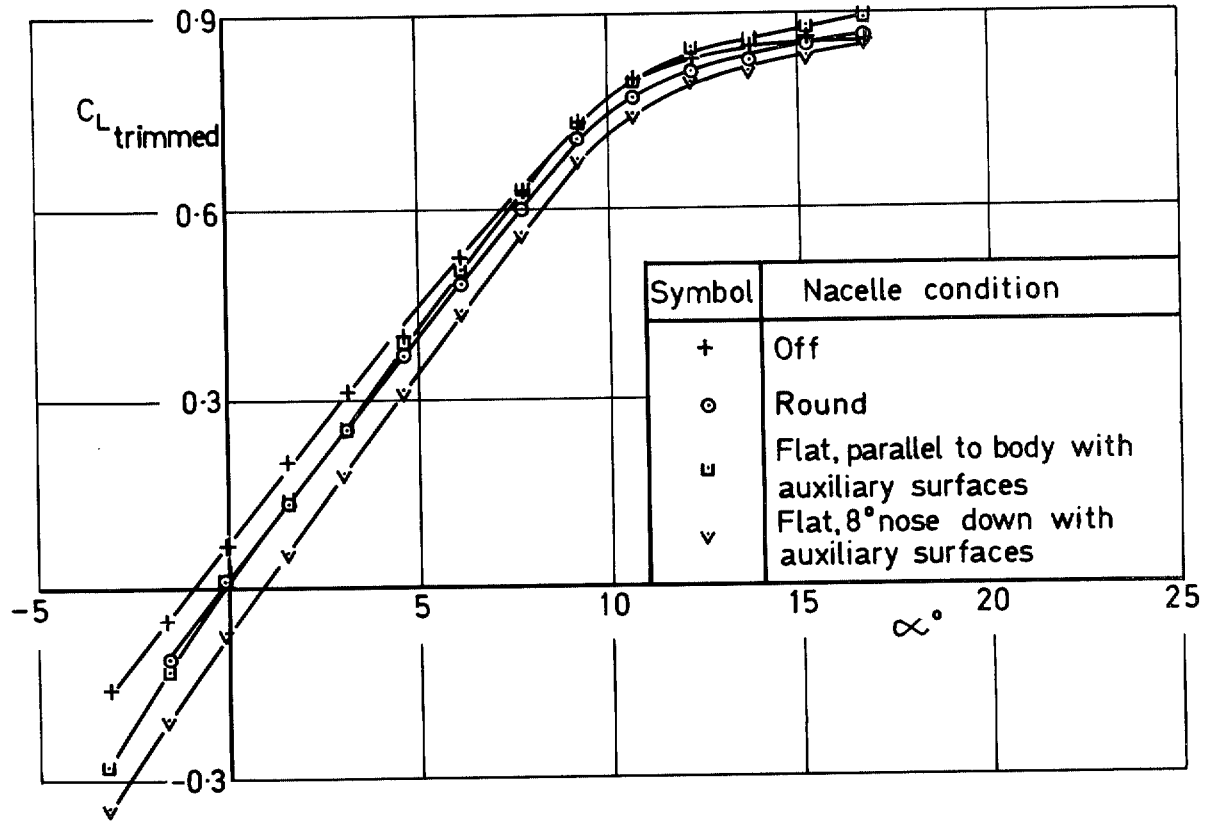

FIG. 53. Trimmed lift coefficient for low-wing model with slats and flaps 0°.

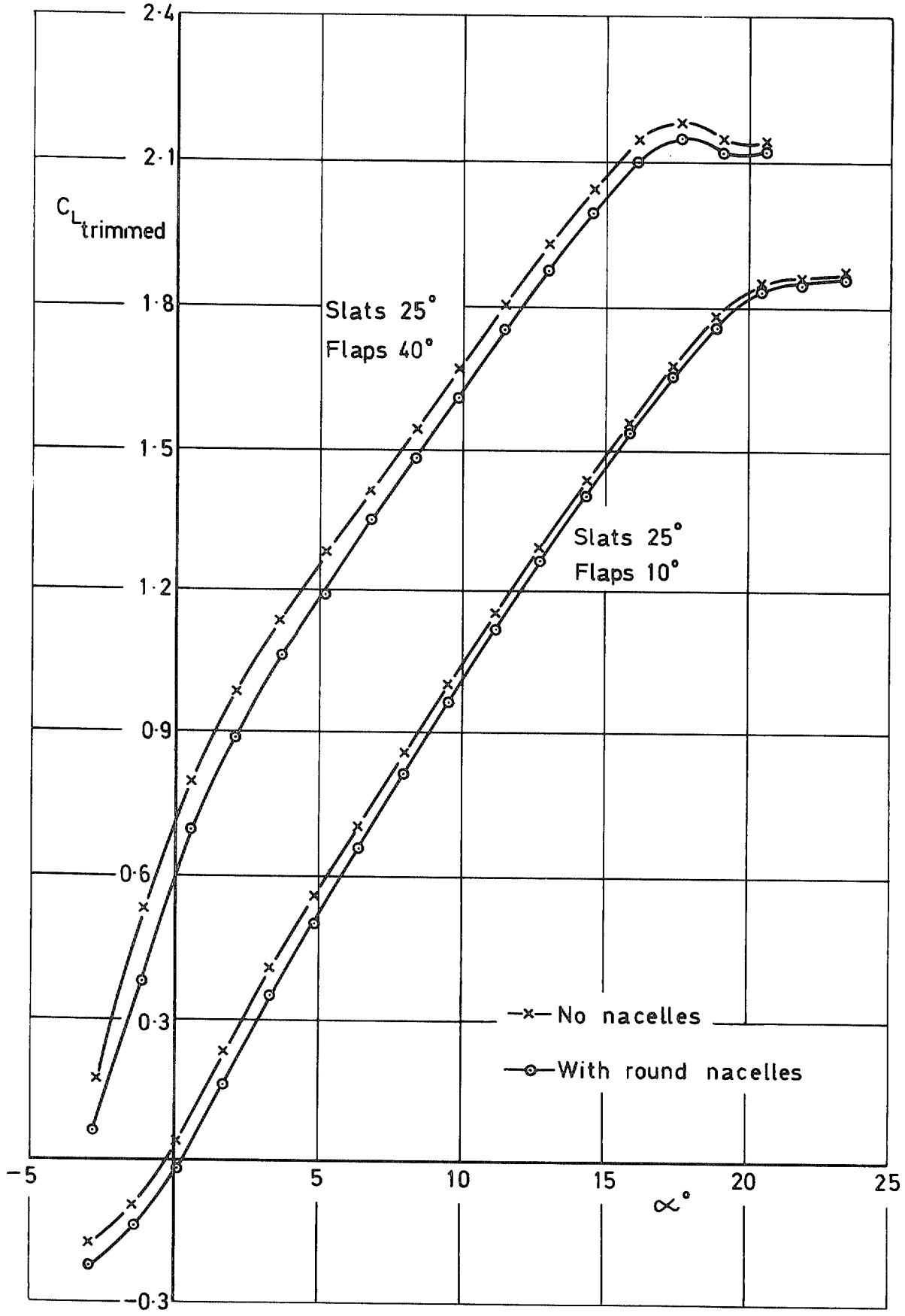

FIG. 54. Trimmed lift coefficient for high-wing model with slats and flaps deflected.

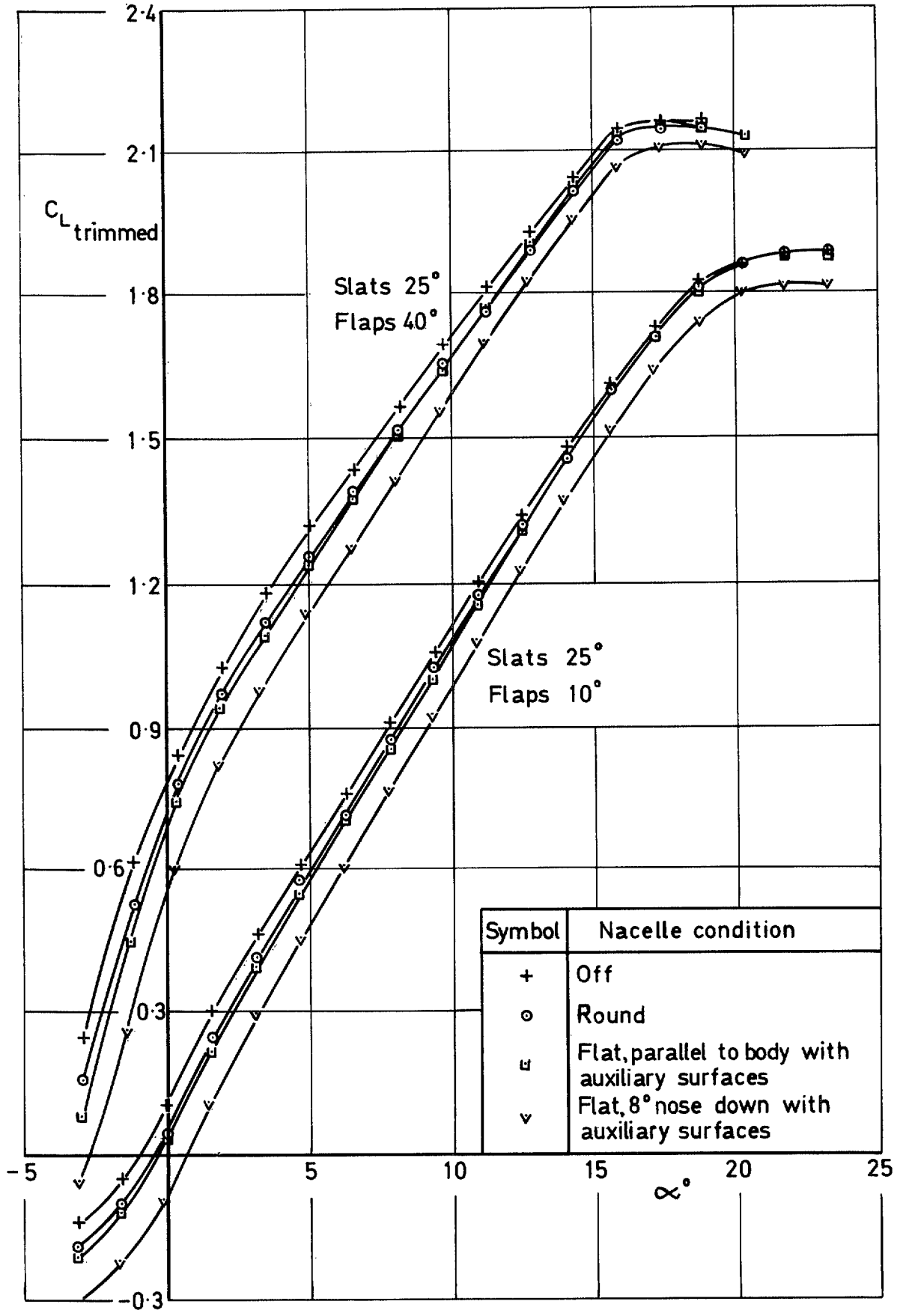

FIG. 55. Trimmed lift coefficient for low-wing model with slats and flaps deflected.

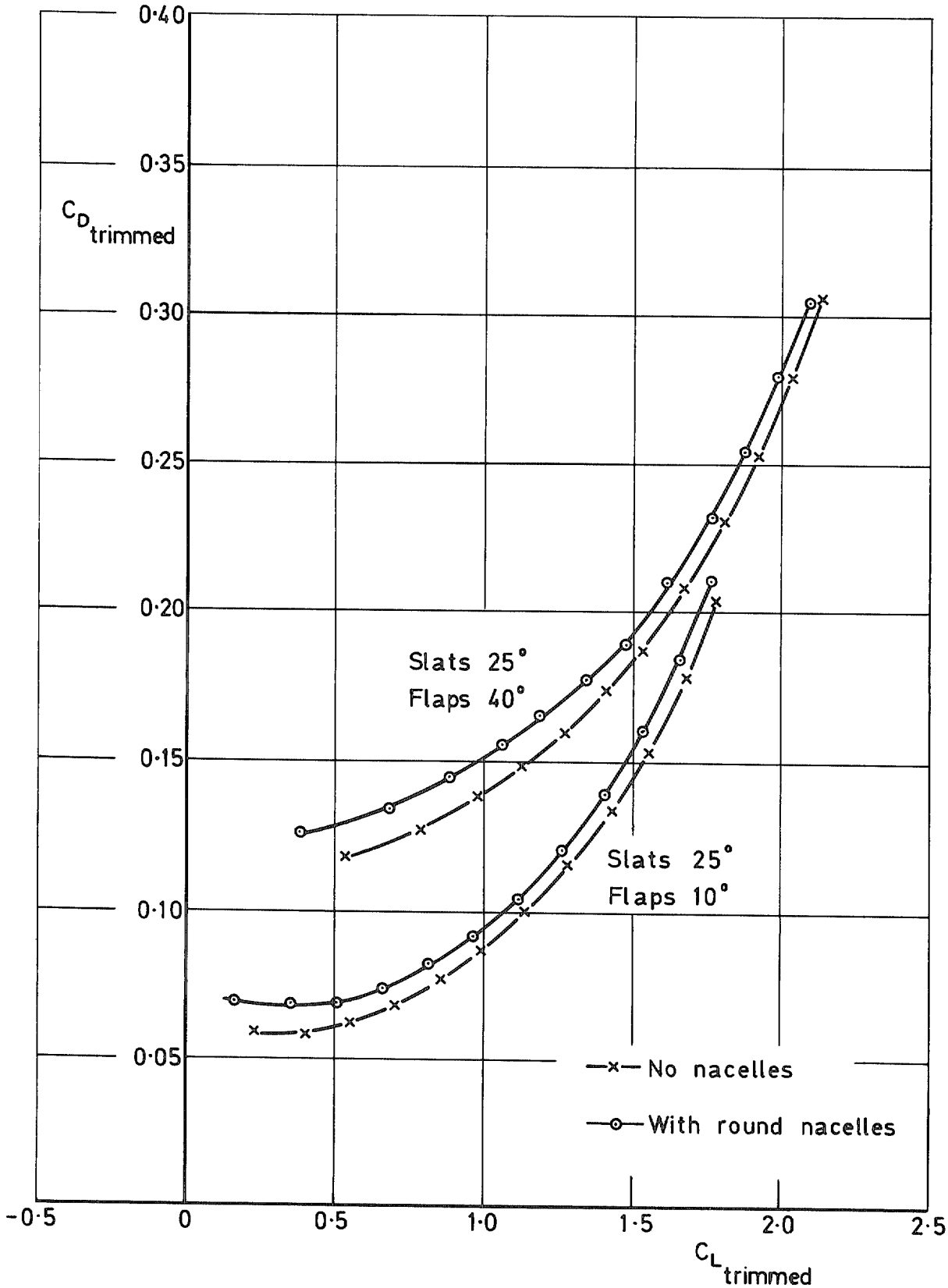

FIG. 56. Trimmed drag coefficient for high-wing model with slats and flaps deflected.

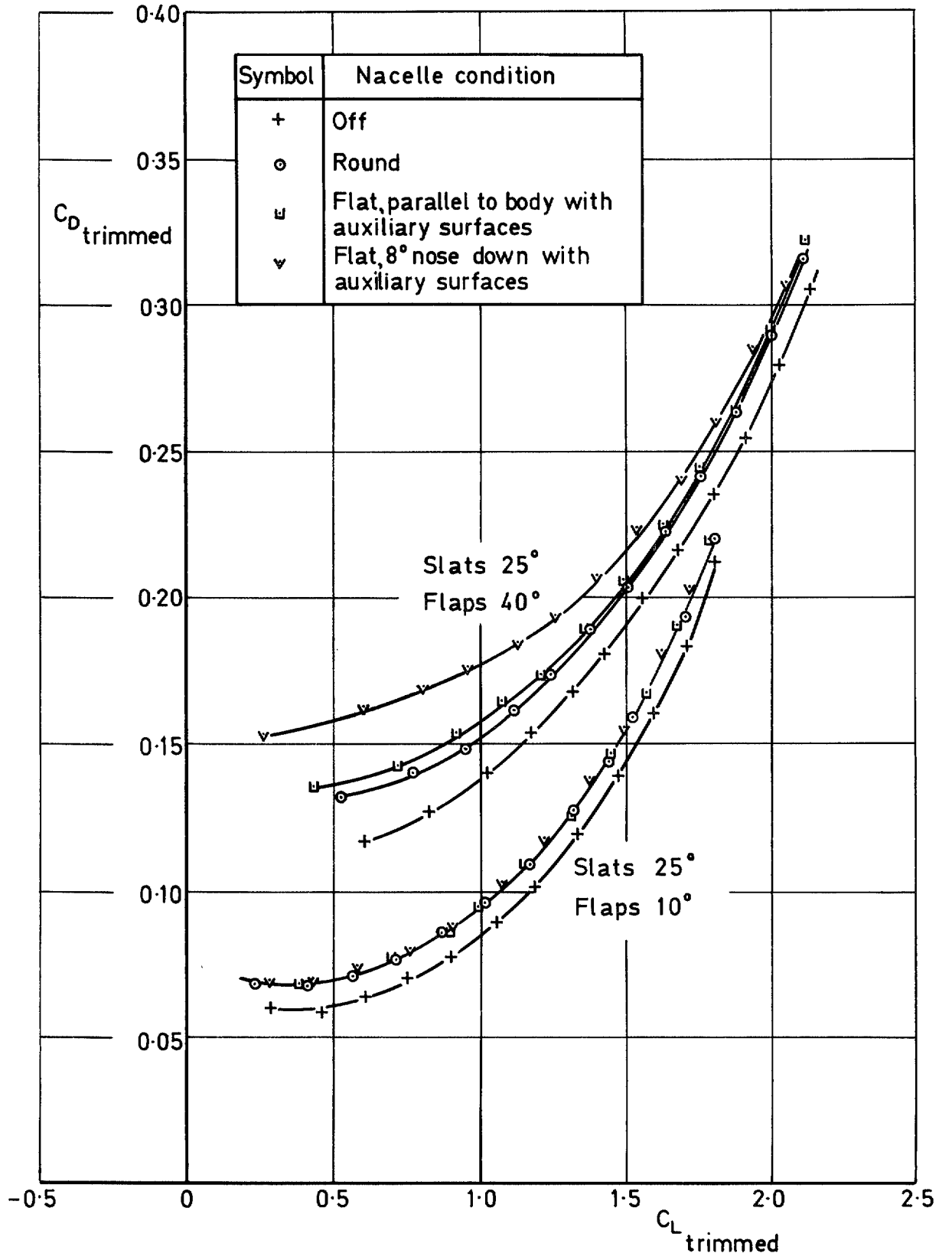

FIG. 57. Trimmed drag coefficient for low-wing model with slats and flaps deflected.

Printed in England for Her Majesty's Stationery Office by J. W. Arrowsmith Ltd., Bristol BS3 2NT
Dd. 587484 K5 7/77

HER MAJESTY'S STATIONERY OFFICE

Government Bookshops

49 High Holborn, London WC1V 6HB
13a Castle Street, Edinburgh EH2 3AR
41 The Hayes, Cardiff CF1 1JW
Brazennose Street, Manchester M60 8AS
Southey House, Wine Street, Bristol BS1 2BQ
258 Broad Street, Birmingham B1 2HE
80 Chichester Street, Belfast BT1 4JY

Government publications are also available through booksellers

ISBN 0 11 470972 6